

GEOLOGIC MAP OF THE CTGH-1 DRILL SITE, CLACKAMAS AND MARION COUNTIES, OREGON

Open-File Report O-88-5

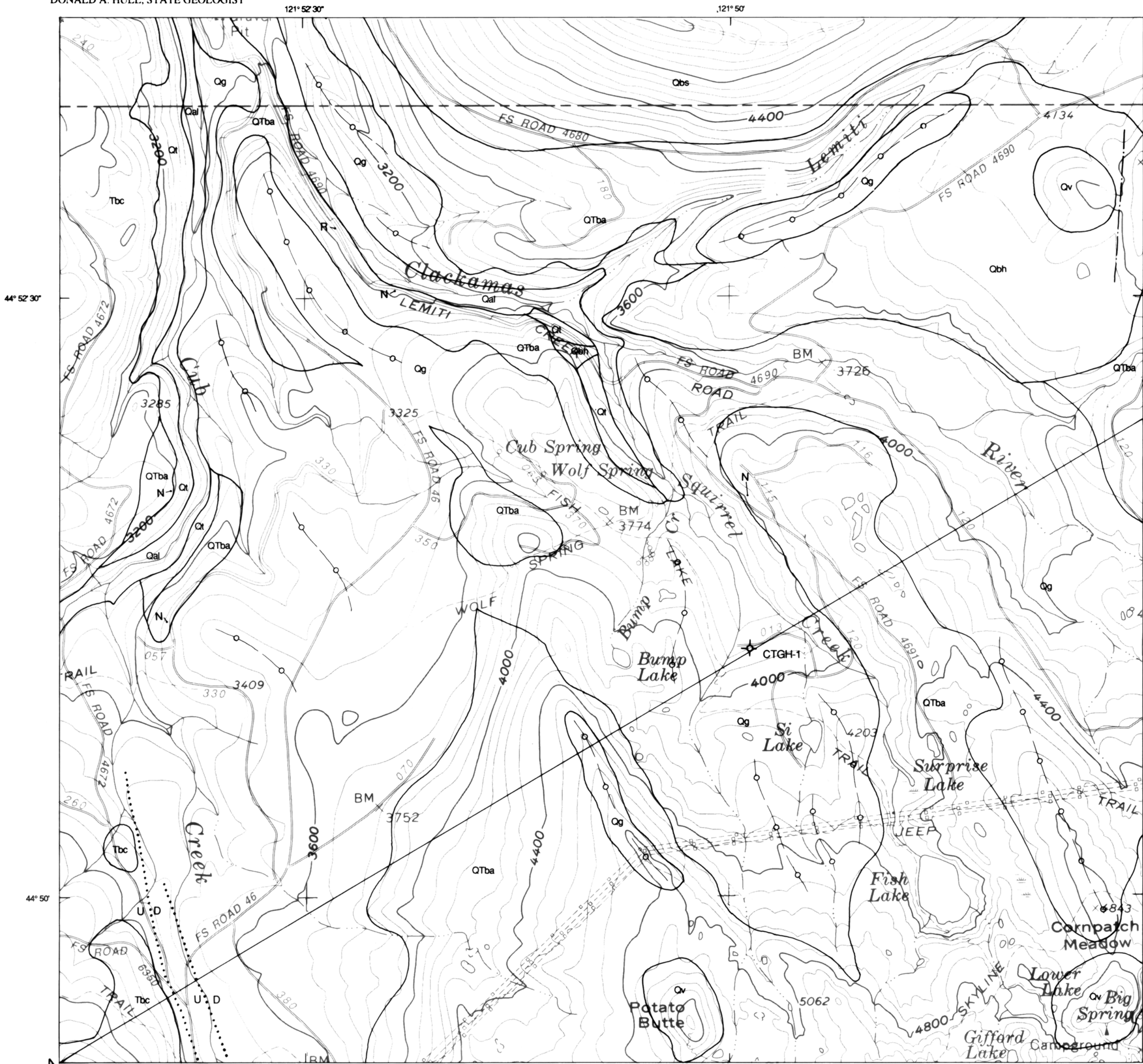
1988

STATE OF OREGON
DEPARTMENT OF GEOLOGY AND MINERAL INDUSTRIES
DONALD A. HULL, STATE GEOLOGIST

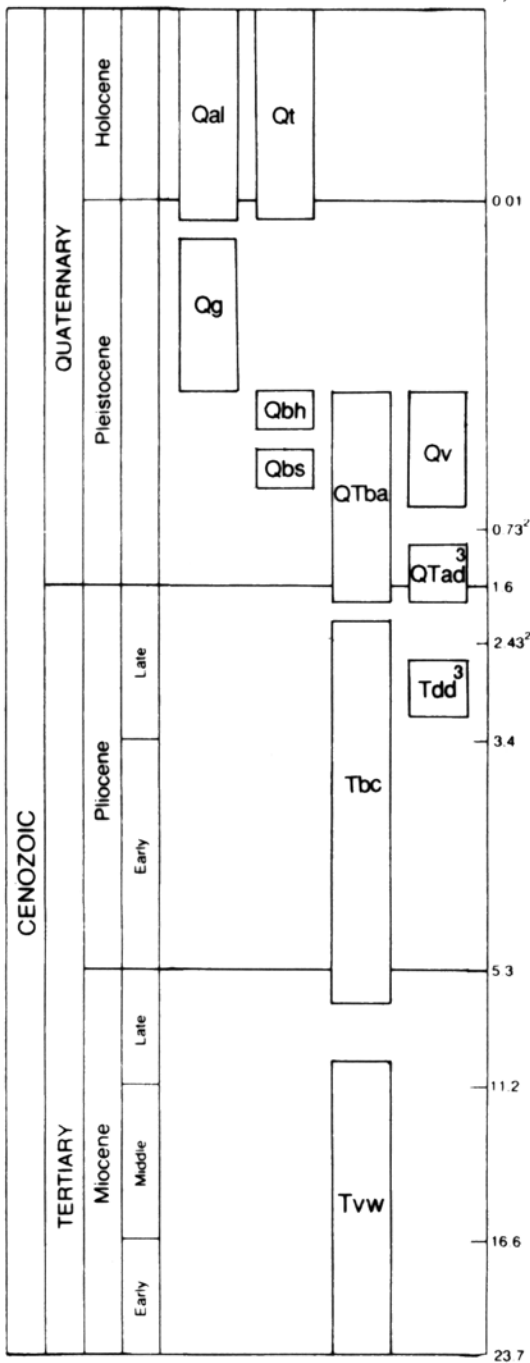
Geology and Geothermal Resources of the Breitenbush-Austin
Hot Springs Area, Clackamas and Marion Counties, Oregon
Edited by David R. Sherrod

Funded in part by U.S. Department of Energy
Grant No. DE-FG07-84 ID 12526

Plate 1



TIME ROCK CHART



¹Dates taken from Palmer (1983)
²Time boundaries of most recent magnetic reversal
³Shown only in cross section

EXPLANATION

- Qal** Alluvium (Holocene and Pleistocene)—Sand and gravel of modern stream floors. Includes deposits that may be outwash from latest Pleistocene glaciation
- Qt** Talus deposits (Holocene and Pleistocene)—Poorly sorted blocks from adjacent basalt and basaltic andesite lava flows. Unit probably formed as a consequence of overstepped valley walls from Pleistocene glaciations
- Qg** Glacial deposits (Pleistocene)—Chiefly unsorted and poorly sorted unstratified till. Unit forms ground and lateral moraines throughout map area. Locally includes minor outwash deposits. Strings of small circles indicate prominent ridge crests in lateral moraines
- Qbh** Hornblende-bearing basaltic andesite (Pleistocene)—Lava flows of hornblende- and olivine-bearing basaltic andesite. Locally clinopyroxene bearing. Normally polarized
- Qbs** Basaltic andesite of Sisi Butte (Pleistocene)—Finely plagioclase-phyric olivine basaltic andesite lava flows. Unit forms moderate-size (3.4 km²) shield volcano (Sisi Butte) centered about 1 km north of map area. Volcano, which is heavily glaciated and normally polarized, probably formed during a relatively short interval between 500,000 and 730,000 yrs ago, on the basis of geomorphic comparisons with other normally and reversely polarized shield volcanoes in the area from Mount Jefferson to Mount Hood
- Qv** Vent rocks (Pleistocene)—Cinders and scoria associated with vents for basaltic andesite and basalt lava flows. Near-vent rocks associated with lava in unit Qbh form poorly exposed hill of cinders in northeast corner of map. Near-vent rocks associated with lava near top of unit QTba form cinder cone at Potato Butte at south edge of map and palagonitized cinder- and lapilli-tuff in cone near Big Spring in southeast corner. No near-vent rocks for lower part of unit QTba have been recognized, probably because of poor exposures, burial by younger flows in the unit, and removal by erosion
- QTba** Basaltic andesite and basalt (Pleistocene and Pliocene)—Lava flows and minor breccia of olivine-bearing basaltic andesite and basalt. Unit contains numerous flows that were erupted from several cinder cones and small shields. Includes rocks with normal and reversed polarity magnetization. Unit thickens from about 250 m at CTGH-1 drill site to at least 750 m thick near the southeast edge of map, which is near the axis of the High Cascades
- QTad** Andesite in drill hole CTGH-1 (Pleistocene or Pliocene)—Slightly porphyritic lava flows and minor breccia and lahatic deposits. Forms interval at 260-479 m in drill hole; shown only on cross-section. Queried where lateral extent unknown. Pleistocene or Pliocene in age, on basis of K-Ar age of about 2.91 Ma from underlying strata at 597 m (Table 1)
- Tdd** Dacite in drill hole CTGH-1 (Pliocene)—Crystal-litic lapilli tuff and welded tuff. Includes andesite breccia and possible surge deposits. Forms interval at 789-831 m in drill hole; shown only on cross-section. Queried where lateral extent unknown. Pliocene in age, on basis of K-Ar ages from bracketing strata: about 2.91 Ma at 597 m and 4.95 Ma at 961 m (Table 1)
- Tbc** Basaltic andesite and basalt of Collawash Mountain (Pliocene and Miocene)—Lava flows and minor breccia of olivine-bearing basaltic andesite and basalt. Unit is extensively exposed southwest and west of map area and forms the upthrown block or blocks of several buried, poorly defined faults at the west edge of the map area. By volume, unit contains about 60 percent basaltic andesite, 30 percent basalt, and 10 percent andesite
- Twv** Volcanic rocks of the Western Cascades (Miocene and Oligocene)—Lava flows and volcanoclastic rocks, including parts of the Breitenbush Formation, lava of Outerson Mountain, and andesite and dacite of Rhododendron Ridge as described by Sherrod and Conrey (1988). Shown only on cross-section

REFERENCES

- Conrey, R.M., and Sherrod, D.R., 1988, Stratigraphy of drill holes and geochemistry of surface rocks, Breitenbush Hot Springs 15-minute quadrangle, Cascade Range, Oregon, in Sherrod, D.R., ed., Geology and geothermal resources of the Breitenbush-Austin Hot Springs area, Clackamas and Marion Counties, Oregon: Oregon Department of Geology and Mineral Industries Open-File Report O-88-5, in press.
- Palmer, A.R., 1983, The Decade of North American Geology 1983 geologic time scale: Geology, v. 11, no. 9, p. 503-504.
- Sherrod, D.R., and Conrey, R.M., 1988, Geologic setting of the Breitenbush-Austin Hot Springs area, Cascade Range, north-central Oregon, in Sherrod, D.R., ed., Geology and geothermal resources of the Breitenbush-Austin Hot Springs area, Clackamas and Marion Counties, Oregon: Oregon Department of Geology and Mineral Industries Open-File Report O-88-5, in press.
- Steiger, R.H., and Jager, E., 1977, Subcommittee on geochronology: Convention on the use of decay constants in geo- and cosmochronology: Earth and Planetary Science Letters, v. 36, p. 359-362.

MAP SYMBOLS

- Contact**—Approximately located. Queried in cross section where lateral continuity is unknown
- Fault**—Approximately located, dotted where buried. D, U indicate downthrown and upthrown block, respectively
- Lineament**
- Thermal remanent magnetization**
- N** Normally polarized
- R** Reversely polarized
- CTGH-1 drill site**

4.95±0.23 Ma Age of drill core sample—See Table 1

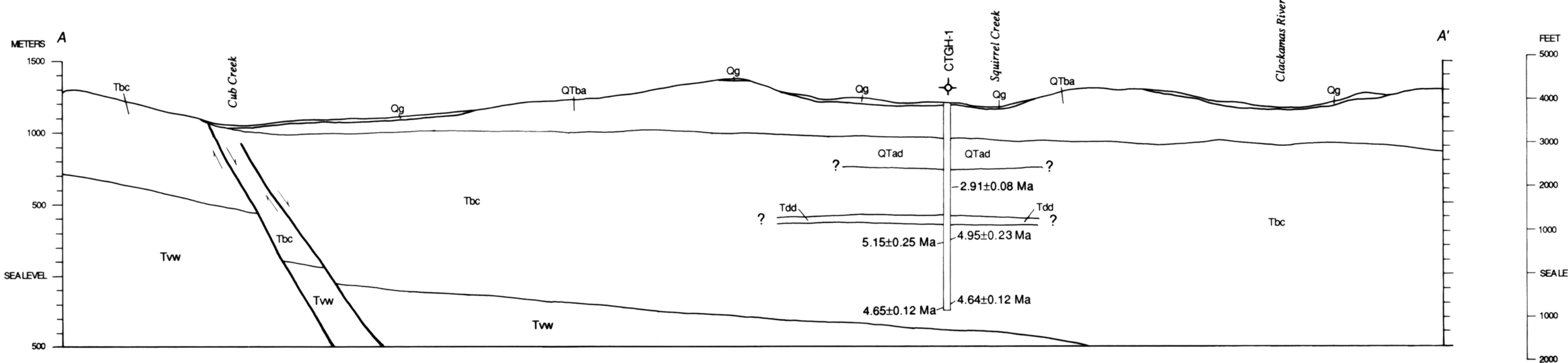
Geology mapped by David R. Sherrod, U.S. Geological Survey and Richard M. Conrey, Washington State University

Field work completed in 1987

Table 1. K-AR AGES FROM CTGH-1 DRILL CORE						
Sample number	Rock type	Material dated ¹	K ₂ O (wt %) ²	⁴⁰ Ar/ ³⁹ Ar ² (10 ⁻¹¹ moles/gm) ²	Percent ⁴⁰ Ar/ ³⁹ Ar ²	Calculated age (Ma) ³
CTGH-1956	Basaltic andesite	Plagioclase concentrate	1.392	0.5845	70	2.91±0.08
CTGH-3152	Basaltic andesite	Plagioclase concentrate	0.615	0.4388	19	4.95±0.23
CTGH-3195	Basaltic andesite	Plagioclase concentrate	0.801	0.5949	17	5.15±0.25
CTGH-4633	Basaltic andesite	Plagioclase concentrate	1.295	0.8664	43	4.64±0.12
CTGH-4740	Basaltic andesite	Plagioclase concentrate	1.379	0.9232	39	4.65±0.12

Notes:
¹Sample preparation and analytical work were done at University of Arizona, Paul E. Damon and Mohammed Shafiqullah, principal investigators.
²Average of several analyses. See Conrey and Sherrod (1988) for complete data.
³K-Ar ages were calculated using the constants for the radioactive decay and abundance of ⁴⁰K recommended by the International Union of Geological Sciences Subcommittee on Geochronology (Steiger and Jager, 1977). These constants are:
 $\lambda_e = 0.580 \times 10^{-10} \text{ yr}^{-1}$, $\lambda_\beta = 4.962 \times 10^{-10} \text{ yr}^{-1}$, and $^{40}\text{K}/\text{K}_{\text{total}} = 1.167 \times 10^{-4} \text{ mol/mol}$.

GEOLOGIC CROSS SECTION



STATE OF OREGON
DEPARTMENT OF GEOLOGY AND MINERAL INDUSTRIES
910 State Office Building
1400 SW Fifth Avenue
Portland, Oregon 97201

OPEN-FILE REPORT O-88-5

**GEOLOGY AND GEOTHERMAL RESOURCES OF THE BREITENBUSH-
AUSTIN HOT SPRINGS AREA, CLACKAMAS AND MARION COUNTIES,
OREGON**

Edited by
David R. Sherrod
U.S. Geological Survey
345 Middlefield Road, Menlo Park, Calif. 94025

1988

Funded in part by
U.S. Department of Energy
Grant No. DE-FG07-84 ID 12526

NOTICE

The Oregon Department of Geology and Mineral Industries is publishing this paper because the subject matter is consistent with the mission of the Department. To facilitate timely distribution of information, camera-ready copy submitted by the editor has not been edited by the staff of the Oregon Department of Geology and Mineral Industries.

CONTENTS

Preface	iv
Chapter 1. Geologic setting of the Breitenbush-Austin Hot Springs area, Cascade Range, north-central Oregon, by David R. Sherrod and Richard M. Conrey	1
Chapter 2. Stratigraphy of drill holes and geochemistry of surface rocks, Breitenbush Hot Springs 15-minute quadrangle, Cascade Range, Oregon, by Richard M. Conrey and David R. Sherrod	15
Chapter 3. Regional patterns of hydrothermal alteration in the Breitenbush-Austin Hot Springs area of the Cascade Range, Oregon, by Terry E.C. Keith	31
Chapter 4. Secondary mineralogy of core from geothermal drill hole CTGH-1, Cascade Range, Oregon, by Keith E. Bargar	39
Chapter 5. Thermal analysis of the Austin and Breitenbush geothermal systems, Western Cascades, Oregon, by David D. Blackwell and Sydney L. Baker	47
Chapter 6. Geologic and geothermal summary of the Breitenbush-Austin Hot Springs area, Clackamas and Marion Counties, Oregon, by David R. Sherrod	63
Appendix 1. Chemical analyses of rocks exposed in the southeastern part of the Breitenbush Hot Springs quadrangle, by Richard M. Conrey	71
Appendix 2. Drill core log for CTGH-1, by David R. Sherrod and Richard M. Conrey	87

Preface

The Breitenbush-Austin Hot Springs area is located about 50 km southeast of Portland, in the Cascade Range of northern Oregon (Figure 1). The area includes the two physiographic subprovinces of the Cascade Range in Oregon: the deeply incised Western Cascades and the relatively uneroded High Cascades. The High Cascades subprovince coincides with an extensive belt of Quaternary and Pliocene volcanic rocks that form a continental volcanic arc related to the subduction of the Juan de Fuca oceanic plate beneath North America.

Several geologic features make the area an appropriate focus for geothermal exploration. It contains the composite volcano of Mount Jefferson, late Pleistocene dacitic to rhyodacitic domes and flows north of Mount Jefferson, many Quaternary basaltic andesite shield volcanoes, and numerous cinder cones and lava flows. Breitenbush Hot Springs Known Geothermal Resource Area (KGRA) is situated in the valley of the Breitenbush River;

Austin Hot Springs KGRA lies 27 km north in the Clackamas River drainage. Additionally, part of the area lies within a region of heat flow in excess of 100 milliwatts per square meter (mW/m^2). Mariner and others (1980) listed Breitenbush Hot Springs as one of the top ten areas of geothermal potential in the state, on the basis of chemical geothermometers.

This open-file report summarizes several ongoing investigations in the Breitenbush-Austin Hot Springs area, including geologic mapping, alteration studies, and the heat-flow results from cooperative drilling programs and previously confidential industry drilling. In Chapter 1, Sherrod and Conrey discuss the geologic setting of the area, which encompasses volcanic rocks ranging in age from Oligocene to Quaternary. Middle Miocene and older volcanic and volcanoclastic rocks were deformed into a broad structural arch (the Breitenbush anticline), whereas relatively undeformed, progressively younger volcanic

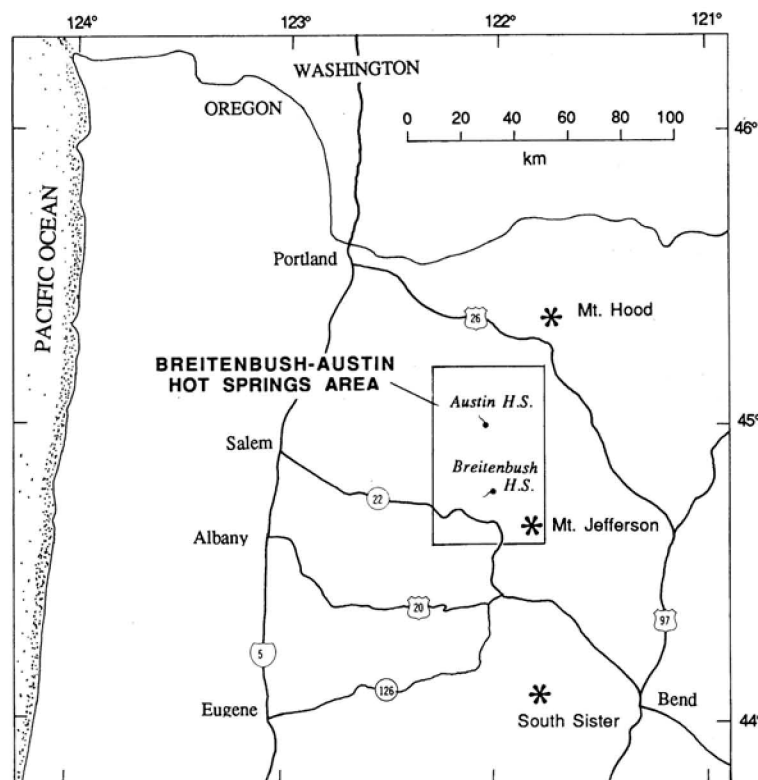


Figure 1. Index map showing location of Breitenbush and Austin Hot Springs and the area of this report, Cascade Range of northern Oregon. Also shown are major highways, towns, and Quaternary composite volcanoes.

Preface

rocks crop out mainly east of the folded units. Upper Pleistocene intermediate and silicic volcanism is restricted to the High Cascades from Mount Jefferson to Olallie Butte, 33 km to the north, and is interpreted as the heat source for geothermal waters at Breitenbush and Austin Hot Springs. In Chapter 2, Conrey and Sherrod summarize the subsurface stratigraphy and correlation of cuttings and core from several drill holes as well as the geochemistry of surface rocks in the Breitenbush Hot Springs 15-minute quadrangle. The 1,463-m-deep CTGH-1 hole, drilled in the High Cascades physiographic subprovince, penetrated chiefly basaltic andesite lava flows ranging in age from late Miocene or early Pliocene to Quaternary. Potassium-argon ages from CTGH-1 core are as old as about 5 Ma.

Chapters 3 and 4 describe alteration in the Breitenbush-Austin Hot Springs area. In Chapter 3, Keith shows that secondary mineralogy is broadly zoned from phyllic to zeolitic outward from the axis of the Breitenbush anticline. This alteration, which indicates that temperatures locally exceeded 200 °C in rocks once buried 1-2 km, probably predates the middle Miocene folding of the Breitenbush anticline and is not related to the active geothermal systems of Breitenbush and Austin Hot Springs. In contrast, exposed upper Miocene and younger rocks are relatively unaltered. In Chapter 4, Bargar applies alteration mineralogy in his study of the CTGH-1 drill core and concludes that downhole temperatures have never exceeded those measured today—about 100 °C at 1,463 m.

In Chapter 5, Blackwell and Baker present a substantial set of new data on thermal conductivity and heat flow, much of it the previously confidential results of exploration by private industry in the early 1980's. By contouring the heat-flow data, Blackwell and Baker show that Breitenbush Hot Springs is at the western edge of a lobe of high heat flow that extends away from the High Cascades into the Western Cascades. At the surface the lobe corresponds to what Priest and others (1987) described as a thermal aquifer, in which hot water migrates in lower Miocene and older units that plunge eastward beneath the High Cascades. The aquifer is probably complex and results from permeability contrasts created by lithology, structure, and alteration.

In Chapter 6, Sherrod combines all the contributions into a geologic cross section showing topography, stratigraphy, structure, isotherms, heat flow, gravity, and hydrology. The picture emerges of an igneous-related conductive thermal regime with heat flow of 100 mW/m² beneath the High Cascades. The conductive gradient decreases to 40 mW/m² in the Western Cascades but is locally perturbed by convective anomalies arising from the migration of heated ground water in fracture zones (Austin Hot Springs) and along the top of impermeable barriers in altered Oligocene and lower Miocene volcanoclastic rocks (Breitenbush Hot Springs).

This model differs from interpretations that extend the igneous-related heat source from the High Cascades into the Western Cascades and thus narrows the area of prime interest for geothermal exploration. Though not fully tested, the model is compatible with the information presently available.

Acknowledgments

Support for this open-file report comes largely from the U.S. Department of Energy, Grant No. DE-FGO7-84 ID 12526. The authors wish to thank numerous reviewers who patiently gave guidance and advice, particularly B.F. Vogt and G.R. Priest of the Oregon Department of Geology and Mineral Industries and S.E. Ingebritsen of the U.S. Geological Survey.

David R. Sherrod, editor
October 1, 1988

REFERENCES CITED

- Mariner, R.H., Swanson, J.R., Orris, G.J., Presser, T.S., and Evans, W.C., 1980, Chemical and isotopic data for water from thermal springs and wells of Oregon: U.S. Geological Survey Open-File Report 80-737, 50 p.
- Priest, G.R., Woller, N.M., and Ferns, M.L., 1987, Geologic map of the Breitenbush River area, Linn and Marion Counties, Oregon: Oregon Department of Geology and Mineral Industries Geological Map Series GMS-46, scale 1:62,500.

Chapter 1

Geologic setting of the Breitenbush-Austin Hot Springs area, Cascade Range, north-central Oregon

by David R. Sherrod, U.S. Geological Survey, Menlo Park, Calif. 94025,
and Richard M. Conrey, Washington State University, Pullman, Wash. 99164

ABSTRACT

The volcanic and structural history of the Breitenbush-Austin Hot Springs area is critical to understanding the geothermal setting and distribution of shallow and deep heat sources in the area. Oligocene to middle Miocene volcanoclastic strata, the oldest rocks in the area, were broadly folded and moderately sheared prior to deposition of lava flows of latest middle Miocene to Quaternary age. Upper Pleistocene intermediate and silicic volcanic rocks are restricted to the area from Mount Jefferson north to Olallie Butte. Northwest-trending strike- and dip-slip faults with displacement less than 250 m cut middle Miocene and older rocks in the northwestern part of the area, and may control the location of Austin Hot Springs. North- to north-northwest-trending normal faults, which probably formed during a regional episode of extension during early Pliocene time, form a zone with cumulative displacement locally of at least 500-600 m.

The Breitenbush-Austin Hot Springs area is appealing for geothermal exploration because it encompasses high heat flow (locally in excess of 100 mW/m²), hot springs, and Quaternary volcanic rocks. If silicic rocks of late Pleistocene age in the Mount Jefferson area are the heat source for upwelling fluid at Breitenbush and Austin Hot Springs, which the heat-flow data suggest, then exploration would be best served by drilling as close to those rocks as possible. Drilling depths as great as 3 km may be necessary to reach geothermal waters flowing laterally above impermeable strata in the Breitenbush Formation; ground water at shallower depths may be moving chiefly downwards in response to hydrologic recharge along the Cascade Range crest.

INTRODUCTION

This chapter describes the stratigraphic and structural setting of the Breitenbush-Austin Hot Springs area as background for interpreting drill hole results (Conrey and Sherrod, this volume; Bargar, this volume) and heat-flow data (Blackwell and Baker, this volume). The geology is interpreted from published sources (White, 1980a; Hammond and others, 1982; Priest and others, 1987; Walker and Duncan, 1988) and our own reconnaissance and detailed mapping during the last three years (D.R. Sherrod and R.M. Conrey, unpublished data).

In overview, this part of the Cascade Range in northern Oregon can be divided into two broadly defined sequences of rock that are separated by an angular unconformity of as much as 24°. The older sequence, assignable to the Breitenbush Formation and lava of Scorpion Mountain of White (1980a), comprises chiefly volcanoclastic strata and fewer lava flows and intrusions (see Figure 1). In surface exposures, these rocks are altered on a regional scale to smectite and mixed-layer smectite-chlorite clay minerals and to zeolites, the most common of which are clinoptilolite and mordenite (Keith, this volume). The age of this part of the sequence probably ranges from about 18 to 25 Ma in the Breitenbush-Austin Hot Springs area. A 2.5-km-deep drill hole (SUNEDCO 58-28) sited 3 km southeast of Breitenbush Hot Springs was completed in this older sequence of rocks.

The younger sequence comprises chiefly lava flows. It includes the Quaternary and Pliocene rocks of the High Cascades as well as petrographically similar rocks that are as old as about 13 Ma. Basaltic andesite and lesser basalt are predominant and are interlayered with as much as 10

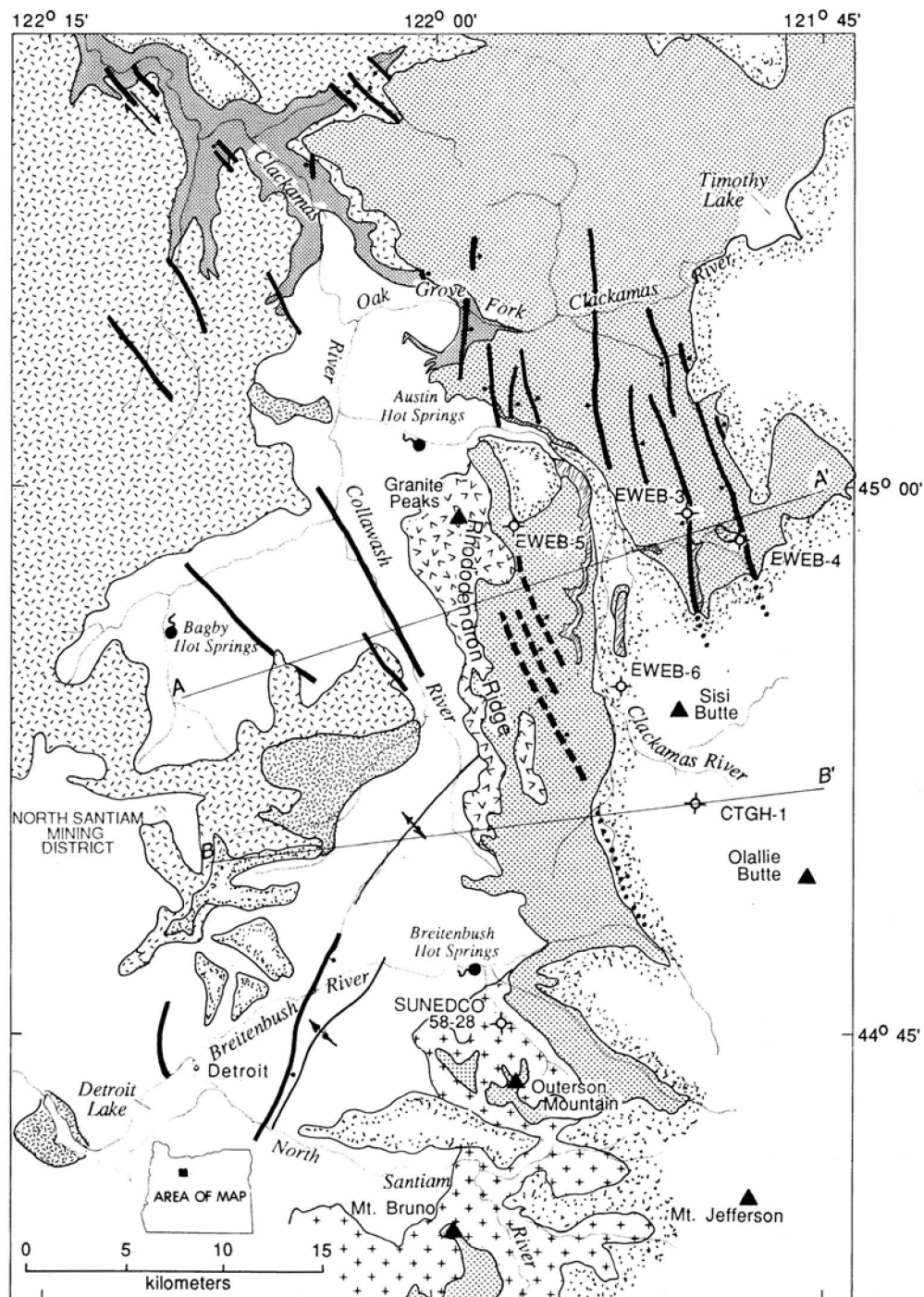
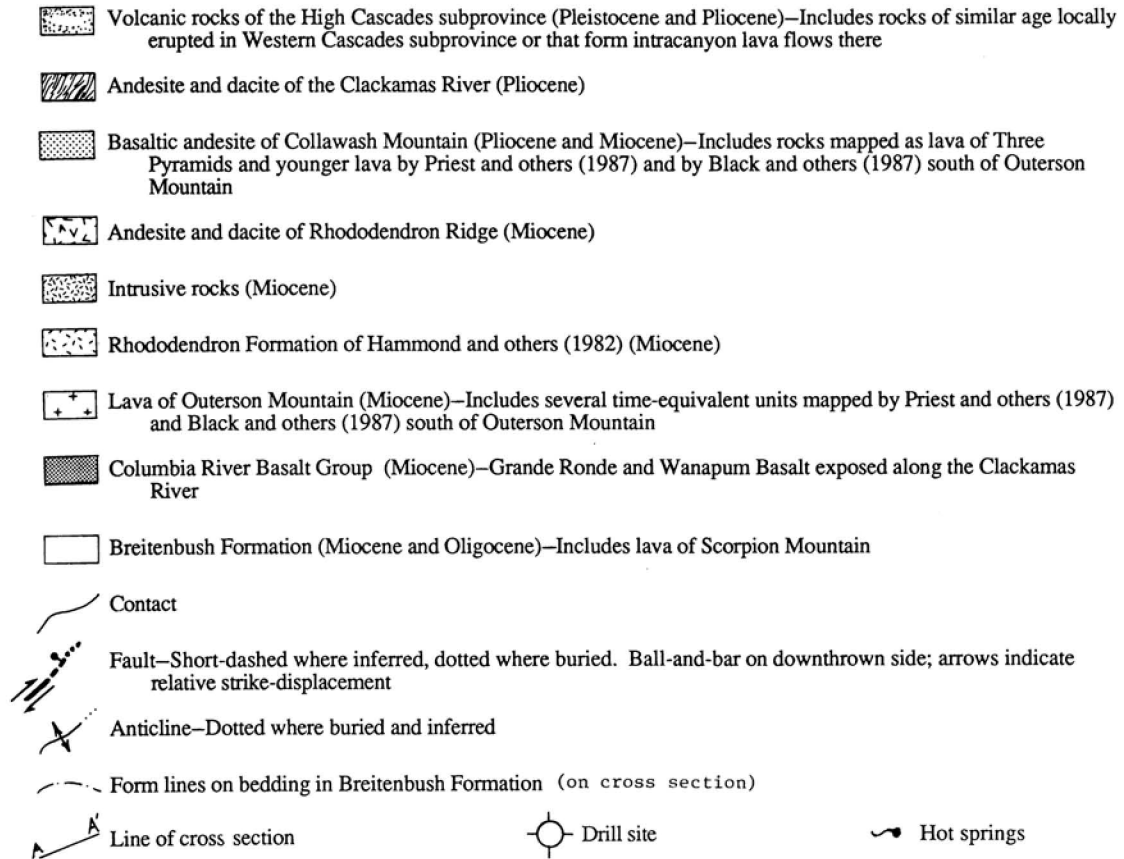


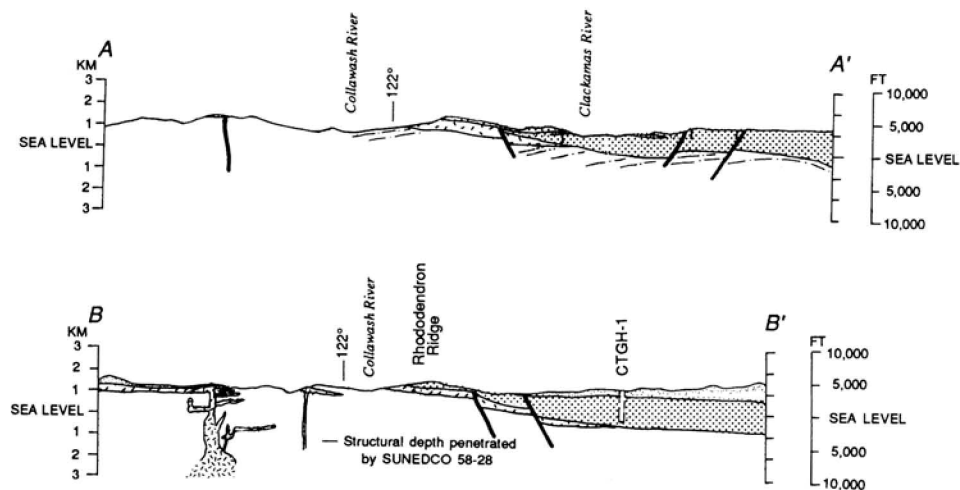
Figure 1. Geologic map and cross sections of the Breitenbush-Austin Hot Springs area, Cascade Range, northern Oregon. Map generalized from White, 1980a; Hammond and others, 1982; Black and others, 1987; Priest and others, 1987; Walker and Duncan, 1988; and D.R. Sherrod and R.M. Conrey, unpublished data, 1987.

Geologic setting of the Breitenbush-Austin Hot Springs area

EXPLANATION



CROSS SECTIONS



Sherrod and Conrey

Table 1. New K-Ar ages from the Breitenbush-Austin Hot Springs area, Cascade Range, northern Oregon

Sample number	Location		Rock type	Material dated	K ₂ O (wt %) ¹	⁴⁰ Ar _{rad} (10 ⁻¹¹ moles/g) ¹	Percent ⁴⁰ Ar _{rad}	Calculated age (Ma) ²
	Latitude (N)	Longitude (W)						
BHS-23	44°45.5'	121°47.6'	Basaltic andesite	Plagioclase concentrate	(0.691)	(0.0649)		0.652±0.045 ³
					0.703	0.0665	19	
					0.681	0.0648	16	
					0.689	0.0611	16	
						0.0670	18	
BHS-20	44°45.7'	121°54.25'	Basaltic andesite	Plagioclase concentrate	(0.812)	(0.1002)		0.857±0.060 ³
					0.817	0.0980	24	
					0.812	0.1041	25	
					0.807	0.0985	24	
BHS-21	44°45.1'	121°54.25'	Andesite	Plagioclase concentrate	(0.880)	(0.1858)		1.47±0.06 ³
					0.889	0.1993	31	
					0.876	0.1887	29	
					0.872	0.1729	27	
					0.881	0.1823	28	
GW-2-85	45°01.7'	121°52.6'	Basaltic andesite	Whole rock	0.916	2.0298	25	1.54±0.74 ⁴
BHS-24	44°46.75'	121°50.3'	Andesite	Whole rock	1.213	0.4043	30	2.31±0.05 ⁴
S5-26	45°09.4'	121°56.45'	Basaltic andesite	Whole rock	(0.848)	(0.3396)		2.78±0.09 ⁵
					0.843	0.3468	33	
					0.843	0.3324	19	
					0.846			
					0.858			
GW-1-85	45°03.9'	121°57.4'	Basaltic andesite	Whole rock	1.012	4.2637	11	2.92±0.13 ⁴
BHS-22	44°46.6'	121°57.0'	Andesite	Whole rock	1.223	1.0528	14	5.97±0.13 ⁴

Notes:

¹For multiple determinations, value in parentheses is arithmetic mean used in age calculation.

²K-Ar ages were calculated using the constants for the radioactive decay and abundance of ⁴⁰K recommended by the International Union of Geological Sciences Subcommittee on Geochronology (Steiger and Jager, 1977). These constants are:
 $\lambda_e = 0.580 \times 10^{-10} \text{ yr}^{-1}$, $\lambda_\beta = 4.962 \times 10^{-10} \text{ yr}^{-1}$, and $^{40}\text{K}/\text{K}_{\text{total}} = 1.167 \times 10^{-4} \text{ mol/mol}$.

³Sample preparation and analytical work were done at University of Arizona, Paul E. Damon and Mohammed Shafiqullah, principal investigators.

⁴Sample preparation and analytical work were done at Oregon State University, Robert A. Duncan, principal investigator.

⁵Sample preparation and analytical work were done at U.S. Geological Survey, Leda Beth G. Pickthorn, principal investigator.

percent andesite. Andesite and dacite are locally extensive, however, forming mappable units. The Quaternary to middle Miocene rocks are generally unaltered except in the lower parts of thick sections exposed in deep canyons. Compared to the older sequence, the younger sequence is more permeable, with fluids moving in interflow breccia and fracture zones. Most of the geothermal gradient holes described in this report have been drilled partly or entirely in lava flows younger than 13 Ma.

POTASSIUM-ARGON (K-Ar) GEOCHRONOLOGY

Absolute ages of volcanic units in the map area have been determined almost entirely by K-Ar geochronology.

Table 1 lists eight new K-Ar ages determined for this report and for regional studies conducted during 1985 (D.R. Sherrod and G.W. Walker, unpublished mapping) from surface exposures throughout the area. Five ages from CTGH-1 drill core are listed in Conrey and Sherrod (this volume).

STRATIGRAPHY

Breitenbush Formation

The oldest rocks in the Breitenbush-Austin Hot Springs area are volcanic and volcanoclastic strata assigned to the Breitenbush Formation of White (1980a) (see Figure 1). Tuff, tuff breccia, and lapilli tuff are predominant and

Geologic setting of the Breitenbush-Austin Hot Springs area

are exposed throughout most of the Breitenbush and Collawash canyons. The volcanoclastic strata are of diverse origin; many originated as pyroclastic flows and lahars. Tuffaceous sandstone and siltstone form a minor part of the series. Lava flows and intrusions occur locally, ranging in composition from basalt to rhyodacite.

The Breitenbush Formation is probably at least 2-3 km thick, on the basis of a 2.5-km-deep drill hole near Breitenbush Hot Springs (SUNEDCO 58-28). The base of the unit is not exposed in the area. The formation presumably extends beneath the younger rocks of the High Cascades and interfingers eastward with similar but more alkalic rocks of the John Day Formation (for example, Robinson and others, 1984).

An absolute age of the Breitenbush Formation is difficult to interpret because some isotopic ages conflict with stratigraphic relations. Priest and others (1987) summarized the geochronologic data and concluded that the Breitenbush Formation exposed in the Breitenbush-Austin area is at least as old as 25 Ma and probably as young as 18 Ma.

The 2.5-km-deep SUNEDCO hole (58-28) was drilled almost entirely in rocks of the Breitenbush Formation (the upper few hundred meters were in middle Miocene lava and volcanoclastic rocks). A thermal aquifer intercepted at 780-800 m is interpreted by Priest and others (1987) as stratal-bound within a quartz-bearing ash-flow tuff near the top of the Breitenbush Formation. We interpret the aquifer as a result of permeability contrasts near the top of the Breitenbush Formation, as will be explained later.

Lava of Scorpion Mountain

The lava of Scorpion Mountain (not shown on Figure 1) was mapped and informally named by White (1980a). Subsequently it was greatly expanded by Priest and others (1987) to encompass a thick accumulation of flows nearly 500 m thick at Scorpion Mountain, 4 km north of Breitenbush Hot Springs. The lava ranges in composition from basalt to dacite (White, 1980a). Several flows in the unit are tholeiitic; that is, their chemical analyses display a trend of iron-enrichment that is characteristic of the tholeiitic rock series, in contrast to the calc-alkaline trends shown by other rock units in the area (White, 1980a).

Scorpion Mountain lava interfingers with the highest strata of the Breitenbush Formation (Priest and others, 1987). White (1980a, b) reported three whole-rock K-Ar ages from rocks he assigned to the Scorpion Mountain: 19.4 ± 0.4 Ma from a lava in the main part of the unit 3 km north of Breitenbush Hot Springs, 24.8 ± 0.3 Ma from an intrusion 4 km southwest of Breitenbush, and 25.5 ± 0.8 Ma from a lava 7 km north of Breitenbush. Priest and others (1987) interpreted the 25.5-Ma rock as an intrusion. In this report, the lava of Scorpion Mountain is assigned an age of early Miocene because it interfingers with the top of the Breitenbush Formation.

Columbia River Basalt Group

Lava of the Columbia River Basalt Group forms a gently northwest-dipping series of flows exposed in the northwest corner of the area (Figure 1). According to Anderson (1978), the exposures there include the Grande Ronde and Wanapum Basalts, which are middle Miocene in age (Swanson and others, 1979).

Rhododendron Formation

The Rhododendron Formation is an assemblage of andesite tuff breccia (chiefly lahars) and fewer lava flows exposed in the area from Mount Hood to Portland (Hodge, 1933; Trimble, 1963). It ranges in age from about 10 to 15 Ma, on the basis of its position between the underlying Columbia River Basalt Group and the overlying Last Chance andesite unit of Priest and others (1982). The formation was extended southward by Hammond and others (1982) to include similar rocks on both flanks of the Breitenbush anticline. We have modified the mapping of Hammond and others (1982) on the east flank of the anticline (Figure 1). The Rhododendron Formation is not discussed further.

Lava of Outerson Mountain

Basaltic andesite and lesser basalt and andesite, which were named the lava of Outerson Mountain by Priest and Woller (1983), form a sequence of flows as much as 550 m thick 6 km south of Breitenbush Hot Springs (Figure 1). These lava flows probably formed several shield volcanoes located in the Outerson Mountain area. They are disconformably overlain by petrographically similar but younger basalt and basaltic andesite in many places. (The lava of Outerson Mountain should not be confused with the Outerson Formation of McBirney and others (1974), a name applied to the younger basalt and basaltic andesite.)

The lava of Outerson Mountain is poorly dated by isotopic methods. It includes rocks with K-Ar ages of 11.52 ± 0.17 Ma and 10.6 ± 1.2 (Sutter, 1978; Hammond and others, 1980; ages reported here are recalculated with new decay constants), and it overlies the Breitenbush Formation, which is as young as 18 Ma. According to Priest and others (1987), the lava of Outerson Mountain fills as much as 400 m of relief on a paleosurface developed on the underlying Breitenbush Formation. Therefore, the lava of Outerson Mountain is probably substantially younger than 18 Ma. We tentatively assign it an age of about 9-13 Ma.

The northern limit of the main part of the lava of Outerson Mountain is controversial, largely because the sequence is commonly overlain by similar but substantially younger rocks. Priest and others (1987) mapped the lava of Outerson Mountain northward along the base of Breitenbush Mountain (east of Breitenbush Hot Springs). However, a recently obtained K-Ar age of 5.97 ± 0.13 Ma (Table 1 and Figure 2) from a sample collected at the base of Breitenbush Mountain indicates that all the lava exposed

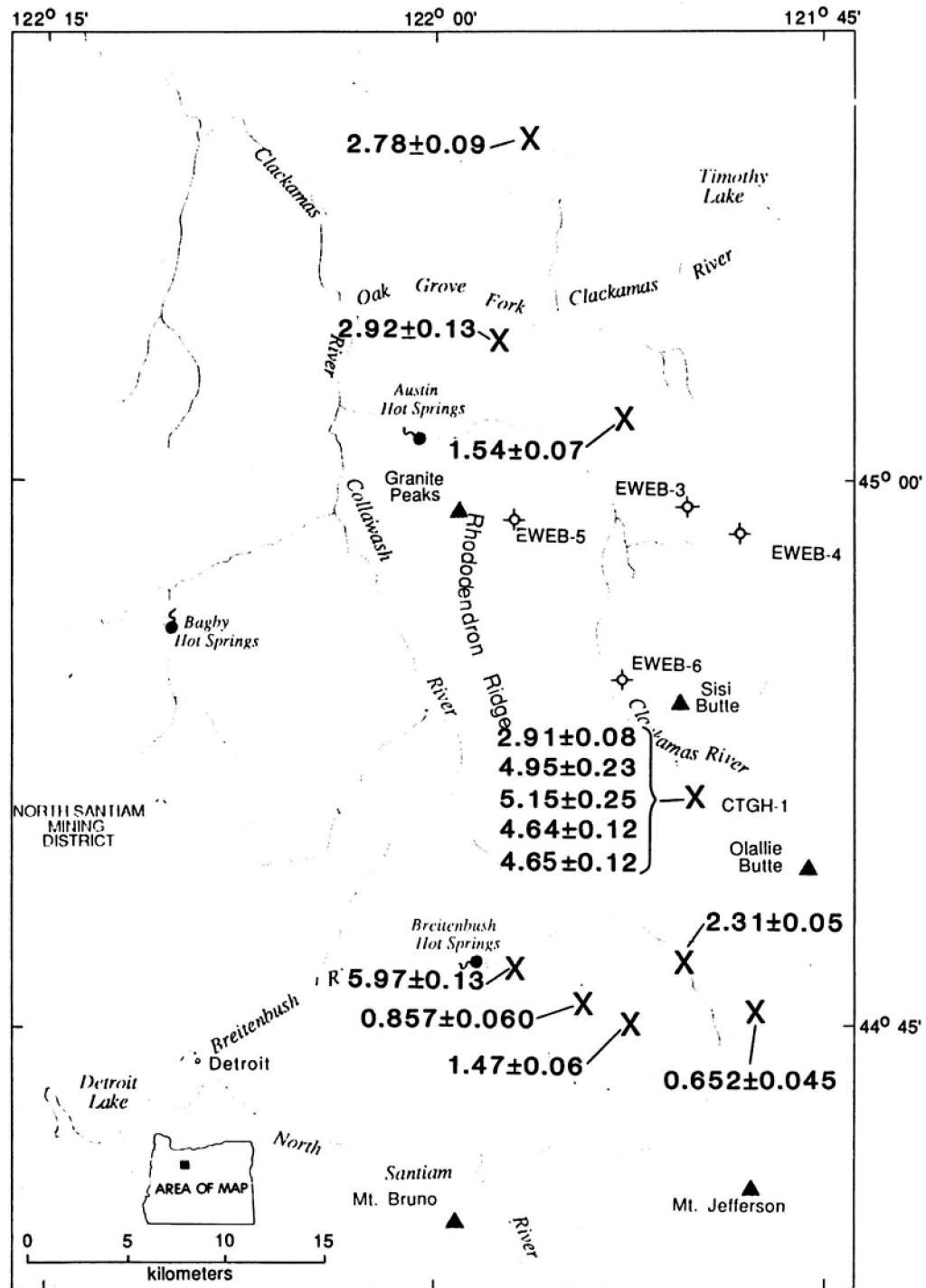


Figure 2. Location map for new K-Ar ages.

Geologic setting of the Breitenbush-Austin Hot Springs area

there could be younger than about 6 Ma. This problem of defining the limit of Outerson Mountain lava can be resolved only by further field and laboratory study.

The 2.5-km-deep SUNEDCO drill hole was sited near the base of the lava of Outerson Mountain. The drill penetrated about 100 m of the lava of Outerson Mountain before passing into volcanoclastic rocks of the Breitenbush Formation.

Andesite and dacite of Rhododendron Ridge

Thick andesite lava flows or domes unconformably overlie the Breitenbush Formation on the west slope of Rhododendron Ridge (Figure 1). They are also locally exposed on the east side of the ridge where erosion has cut through younger basaltic andesite. Hornblende-bearing dacite domes and tuff breccia are predominant in the Granite Peaks area at the north end of the ridge. The andesite and dacite are poorly dated: they are younger than 18 Ma, which is the age assigned to the top of the Breitenbush Formation, and they are older than 6.1 Ma, the oldest age obtained from overlying basalt and basaltic andesite of Collawash Mountain (White, 1980a; Hammond and others, 1980; Priest and others, 1987). These rocks were assigned by White (1980a) to his Elk Lake Formation, a unit that combined all middle and upper(?) Miocene basalt, basaltic andesite, andesite, and dacite. White (1980a) reported two K-Ar ages from rocks we assign to the andesite and dacite of Rhododendron Ridge: 11.8 ± 0.4 Ma (andesite lava flow) and 9.83 ± 0.46 (dacite dike). Provisionally the unit is about 9-13 Ma, coeval with the lava of Outerson Mountain.

Basaltic andesite of Collawash Mountain

Lava flows and breccia of basaltic andesite and lesser basalt and andesite are widespread from the Breitenbush River north beyond Austin Hot Springs (Figure 1). They disconformably overlie the andesite and dacite of Rhododendron Ridge and extend eastward beneath the volcanic rocks of the High Cascades. They also disconformably overlie the lava of Outerson Mountain, but that contact is poorly understood because of the lithologic similarity between the two units.

The basaltic andesite of Collawash Mountain is late Miocene and Pliocene in age on the basis of several K-Ar ages. These ages range from about 6 to 4 Ma in the Collawash Mountain area 2 km northeast of Breitenbush Hot Springs (Priest and others, 1987, and this report). Ages as young as about 2.8 Ma have been obtained from a stratigraphically and petrographically similar sequence of rocks at localities 10 km north and 15 km northeast of Austin Hot Springs (Table 1). We group all these rocks together, recognizing that future mapping, chemistry, and isotopic dating may lead to meaningful subdivisions within the sequence.

Most of the holes drilled by the Eugene Water and Electric Board (EWEB-3, -4, -5, and -6) were completed in the basaltic andesite of Collawash Mountain. The 1,463-m-deep CTGH-1 hole bottomed in 4- to 5-Ma basaltic andesite of this unit. The K-Ar ages from CTGH-1 are not progressively older downsection (Figure 1 and Plate 1) but the 4- to 5-Ma ages, which were obtained from samples purposely collected from the same unit (Conrey and Sherrod, this volume), nearly overlap within the error limits. As noted by Bargar (this volume), CTGH-1 core is generally fresh or only slightly altered, and the secondary mineralogy indicates that temperatures were never much greater than about 100 °C, so the K-Ar geochronology is probably relatively undisturbed.

Andesite and dacite of the Clackamas River

Andesite and dacite lava flows of uncertain age crop out near the Clackamas River north of Sisi Butte (Figure 1). Similar lava flows are exposed in fault escarpments east of the Clackamas River. The lava is overlain by the basaltic andesite of Collawash Mountain in many exposures, and west of the Clackamas River it is underlain by poorly exposed, undated basalt or basaltic andesite that we tentatively include with the basaltic andesite of Collawash Mountain. On the basis of these relationships, the andesite and dacite of the Clackamas River interfingers with the basaltic andesite of Collawash Mountain.

In contrast, White (1980a) interpreted most of the andesite and dacite in the Clackamas River area north of Sisi Butte as eastward extensions of the andesite and dacite exposed at Rhododendron Ridge, to which he assigned a middle or earliest late Miocene age. As an exception, he assigned the easternmost exposure to his next younger unit, probably on the basis of a K-Ar age of 4.04 ± 0.17 Ma. We reinterpret White's mapping for these reasons: (1) the andesite and dacite lava flows near and east of the Clackamas River are all exposed at a similar stratigraphic position; (2) they lack hornblende, which is common in the dacitic part of the unit of andesite and dacite of Rhododendron Ridge; and (3) they have more Rb than the andesite and dacite of Rhododendron Ridge (Conrey and Sherrod, this volume). Tentatively, the andesite and dacite of the Clackamas River is Pliocene in age, on the basis of White's (1980a) K-Ar age of 4.04 Ma.

Volcanic rocks of the High Cascades

The eastern part of the study area includes several youthful-looking volcanoes in the High Cascades subprovince of the Cascade Range. In the northeastern part, these volcanoes are mostly cinder cones and small- to moderate-volume shields that erupted lava flows of basaltic andesite and lesser basalt. In contrast, andesite, dacite, and rhyodacite are predominant in the area between Mount Jefferson and Olallie Butte in the southeastern part, with Mount Jefferson itself being probably the youngest of these

rocks in the area. Thus, the Mount Jefferson area is distinguished compositionally from other parts of the High Cascades where basaltic andesite and basalt form most of the volcanic rocks (for example, Davie, 1980; Smith and others, 1982; Sherrod, 1986; Taylor and others, 1987).

The andesite, dacite, and rhyodacite in the Mount Jefferson area chiefly form thick stubby lava flows and domes; pyroclastic flows and falls are sparse. Ingebritsen and others (1988) suggested that intermediate and silicic rocks in the Mount Jefferson area may be the heat source for thermal waters that rise at Breitenbush Hot Springs. The detailed contouring of heat-flow data by Blackwell and Baker (this volume) corroborates this interpretation of source, because the heat flow at Breitenbush Hot Springs is at the western edge of a narrow heat-flow lobe that extends eastward towards Quaternary silicic rocks in the Mount Jefferson area.

Generally, the volcanic rocks of the High Cascades are thickest near the crest of the range. For example, cross section B-B' (Figure 1) shows a representative thickness of 700-800 m near B' (range crest). The unit is locally thicker near the larger shields and at the Mount Jefferson composite volcano. At its apex, Mount Jefferson accounts for about 1.4 km of the entire unit, which may be as thick as 2.2-2.3 km. North of Sisi Butte, the volume of Quaternary rocks diminishes greatly, and the Cascade Range crest is built up by chiefly reversely polarized early Quaternary basaltic andesite shield volcanoes and Pliocene andesite and dacite lava flows and domes (D.R. Sherrod, unpublished data). In the study area, the volcanic rocks of the High Cascades disconformably to conformably overlie the basalt and basaltic andesite of Collawash Mountain.

The volcanic rocks of the High Cascades in the Breitenbush-Austin Hot Springs area are probably almost entirely of Pleistocene age, but some latest Pliocene lava is included in the area outlined on Figure 1. The oldest rocks assigned to the unit have K-Ar ages of about 2.31 Ma (Table 1). The youngest rocks, which are undated, have been glaciated and therefore are at least 11,000 years old (for example, Scott, 1977). Till and outwash deposits abound at the middle elevations (700-1500 m) of the High Cascades.

The youngest part of the Mount Jefferson composite volcano is presumably about $76,000 \pm 34,000$ yrs, on the basis of preliminary chemical correlation of Mount Jefferson tephra with an ash bed found near Arco, Idaho (A.M. Sarna-Wojcicki and N.D. Naeser, personal communications, 1988). At the Idaho site, the tentative Mount Jefferson ash closely underlies a Yellowstone-derived ash that yielded the 76,000-yr fission-track age (Pierce, 1985). Yellowstone plateau-forming rhyolites yield K-Ar ages ranging from 150,000 to 70,000 yrs (Christiansen, 1982), so despite the large analytical error from the fission-track-dated ash, the underlying Jefferson ash is probably not younger than about 76,000-70,000 yrs.

Because of young age, Quaternary volcanic rocks exposed in the High Cascades are significant for igneous-related geothermal resources. However, the volume of late Miocene and Pliocene volcanic rocks in the map area may be 3-4 times greater than that of latest Pliocene and Quaternary volcanic rocks, and as much as 50 percent of the late Miocene and Pliocene volume erupted between 6 and 4.5 Ma, a conclusion based on the thickness and distribution of rocks shown on the maps and cross sections of Figure 1 and Plate 1. The eruptions from 6 to 4.5 Ma may have coincided with regional extension (see discussion in this paper, *Structure, north- and north-northwest-trending faults*). In terms of rate, late Miocene and Pliocene volcanoes (6-2.5(?) Ma) in the Breitenbush-Austin Hot Springs area may have erupted 2-3 times more magma per unit time than latest Pliocene and Quaternary volcanoes (<2.5 Ma).

Summary

In summary, an angular unconformity separates lower Miocene and older rocks from middle Miocene to Quaternary rocks in the study area. The older sequence of rocks comprises chiefly volcanoclastic strata that have been altered to low-grade secondary minerals on a regional scale. In contrast, the younger sequence of middle Miocene to Quaternary rocks comprises chiefly lava flows that are generally fresh or only slightly altered. The youngest intermediate and silicic volcanic rocks in the Breitenbush-Austin Hot Springs area were erupted near Mount Jefferson as recently as about 76,000 yrs ago.

STRUCTURE

Folds

The Breitenbush Formation and the lava of Scorpion Mountain have been deformed into a broad arch that includes several lesser folds. However, the precise location and orientation of major and minor fold axes remains poorly constrained (for example, compare maps of Thayer, 1936, 1939; Peck and others, 1964; Hammond and others, 1980, 1982; White, 1980a, b; Priest and others, 1987; Walker and Duncan, 1988). The Breitenbush anticline is the best-known of these fold axes: a northeast-trending, northwest-verging asymmetric fold in which the northwest limb dips up to 60° and the southeast limb dips 20° (White, 1980b). For convenience of discussion, we follow the custom of applying the name "*Breitenbush anticline*" to the entire arch. Fold axes in Figure 1 are from the map by Priest and others (1987), modified somewhat to reflect our reconnaissance mapping in the Collawash River.

Folding probably began after about 18 Ma, because strata in the Breitenbush Formation are approximately concordant. However, the Breitenbush Formation in much of the Breitenbush-Austin Hot Springs area is insufficiently mapped and poorly exposed, so there remains the

Geologic setting of the Breitenbush-Austin Hot Springs area

possibility that folding may have begun sometime before about 18 Ma. The episode was largely ended by about 12 Ma, because the folded Breitenbush Formation was beveled by erosion prior to the deposition of the andesite and dacite of Rhododendron Ridge and the lava of Outerson Mountain. Subsequent folding, if any, has been minor.

The Breitenbush anticline projects beneath the volcanic rocks of the High Cascades and into an east-trending

anticline exposed 15 km east of the Cascade Range crest in the southern Laughlin Hills and Mutton Mountains (Waters, 1968; Swanson and others, 1981; Bela, 1982). Figure 3 is a structure-contour diagram drawn on the top of the Columbia River Basalt Group (CRBG) or older rocks. This horizon in the Breitenbush-Austin Hot Springs area corresponds to the top of the Breitenbush Formation in most places. The contours show the minimum relief because of

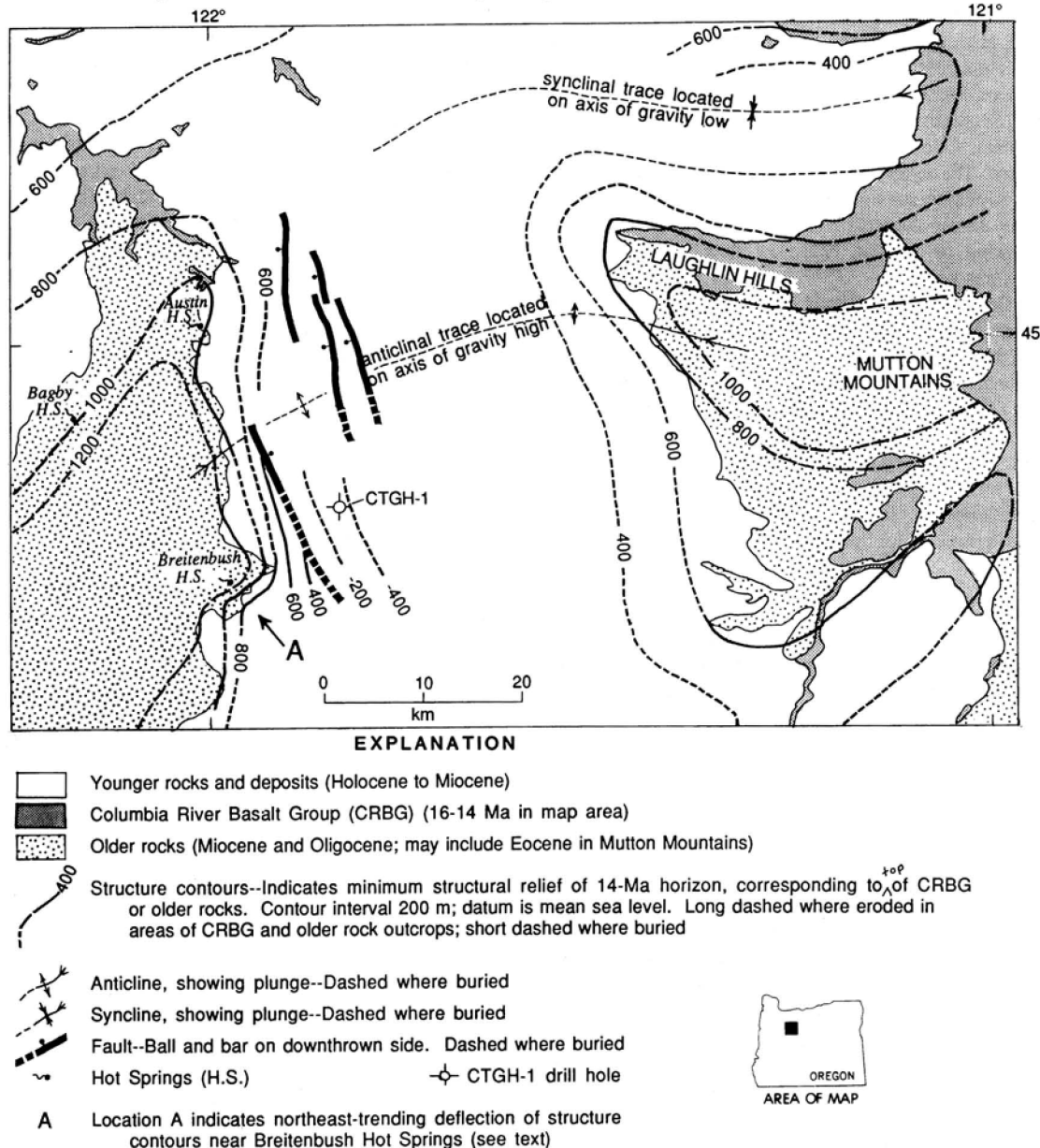


Figure 3. Structure-contour map, north-central Cascade Range, Oregon. Contours are drawn on top of Columbia River Basalt Group or older volcanic rocks and generally correspond to surface about 14 Ma. Location A indicates northeast-trending deflection of structure contours near Breitenbush Hot Springs.

subsequent erosion of CRBG and older rocks. Also, the CTGH-1 drill hole never penetrated below upper Miocene rocks. Its base is about 300 m below sea level.

The structure-contour diagram is highly interpretive because there are virtually no data in the area buried by rocks younger than CRBG. The buried traces of the anticline and syncline are drawn to coincide with gravity anomalies (high and low, respectively) on the Bouguer gravity anomaly map (Couch and others, 1981). More secure, however, is the short northeast-trending deflection of structure contours near Breitenbush Hot Springs (location A on Figure 3). The deflection could result from a localized stratigraphic buildup of the lava of Scorpion Mountain, which is mapped by Priest and others (1987) in that area. The deflection may indicate structure as well, for it roughly coincides with the northern edge of the heat-flow lobe in the Breitenbush Hot Springs area, as defined by contouring of detailed heat-flow data (Blackwell and Baker, this volume).

Breitenbush and Austin Hot Springs are located near the eastern limit of Breitenbush Formation. This location could be controlled partly by the permeability contrast between clay- and zeolite-altered Oligocene volcanoclastic rocks (lower parts of Breitenbush Formation; Keith, this volume) and overlying middle Miocene to Quaternary lava flows. Thus, the depth to the relatively impermeable layers in the Breitenbush Formation may be of critical importance to geothermal exploration in the eastern part of the Breitenbush-Austin Hot Springs area.

Faults

On outcrop scale, numerous shears are the most conspicuous structural feature exposed in strata of the Breitenbush Formation and the lava of Scorpion Mountain. Fewer faults cut the post-early Miocene strata. Slickensides occur in all orientations on the fracture surfaces. Locally the shear fractures form zones that range in width from meters to tens of meters. Nevertheless, few of these faults or fault zones offset the map units by more than 100 meters.

Northwest-trending faults and lineaments of the Clackamas River: Several northwest-trending vertical or near-vertical faults were delineated by Anderson (1978) along the Clackamas River northwest of Austin Hot Springs (Figure 1). He measured displacements ranging up to 200 m and showed that some faults have chiefly strike-slip displacement whereas others have chiefly dip-slip displacement, on the basis of slickensides and offset strata in the Columbia River Basalt Group. The faulting described by Anderson (1978) in the Clackamas River northwest of Austin Hot Springs is younger than middle Miocene, which is the age of that part of the Columbia River Basalt Group exposed there, and older than early Quaternary or Pliocene intracanyon lava in the Clackamas River drainage, which remains undeformed.

nary or Pliocene intracanyon lava in the Clackamas River drainage, which remains undeformed.

Hammond and others (1982) showed many more faults than Anderson in the same map area: they defined a zone of northwest-trending faults about 10 km wide that extends from Rhododendron Ridge northwest along the south side of the Clackamas River. Those authors acknowledge, however, that few of their faults juxtapose rock units. Indeed, many of their faults are perhaps best considered lineaments along a fracture zone of uncertain origin. This zone was informally named the Clackamas River fault zone by Priest (1982, his Figure 1).

As pointed out by Hammond and others (1982), the zone of northwest-trending lineaments and faults along the Clackamas River is aligned with the Portland Hills, a faulted, northwest-trending asymmetrical anticline (Beeson and others, 1985). Perhaps significantly, two stream segments east of the Cascade Range are also aligned with this trend: a 20-km stretch of the Metolius River and a 10-km stretch of the Crooked River (Figure 4). These alignments suggest that some ancient structure has subsequently controlled the orientation and locus of some faulting or fracturing in the Cascade Range. If the separate lineaments mark a continuous structure, the structure passes geographically beneath Olallie and Sisi Buttes in the High Cascades part of the Breitenbush-Austin Hot Springs area.

Such a structural zone, if marked by fracture permeability at depth, could exert a significant control on the lateral migration of hot water and might explain the location of Austin Hot Springs. Austin lies 35 km northwest of the late Quaternary silicic rocks of the Mount Jefferson area, which are the closest candidates for an igneous-related heat source. In contrast, volcanic rocks in the High Cascades directly east of Austin Hot Springs are chiefly lava flows of reversely polarized basaltic andesite that were erupted from small- to intermediate-volume shield volcanoes more than 0.73 Ma. That magmatism probably didn't carry enough heat into the upper crust to create a significant, long-lived thermal anomaly.

North- to north-northwest-trending faults east of Rhododendron Ridge: The only structures exposed east of Rhododendron Ridge are north- to north-northwest-trending normal faults. The faults form gentle to steep escarpments in the upper Miocene and Pliocene basaltic andesite of Collawash Mountain north and west of Sisi Butte. Dip separation of as much as 250-300 m is inferred from the escarpment heights. These estimates are probably minimum values, however, because erosion has reduced the escarpment height. Also, younger lava flows and glaciogenic deposits have locally buried the downthrown blocks, further reducing escarpment height. Cumulative displacement across these faults may locally exceed 500-600 m (for example, Plate 1).

Geologic setting of the Breitenbush-Austin Hot Springs area

The age of the north- and north-northwest-trending faults is imprecisely known. The faults are along or near the boundary between the High Cascades and Western Cascades, the two physiographic subprovinces of the Cascade Range in Oregon (Callaghan and Buddington, 1938). Regionally, a major episode of faulting and local graben formation occurred along this boundary in late Miocene or early Pliocene time (for example, Smith and Taylor, 1983; Sherrod, 1986), and probably the north- and north-northwest-trending faults in the Breitenbush-Austin Hot Springs area are part of the same event. Clearly some of the faulting is early Pliocene or younger because lower Pliocene strata are offset by the faults.

Lineaments with the same north to north-northwest trend are defined by stream drainages in the High Cascades, suggesting some very minor movement on poorly exposed faults during Quaternary time. The lineaments lose expression in rocks younger than about 0.73 Ma.

commonplace in rocks older than middle Miocene. Fewer faults cut middle Miocene and younger rocks. Statistically, too few faults are mapped to define preferred trends in rocks younger than middle Miocene, but northwest and northeast trends might be expected if reactivation of older structures is important. A northwest-trending zone of faults along the Clackamas River northwest of Austin Hot Springs presumably marks a reactivated ancient zone of uncertain origin. Offset of middle Miocene units along this zone is as great as 250 m and includes both strike- and dip-slip components as interpreted from slickensides and displaced contacts. This zone is buried by late Miocene and younger rocks in the map area. Several north- to north-northwest-trending faults cut Pliocene and younger rocks in the area east of Austin and Breitenbush Hot Springs. Individually these faults have dip-separation of about 300 m or less but locally form a zone near Cub Creek with cumulative displacement of at least 500-600 m (Plate 1).

Summary

In summary, early Miocene and older rocks were folded along northeast-trending fold axes in either latest early Miocene or middle Miocene time. Middle Miocene and younger rocks in the map area are unfolded. Northeast- and northwest-trending faults with small displacement are

CONCLUSIONS

The Breitenbush-Austin Hot Springs area is appealing for geothermal exploration because it encompasses high heat flow (locally in excess of 100 mW/m²), hot

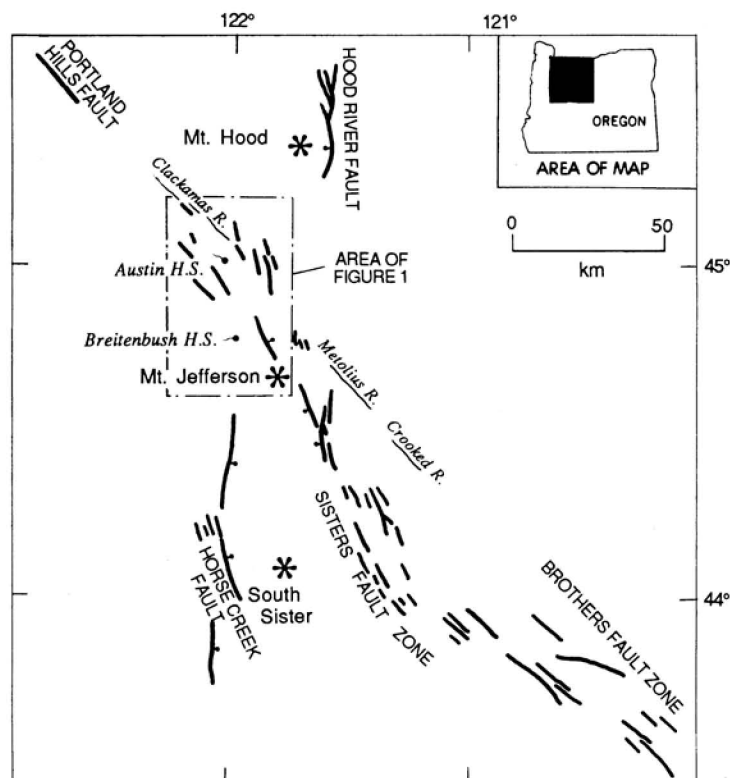


Figure 4. Map showing faults (bold) and lineaments (light) in Cascade Range and adjacent areas, northern Oregon.

springs, and late Quaternary intermediate and silicic volcanic rocks. The heat flow, presumably igneous-related, is a product of Quaternary magmatism along and beneath the crest of the Cascade Range. The heat supplied to the upper crust is not directly related to the distribution of volcanic rocks but instead depends on the relative proportion of intrusive and extrusive rocks, which remains unknown. Because of greater viscosity, however, magmas intermediate to silicic in composition are more likely to form shallow crustal reservoirs and supply more heat to the upper crust than an equivalent amount of mafic magma (Smith and Shaw, 1975).

The contouring of heat-flow data by Blackwell and Baker (this volume) and of 100-°C isotherms by Ingebritsen and others (1988) strongly suggests a connection between upwelling hot water at Breitenbush Hot Springs and late Quaternary silicic volcanic rocks in the Mount Jefferson area in the southeast part of the study area. The connection between Austin Hot Springs and late Quaternary volcanic centers is less clear. Austin Hot Springs are located along a fracture zone that probably extends beneath the High Cascades just north of the Mount Jefferson area (Figure 4). Conceivably the Austin circulation is controlled by that structural zone. The location of both Austin and Breitenbush Hot Springs probably results in part from permeability barriers owing to pronouncedly greater clay- and zeolite-alteration in the chiefly volcanoclastic Breitenbush Formation, compared to overlying lava flows.

If the late Quaternary silicic rocks in the Mount Jefferson area are the heat source for upwelling fluid at Breitenbush and Austin Hot Springs, then exploration would best be served by drilling as close to those rocks as possible. Drilling depths as great as 3 km may be necessary to reach water flowing laterally above impermeable strata in the Breitenbush Formation; ground water at shallower depths may be moving chiefly downwards in response to hydrologic recharge along the Cascade Range crest.

ACKNOWLEDGMENTS

The authors wish to thank G.L. Black (Oregon Department of Geology and Mineral Industries) and G.W. Walker (U.S. Geological Survey) for sincere and careful reviews. N.S. MacLeod (U.S. Geological Survey) first pointed out to Sherrod the remarkable alignment of the Brothers fault zone with segments of the Crooked and Metolius Rivers. Financial support for Sherrod was made possible by subcontracted funds from U.S. Department of Energy Grant No. DE-FG07-84 ID 12526 to the Oregon Department of Geology and Mineral Industries, and matching funds from the U.S. Geological Survey's Office of Mineral Resources.

REFERENCES CITED

- Anderson, J.L., 1978, The structure and stratigraphy of the Columbia River Basalt in the Clackamas River drainage: Portland, Oreg., Portland State University master's thesis, 136 p.
- Bargar, K.E., 1988 (this volume), Secondary mineralogy of core from geothermal drill hole CTGH-1, Cascade Range, Oregon, *in* Sherrod, D.R., ed., Geology and geothermal resources of the Breitenbush-Austin Hot Springs area, Clackamas and Marion Counties, Oregon: Oregon Department of Geology and Mineral Industries Open-File Report O-88-5, in press.
- Beeson, M.H., Fecht, K.R., Reidel, S.P., and Tolan, T.L., 1985, Regional correlations within the Frenchman Springs member of the Columbia River Basalt Group: new insights into the middle Miocene tectonics of northwest Oregon: Oregon Geology, v. 47, no. 8, p. 87-96.
- Bela, J.L., 1982, Geologic and neotectonic evaluation of north-central Oregon: The Dalles 1°x2° quadrangle: Oregon Department of Geology and Mineral Industries Geological Map Series GMS-27, scale 1:250,000.
- Black, G.L., Woller, N.M., and Ferns, M.L., 1987, Geologic map of the Crescent Mountain area, Linn County, Oregon: Oregon Department of Geology and Mineral Industries Geological Map Series GMS-47, scale 1:62,500.
- Blackwell, D.D., and Baker, S. L., 1988 (this volume), Thermal analysis of the Austin and Breitenbush geothermal systems, Western Cascades, Oregon, *in* Sherrod, D.R., ed., Geology and geothermal resources of the Breitenbush-Austin Hot Springs area, Clackamas and Marion Counties, Oregon: Oregon Department of Geology and Mineral Industries Open-File Report O-88-5, in press.
- Callaghan, Eugene, and Buddington, A.F., 1938, Metalliferous mineral deposits of the Cascade Range in Oregon: U.S. Geological Survey Bulletin 893, 141 p.
- Christiansen, R.L., 1982, Late Cenozoic volcanism of the Island Park area, eastern Idaho, *in* Bonnichsen, Bill, and Breckenridge, R.M., eds., Cenozoic Geology of Idaho: Idaho Bureau of Mines and Geology Bulletin 26, p. 345-368.
- Conrey, R.M., and Sherrod, D.R., 1988 (this volume), Stratigraphy of drill holes and geochemistry of surface rocks, Breitenbush Hot Springs 15-minute quadrangle, Cascade Range, Oregon, *in* Sherrod, D.R., ed., Geology and geothermal resources of the Breitenbush-Austin Hot Springs area, Clackamas and Marion Counties, Oregon: Oregon Department of Geology and Mineral Industries Open-File Report O-88-5, in press.

Geologic setting of the Breitenbush-Austin Hot Springs area

- Couch, R.W., Pitts, G.S., Braman, D.E., and Gemperle, M., 1981, Free-air gravity anomaly map and complete Bouguer gravity anomaly map, Cascade Mountain Range, northern Oregon: Oregon Department of Geology and Mineral Industries Geological Map Series GMS-15, scale 1:250,000.
- Davie, E.I., 1980, The geology and petrology of Three Fingered Jack, a High Cascade volcano in central Oregon: Eugene, Oreg., University of Oregon master's thesis, 138 p.
- Hammond, P.E., Anderson, J.L., and Manning, K.J., 1980, Guide to the geology of the upper Clackamas and North Santiam Rivers area, northern Oregon Cascade Range, in Oles, K.F., Johnson, J.G., Niem, A.R., and Niem, W.A., eds., Geologic field trips in western Oregon and southwestern Washington: Oregon Department of Geology and Mineral Industries Bulletin 101, p. 133-167.
- Hammond, P.E., Geyer, K.M., and Anderson, J.L., 1982, Preliminary geologic map and cross-sections of the upper Clackamas and North Santiam Rivers area, northern Oregon Cascade Range: Portland, Oreg., Portland State University Department of Earth Sciences, scale 1:62,500.
- Hodge, E.T., 1933, Age of Columbia River and lower canyon [abs.]: Geological Society of America Bulletin, v. 44, pt. 1, p. 156-157.
- Ingebritsen, S.E., Mariner, R.H., and Sherrod, D.R., 1988, Heat flow and hydrothermal circulation in the Cascade Range, north-central Oregon [abs.]: EOS, v. 69, no. 16, p. 471.
- Keith, T.E.C., 1988 (this volume), Regional patterns of hydrothermal alteration in the Breitenbush-Austin Hot Springs area, Cascade Range, Oregon, in Sherrod, D.R., ed., Geology and geothermal resources of the Breitenbush-Austin Hot Springs area, Clackamas and Marion Counties, Oregon: Oregon Department of Geology and Mineral Industries Open-File Report O-88-5, in press.
- McBirney, A.R., Sutter, J.F., Naslund, H.R., Sutton, K.G., and White, C.M., 1974, Episodic volcanism in the central Oregon Cascade Range: Geology, v. 2, p. 585-589.
- Peck, D.L., Griggs, A.B., Schlicker, H.G., Wells, F.G., and Dole, H.M., 1964, Geology of the central and northern parts of the Western Cascade Range in Oregon: U.S. Geological Survey Professional Paper 449, 56 p.
- Pierce, K.L., 1985, Quaternary history of faulting on the Arco segment of the Lost River fault, central Idaho, in Stein, R.S., and Bucknam, R.C., eds., Proceedings of Workshop XXVIII on the Borah Peak, Idaho, Earthquake: U.S. Geological Survey Open-File Report 85-290-A, p. 195-206.
- Priest, G.R., 1982, Overview of the geology and geothermal resources of the Mount Hood area, Oregon, in Priest, G.R., and Vogt, B.F., eds., Geology and geothermal resources of the Mount Hood area, Oregon: Oregon Department of Geology and Mineral Industries Special Paper 14, p. 6-15.
- Priest, G.R., and Woller, N.M., 1983, Preliminary geology of the Outerson Mountain-Devils Creek area, Marion County, Oregon, in Priest, G.R., and Vogt, B.F., eds., Geology and geothermal resources of the central Oregon Cascade Range: Oregon Department of Geology and Mineral Industries Special Paper 15, p. 29-38.
- Priest, G.R., Woller, N.M., and Ferns, M.L., 1987, Geologic map of the Breitenbush River area, Linn and Marion Counties, Oregon: Oregon Department of Geology and Mineral Industries Geological Map Series GMS-46, scale 1:62,500.
- Robinson P.T., Brem, G.F., and McKee, E.H., 1984, John Day Formation of Oregon: a distal record of early Cascade volcanism: Geology, v. 12, no. 4, p. 229-232.
- Scott, W.E., 1977, Quaternary glaciation and volcanism, Metolius River area, Oregon: Geological Society of America Bulletin, v. 88, p. 113-124.
- Sherrod, D.R., 1986, Geology, petrology, and volcanic history of a portion of the Cascade Range between latitudes 43°-44° N, central Oregon, U.S.A.: Santa Barbara, University of California doctoral dissertation, 320 p.
- Smith, G.A., and Taylor, E.M., 1983, The central Oregon High Cascade graben: What? Where? When?: Geothermal Resources Council Transactions, v. 7, p. 275-279.
- Smith, J.G., Page, N.J., Johnson, M.G., Moring, B.C., and Gray, Floyd, 1982, Preliminary geologic map of the Medford 1°x2° quadrangle, Oregon and California: U.S. Geological Survey Open-File Report 82-955, scale 1:250,000.
- Smith, R.L., and Shaw, H.R., 1975, Igneous-related geothermal systems, in White, D.E., and Williams, D.L., eds., Assessment of Geothermal Resources of the United States—1975: U.S. Geological Survey Circular 726, p. 58-83.
- Steiger, R.H., and Jager, E., 1977, Subcommission on geochronology: Convention on the use of decay constants in geo- and cosmochronology: Earth and Planetary Science Letters, v. 36, p. 359-362.
- Sutter, J.F., 1978, K/Ar ages of Cenozoic volcanic rocks from the Oregon Cascades west of 121° 30': Isochron/ West, no. 21, p. 15-21.
- Swanson, D.A., Wright, T.L., Hooper, P.R., and Bentley, R.D., 1979, Revisions in stratigraphic nomenclature of the Columbia River Basalt Group: U.S. Geological Survey Bulletin 1457-G, 59 p.
- Swanson, D.A., Anderson, J.L., Camp, V.E., Hooper, P.R., Taubeneck, W.H., and Wright, T.L., 1981, Reconnaissance geologic map of the Columbia River Basalt Group, northern Oregon and western Idaho: U.S.

Sherrod and Conrey

- Geological Survey Open-File Report 81-797, scale 1:250,000.
- Taylor, E.M., MacLeod, N.S., Sherrod, D.R., and Walker, G.W., 1987, Geologic map of the Three Sisters Wilderness, Deschutes, Lane, and Linn Counties, Oregon: U.S. Geological Survey Miscellaneous Field Studies Map MF-1952, scale 1:63,360.
- Thayer, T.P., 1936, Structure of the North Santiam River section of the Cascade Mountains in Oregon: *Journal of Geology*, v. 44, p. 701-716.
- Thayer, T.P., 1939, Geology of the Salem Hills and the North Santiam River basin, Oregon: Oregon Department of Geology and Mineral Industries Bulletin 15, 40 p.
- Trimble, D.E., 1963, Geology of Portland, Oregon, and adjacent areas: U.S. Geological Survey Bulletin 1119, 119 p.
- Walker, G.W., and Duncan, R.A., 1988, Geologic map of the Salem 1°x2° sheet, Oregon: U.S. Geological Survey Miscellaneous Investigations Map I-1893, scale 1:250,000.
- Waters, A.C., 1968, Reconnaissance geologic map of the Dufur quadrangle, Hood River, Sherman, and Wasco Counties, Oregon: U.S. Geological Survey Miscellaneous Geologic Investigations Map I-556, scale 1:125,000.
- White, C.M., 1980a, Geology of the Breitenbush Hot Springs quadrangle, Oregon: Oregon Department of Geology and Mineral Industries Special Paper 9, 26 p.
- 1980b, Geology and geochemistry of volcanic rocks in the Detroit area, Western Cascade Range, Oregon: Eugene, Oreg., University of Oregon doctoral dissertation, 177 p.

Chapter 2

Stratigraphy of drill holes and geochemistry of surface rocks, Breitenbush Hot Springs 15-minute quadrangle, Cascade Range, Oregon

by Richard M. Conrey, Washington State University, Pullman, Wash. 99164,
and David R. Sherrod, U.S. Geological Survey, Menlo Park, Calif. 94025

ABSTRACT

Core hole CTGH-1 and rotary-drilled holes EWEB-3, -4, -5, and -6 in the High Cascades part of the Breitenbush Hot Springs 15-minute quadrangle penetrated upper Miocene and younger basaltic andesite lava flows and breccia and fewer basalt and andesite flows. Locally, thick dacite and rhyodacite domes, flows, and pyroclastic rocks were penetrated in three holes. Five new K-Ar ages on core from CTGH-1, a 1,463-m-deep hole drilled in 1986, range from about 2.91 Ma at 596-m depth to 4-5 Ma at depths of 961 and 1,445 m. Forty chemical analyses from CTGH-1 core and eight analyses from EWEB cuttings substantiate the lithologic logs presented here for these holes. Two analyses of cuttings from SUNEDCO 58-28 were obtained.

Correlations between drilled strata and rocks exposed at the surface are supported by chemical comparisons. Chemically, the surface rocks define four major sequences, described here as two pairs of titanium- and rubidium-rich units succeeded by titanium- and rubidium-poor units. Thus, it may be possible to discriminate rocks of different age sequences when comparing andesite, dacite, and rhyodacite. The method fails for basaltic andesite and basalt of different ages, which can't be distinguished by titanium and rubidium.

INTRODUCTION

This chapter describes the stratigraphic, geochronologic, and geochemical findings of core from CTGH-1 and

cuttings from EWEB-3, -4, -5, -6, and SUNEDCO 58-28. Five new K-Ar ages and 40 chemical X-ray fluorescence (XRF) analyses were obtained from CTGH-1 core; a total of ten sets of cuttings from the others holes were chemically analyzed. Also, 143 samples from surface exposures were analyzed to define the chemical characteristics of lower Miocene to Quaternary rock units exposed in and near the Breitenbush Hot Springs 15-minute quadrangle.

DRILL-HOLE STRATIGRAPHY AND GEOCHEMISTRY

EWEB holes

Four holes were rotary-drilled in the Breitenbush-Austin Hot Springs area in the summer of 1979 as part of a geothermal-gradient drilling program. The program was funded chiefly by the U.S. Department of Energy, with the Eugene Water and Electric Board (EWEB) as principal contractor. The drilling results were summarized by Youngquist (1980). Cuttings collected at 3-m intervals were used to interpret lithology and alteration of the drilled stratigraphic sections, using microscopic examination and X-ray diffraction methods (Keith and Boden, 1980a, b; 1981a, b). No chemical analyses were available prior to our study.

The holes were drilled mainly in basalt and basaltic andesite lava that ranges in age from late Miocene or Pliocene to Pleistocene (Sherrod and Conrey, this volume). Andesite and dacite form locally thick accumulations, and one new chemical analysis indicates rhyodacite in the sub-

surface. The correlation of units for the three shallow EWEB holes (less than 300 m deep) is fairly secure, because erosion has cut sufficiently deep in nearby valleys that mapped units can be projected with confidence into the subsurface. The correlations are more tenuous, however, for the 460-m-deep EWEB-6 hole located in the Clackamas River valley west of Sisi Butte. There are no isotopic ages from EWEB cuttings.

We selected eight sets of cuttings for chemical analysis (Table 1) because they were relatively homogeneous samples. These samples are chiefly from thick domes or flows of andesite or dacite. In contrast, cuttings from most sequences of thin flows (2-10 m) and breccia are commonly inhomogeneous and too varied to warrant chemical analysis. The chemical analyses are used as a tool of tentative stratigraphic correlation.

EWEB-3 (Poop Creek, total depth 293 m): This hole penetrated 250 m of basaltic andesite and minor basalt and andesite, then 43 m of an underlying rhyodacite (Figure 1). The basaltic andesite, basalt, and andesite are correlated with upper Miocene and Pliocene lava flows exposed at the surface in the area of the drill hole. The rhyodacite, which contains about 72 percent SiO_2 (analysis POOP-940; Table 1), is correlated with other upper Miocene or Pliocene silicic rocks in the area on the basis of its elevated TiO_2 (0.30 percent) and Rb (129 ppm).

EWEB-4 (Cinder cone, total depth 354 m): This hole penetrated mainly basaltic andesite and minor basalt and andesite (Figure 1). The cuttings show no abrupt changes in alteration, so presumably no major contacts were crossed (Keith and Boden, 1980b). The lavas in EWEB-4 are tentatively correlated with upper Miocene and Pliocene rocks exposed near the drill hole. Two analyses from EWEB-4 cuttings, an andesite and a basalt, are listed in Table 1.

EWEB-5 (Tarzan Springs, total depth 223 m): This hole penetrated only basaltic andesite and minor basalt (Figure 1), despite its proximity to dacite exposed at Granite Peaks (part of the andesite and dacite of Rhododendron Ridge; Sherrod and Conrey, this volume). The basaltic andesite and basalt are correlated with the upper Miocene and Pliocene basaltic andesite of Collawash Mountain (Sherrod and Conrey, this volume). This unit laps on or is faulted against the Granite Peaks dacite 1 km west of the EWEB-5 site; the contact there is steep but not exposed. The thickness of EWEB-5 basalt and basaltic andesite indicates only that the contact separating Granite Peaks dacite from the younger mafic lavas dips at least 13° eastward from Granite Peaks to the Tarzan Springs area. Two analyses from EWEB-5 cuttings, both basaltic andesite, are listed in Table 1.

EWEB-6 (Sisi Creek, total depth 460 m): This hole sampled the most diverse section of the four EWEB holes in the Breitenbush-Austin Hot Springs area, penetrating (from top to bottom) 171 m of basaltic andesite and basalt, 225 m of hornblende dacite, and 64 m of andesite and dacite (Figure 1). The basaltic andesite and basalt in the upper 171 m range in age from Pleistocene to Pliocene. The andesite and dacite in the lower 289 m are Pliocene in age, on the basis of correlation with dated rocks in the CTGH-1 drill hole. Three analyses of EWEB-6 andesite and dacite are listed in Table 1.

The EWEB-6 hole is 7 km northwest of the 1,463-m-deep CTGH-1 hole, which penetrated basaltic andesite lava and breccia at most intervals. In CTGH-1, an interval of Pliocene crystal-lithic lapilli tuff and welded tuff 21 m thick (elevation 361-382 m above sea level [ASL]) probably correlates with the 289-m-thick sequence of andesite and dacite in the bottom of the EWEB-6 hole (elevation 393-682 m ASL). The Pliocene age is established by K-Ar ages of about 3 Ma and 4-5 Ma from stratigraphically higher and lower units, respectively, in hole CTGH-1 (Table 2).

The correlation between EWEB-6 and CTGH-1 (Figure 1) is speculative and limited by the few distinctive units in CTGH-1. Indeed, there would be no basis for lithologic correlation if the welded tuff in CTGH-1 had pinched out completely in the 7 km that separates the two holes. This dilemma of correlation points out the pitfalls encountered when comparing drilled strata in volcanic terranes. Volcanic rocks can change thickness and facies rapidly along strike. During deposition, some flows may be diverted around the constructional aprons of domes or shields; faulting prior to or during volcanism can create structural depressions and highs that control the distribution of units; and subsequent tectonism can create apparent thickening or thinning of units by reverse or normal faulting, respectively.

Thermal Power Company CTGH-1 (Clackamas River, total depth 1,463 m)

The Clackamas River drill hole resulted from a cost-sharing program involving private industry and the U.S. Department of Energy. The hole was drilled by Thermal Power Company of Santa Rosa, California, at a site near the headwaters of the Clackamas River, about 5 km south of Sisi Butte. The hole, begun on June 7, 1986, was drilled with rotary equipment to a depth of about 150 m, and then cased and drilled with diamond corehead equipment to the final depth of 1,463 m. Core recovery was virtually 100 percent. Drilling was completed by September 7, 1986. The drill log is summarized in Figure 1 and described greater detail in Appendix 2.

With few exceptions the drill penetrated a monotonous series of lava flows and breccia comprising basaltic andesite and minor andesite and basalt (Figure 1 and Table 2). Andesite and dacite lavas were drilled at intervals 260-339

Drill hole stratigraphy and geochemistry

m and 394-479 m, and welded tuff and crystal-lithic lapilli-tuff were drilled from 788-810 m. A thick, homogeneous section of coarse-grained basalt, probably a sill, occurs at 621-683 m. The lowest rocks, from 810 to 1,463 m, consist entirely of basaltic andesite lava flows. Below 903 m these flows form two homogeneous sequences that are interpreted to form the flanks of two moderate-sized shield volcanoes, on the basis of their lithologic similarity and trace-element characteristics.

Five K-Ar ages were obtained from rock cored in the CTGH-1 drill hole (Table 3). The ages and sample depths are 2.91 ± 0.08 Ma at 596 m, 4.95 ± 0.23 Ma at 961 m, 5.15 ± 0.25 Ma at 974 m, 4.64 ± 0.12 Ma at 1,412 m, and 4.65 ± 0.12 Ma at 1,445 m. These depths and ages are shown on the cross-section of Plate 1.

The ages are not progressively older downsection. As noted by Bargar (this volume), the alteration mineralogy in the core indicates relatively low temperatures (not much

greater than 100°C), and the rocks are generally fresh or only slightly altered. Consequently, for most of the rocks there should be essentially no disturbance in the K-Ar systematics. Therefore, we tentatively accept the 2.91-Ma date as the absolute age of the lava at 596 m depth. The 4- to 5-Ma ages were purposely collected from lava flows that we interpret as the same unit; these ages largely overlap in the given limits of error (Table 3). Also, the geochemistry of the 4- to 5-Ma lavas penetrated by the drilling is similar to dated 4- to 6-Ma rocks exposed at the surface in the study area (basaltic andesite of Collawash Mountain); the chemical correlation is discussed elsewhere in this paper. Slight alteration has probably modified either the potassium concentration of the rocks at 961-974 m (potassium loss, age too old) or the argon of the rocks at 1,412-1,445 m (argon loss, age too young). In conclusion, the clustering of ages at about 4-5 Ma indicates the approximate range of age for the lavas that form the shield volcanoes in the bottom of the CTGH-1 drill hole.

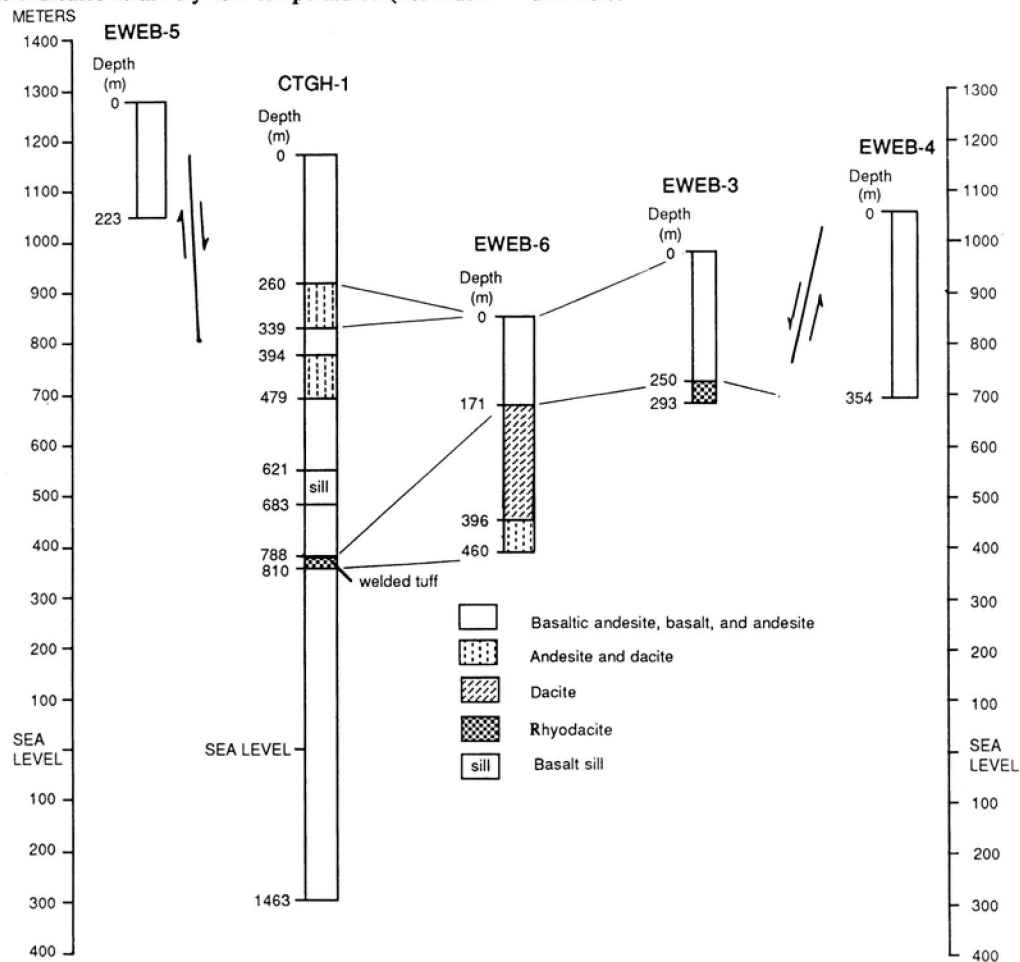


Figure 1. Generalized lithologic logs and correlation of EWEB-3, -4, -5, -6, and CTGH-1. Normal faults with displacement arrows show structural position of EWEB-4 and -5 relative to the other holes.

Table 1. Chemical analyses of cuttings from EWEB-3, -4, -5, -6, and SUNEDCO 58-28.

Drill hole	EWEB-3	EWEB-4		EWEB-5		EWEB-6			SUNEDCO 58-28	
Sample no.	POOP-940	CINC-600	CINC-1120	TRZ-540	TRZ-600	SISI-870	SISI-1430	SISI-1490	SUN-7915	SUN-8015
Unnormalized results (wt. %):										
SiO ₂	73.38	61.75	53.84	54.18	54.71	65.40	59.97	66.29	78.69	81.1
Al ₂ O ₃	14.61	17.27	17.75	17.71	17.87	17.76	17.24	16.44	11.73	11.24
TiO ₂	0.308	1.062	1.431	1.570	1.495	0.645	1.015	0.735	0.211	0.201
FeO*	2.68	6.59	8.07	9.22	8.70	4.60	6.79	5.15	2.02	1.61
MnO	0.040	0.108	0.125	0.148	0.142	0.083	0.118	0.085	0.036	0.028
CaO	0.91	6.02	8.86	7.94	7.59	5.05	6.25	4.00	0.96	0.85
MgO	0.11	3.15	4.62	5.65	4.97	2.31	2.99	1.21	0.07	0.15
K ₂ O	4.61	1.58	1.41	0.95	0.99	1.62	1.50	2.14	4.71	4.72
Na ₂ O	4.78	4.08	4.16	4.09	4.05	4.34	4.22	4.54	1.82	1.32
P ₂ O ₅	0.026	0.262	0.672	0.296	0.303	0.130	0.260	0.238	0.023	0.020
Total	101.45	101.87	100.94	101.75	100.82	101.94	100.35	100.83	100.27	101.26
Normalized results (wt. %):										
SiO ₂	72.14	60.23	52.92	52.77	53.80	63.87	59.36	65.41	78.48	80.11
Al ₂ O ₃	14.36	16.84	17.45	17.25	17.57	17.34	17.06	16.22	11.70	11.10
TiO ₂	0.30	1.04	1.41	1.53	1.47	0.63	1.00	0.73	0.210	0.199
Fe ₂ O ₃ *	2.90	7.07	8.72	9.88	9.41	4.94	7.39	5.59	2.01	1.59
MnO	0.04	0.11	0.12	0.14	0.14	0.08	0.12	0.08	0.036	0.028
CaO	0.89	5.87	8.71	7.73	7.46	4.93	6.19	3.95	0.96	0.84
MgO	0.11	3.07	4.54	5.50	4.89	2.26	2.96	1.19	0.07	0.15
K ₂ O	4.53	1.54	1.39	0.93	0.97	1.58	1.48	2.11	4.70	4.66
Na ₂ O	4.70	3.98	4.09	3.98	3.98	4.24	4.18	4.48	1.82	1.30
P ₂ O ₅	0.03	0.26	0.66	0.29	0.30	0.13	0.26	0.23	0.023	0.02
Trace elements (ppm):										
Ni	14	37	50	89	81	17	21	16	22	20
Cr	0	49	65	94	79	10	47	6	0	1
Sc	6	18	25	28	26	16	21	14	11	11
V	12	111	187	214	194	77	116	60	14	7
Ba	806	412	988	303	360	370	391	588	1703	1643
Rb	129	31	16	11	11	27	36	54	147	143
Sr	90	426	1547	668	643	540	417	344	84	62
Zr	346	202	245	146	165	138	181	220	239	236
Y	41	22	24	23	24	16	22	24	62	57
Nb	37.0	16.1	15.9	10.7	10.9	7.0	11.7	13.3	23.6	22.0
Ga	21	21	19	19	20	20	21	23	17	17
Cu	12	38	49	56	55	34	31	19	19	11
Zn	65	79	92	87	86	59	104	73	105	93

Conroy and Sherrod

Table 2. Chemical analyses of CTGH-1 drill core.

Sample no.	CTGH-546	CTGH-639	CTGH-693	CTGH-708A	CTGH-804	CTGH-838	CTGH-960	CTGH-1217	CTGH-1583	CTGH-1662
Unnormalized results (wt. %):										
SiO ₂	55.31	55.98	54.05	54.46	54.44	54.06	61.46	56.94	58.89	56.22
Al ₂ O ₃	18.40	18.59	18.12	18.07	18.22	18.09	18.38	19.31	18.26	17.76
TiO ₂	1.070	1.084	1.141	1.175	1.169	1.567	0.783	0.968	0.900	1.478
FeO*	7.82	7.74	8.36	8.17	8.36	9.12	5.19	7.08	6.51	8.47
MnO	0.136	0.135	0.142	0.143	0.144	0.154	0.090	0.117	0.110	0.141
CaO	8.12	8.08	8.34	8.29	8.42	7.83	6.75	8.34	7.19	7.41
MgO	5.08	4.99	5.44	5.41	5.45	5.13	3.12	3.72	3.79	4.24
K ₂ O	0.90	0.95	0.88	0.88	1.01	0.88	0.95	0.79	1.07	1.03
Na ₂ O	3.85	3.94	3.89	3.86	3.80	4.17	4.34	4.10	4.03	4.06
P ₂ O ₅	<u>0.273</u>	<u>0.296</u>	<u>0.283</u>	<u>0.291</u>	<u>0.311</u>	<u>0.321</u>	<u>0.172</u>	<u>0.150</u>	<u>0.200</u>	<u>0.362</u>
Total	100.96	101.79	100.65	100.75	101.32	101.32	101.23	101.51	100.95	101.17
Normalized results (wt. %):										
SiO ₂	54.36	54.58	53.26	53.62	53.29	52.88	60.40	55.70	57.96	55.11
Al ₂ O ₃	18.09	18.13	17.86	17.79	17.83	17.69	18.06	18.89	17.97	17.41
TiO ₂	1.05	1.06	1.12	1.16	1.14	1.53	0.77	0.95	0.89	1.45
Fe ₂ O ₃ *	8.45	8.30	9.06	8.85	9.00	9.81	5.61	7.62	7.05	9.13
MnO	0.13	0.13	0.14	0.14	0.14	0.15	0.09	0.11	0.11	0.14
CaO	7.98	7.88	8.22	8.16	8.24	7.66	6.63	8.16	7.08	7.26
MgO	4.99	4.87	5.36	5.33	5.33	5.02	3.07	3.64	3.73	4.16
K ₂ O	0.88	0.93	0.87	0.87	0.99	0.86	0.93	0.77	1.05	1.01
Na ₂ O	3.78	3.84	3.83	3.80	3.72	4.08	4.27	4.01	3.97	3.98
P ₂ O ₅	0.27	0.29	0.28	0.29	0.30	0.31	0.17	0.15	0.20	0.35
Trace elements (ppm):										
Ni	68	66	74	73	73	63	24	30	38	49
Cr	91	80	92	88	81	89	26	32	49	48
Sc	25	25	28	24	26	24	18	23	19	23
V	181	185	191	199	187	199	121	207	160	162
Ba	319	347	301	292	286	275	205	226	284	338
Rb	13	13	14	12	14	6	12	9	18	13
Sr	635	649	615	608	648	630	1016	758	652	495
Zr	142	150	140	142	146	110	135	110	146	161
Y	21	21	22	24	24	22	14	15	17	23
Nb	9.0	9.3	7.9	8.7	9.4	4.8	5.4	4.7	7.2	13.4
Ga	18	21	17	20	20	22	21	19	18	20
Cu	78	64	67	111	69	70	33	74	48	56
Zn	77	76	80	78	80	92	59	66	66	89

(Table 2, continued)

Sample no.	CTGH-1662D	CTGH-1697	CTGH-1782	CTGH-1847	CTGH-1974	CTGH-2005	CTGH-2047	CTGH-2099	CTGH-2135	CTGH-2174
Unnormalized results (wt. %):										
SiO ₂	55.91	55.21	57.61	54.23	53.67	54.32	49.34	48.71	49.65	48.52
Al ₂ O ₃	17.66	17.70	16.83	17.69	17.59	17.73	18.00	16.57	17.25	16.57
TiO ₂	1.469	1.097	1.037	1.591	1.176	1.216	1.443	1.475	1.527	1.501
FeO*	8.68	8.28	7.87	8.33	8.02	8.26	10.40	11.06	10.76	11.39
MnO	0.142	0.142	0.143	0.135	0.145	0.150	0.157	0.177	0.162	0.180
CaO	7.36	8.47	7.86	8.19	8.26	8.48	10.34	10.12	10.24	10.27
MgO	4.23	5.52	5.20	5.32	5.83	5.90	6.39	7.35	6.65	7.19
K ₂ O	1.03	0.40	0.94	0.75	0.87	0.92	0.27	0.20	0.25	0.20
Na ₂ O	4.09	3.72	3.82	3.84	3.88	3.97	2.93	2.62	2.85	2.73
P ₂ O ₅	<u>0.360</u>	<u>0.174</u>	<u>0.184</u>	<u>0.338</u>	<u>0.371</u>	<u>0.413</u>	<u>0.139</u>	<u>0.142</u>	<u>0.147</u>	<u>0.147</u>
Total	100.93	100.71	101.49	100.41	99.81	101.36	99.41	98.42	99.49	98.70
Normalized results (wt. %):										
SiO ₂	54.92	54.37	56.33	53.56	53.34	53.16	49.12	48.94	49.37	48.60
Al ₂ O ₃	17.35	17.43	16.45	17.47	17.48	17.35	17.92	16.65	17.15	16.60
TiO ₂	1.44	1.08	1.01	1.57	1.17	1.19	1.44	1.48	1.52	1.50
Fe ₂ O ₃ *	9.38	8.97	8.46	9.05	8.77	8.89	11.39	12.22	11.77	12.55
MnO	0.14	0.14	0.14	0.13	0.14	0.15	0.16	0.18	0.16	0.18
CaO	7.23	8.34	7.68	8.09	8.21	8.30	10.29	10.17	10.18	10.29
MgO	4.16	5.44	5.08	5.25	5.79	5.77	6.36	7.38	6.61	7.20
K ₂ O	1.01	0.39	0.92	0.74	0.86	0.90	0.27	0.20	0.25	0.20
Na ₂ O	4.02	3.66	3.73	3.79	3.86	3.89	2.92	2.63	2.83	2.73
P ₂ O ₅	0.35	0.17	0.18	0.33	0.37	0.40	0.14	0.14	0.15	0.15
Trace elements (ppm):										
Ni	51	57	55	74	104	99	81	81	74	85
Cr	54	123	121	113	169	148	203	225	219	229
Sc	23	24	26	26	25	28	33	32	31	34
V	158	140	157	166	176	185	234	212	195	216
Ba	328	331	304	312	387	427	56	98	99	82
Rb	14	4	14	8	8	8	4	2	2	3
Sr	493	476	435	498	826	853	256	394	272	351
Zr	164	115	111	170	144	149	88	98	94	97
Y	23	19	20	25	23	22	23	22	22	22
Nb	13.6	7.1	7.9	17.6	8.5	8.7	6.8	7.0	6.1	8.6
Ga	18	22	19	21	18	21	21	15	20	18
Cu	63	44	44	46	52	60	52	65	56	58
Zn	89	79	72	79	77	84	85	92	87	89

Conrey and Sherrod

(Table 2, continued)

Sample no.	CTGH-2206	CTGH-2301	CTGH-2431	CTGH-2525	CTGH-2576	CTGH-2630	CTGH-2968	CTGH-3012	CTGH-3066	CTGH-3360
Unnormalized results (wt. %):										
SiO ₂	50.05	48.96	52.03	52.64	43.31	62.79	52.68	56.06	56.30	57.31
Al ₂ O ₃	17.48	17.12	18.02	17.77	11.23	16.41	19.58	19.19	18.85	18.46
TiO ₂	1.329	1.260	1.985	1.121	3.564	1.080	1.159	1.101	1.110	1.037
FeO*	10.07	11.86	9.86	7.42	11.60	5.90	7.79	7.34	7.21	6.84
MnO	0.164	0.177	0.129	0.144	0.170	0.136	0.140	0.158	0.127	0.121
CaO	10.33	9.12	8.63	9.89	12.95	4.40	7.42	8.50	8.37	7.93
MgO	7.23	6.92	4.73	6.93	11.33	2.08	4.80	4.27	4.30	3.81
K ₂ O	0.20	0.14	0.83	0.57	0.68	2.31	0.78	0.52	0.57	0.99
Na ₂ O	2.92	2.73	3.73	3.41	3.01	3.99	3.52	3.85	3.84	4.03
P ₂ O ₅	<u>0.152</u>	<u>0.092</u>	<u>0.365</u>	<u>0.236</u>	<u>1.234</u>	<u>0.288</u>	<u>0.247</u>	<u>0.196</u>	<u>0.195</u>	<u>0.204</u>
Total	99.92	98.38	100.31	100.13	99.08	99.38	98.12	101.19	100.87	100.73
Normalized results (wt. %):										
SiO ₂	49.59	49.17	51.36	52.18	43.21	62.81	53.27	55.00	55.42	56.51
Al ₂ O ₃	17.32	17.19	17.79	17.62	11.20	16.41	19.80	18.83	18.55	18.20
TiO ₂	1.32	1.27	1.96	1.11	3.56	1.08	1.17	1.08	1.09	1.02
Fe ₂ O ₃ *	10.97	13.10	10.71	8.09	12.73	6.49	8.66	7.92	7.81	7.42
MnO	0.16	0.18	0.13	0.14	0.17	0.14	0.14	0.16	0.13	0.12
CaO	10.23	9.16	8.52	9.80	12.92	4.40	7.50	8.34	8.24	7.82
MgO	7.16	6.95	4.67	6.87	11.30	2.08	4.85	4.19	4.23	3.76
K ₂ O	0.20	0.14	0.82	0.57	0.68	2.31	0.79	0.51	0.56	0.98
Na ₂ O	2.89	2.74	3.68	3.38	3.00	3.99	3.56	3.78	3.78	3.97
P ₂ O ₅	0.15	0.09	0.36	0.23	1.23	0.29	0.25	0.19	0.19	0.20
Trace elements (ppm):										
Ni	67	108	44	68	221	12	27	22	23	21
Cr	199	222	34	239	410	4	46	50	49	48
Sc	32	30	26	31	32	18	27	26	25	23
V	199	183	221	213	237	60	168	196	195	195
Ba	111	42	287	313	650	509	282	265	290	298
Rb	1	3	11	9	45	45	9	12	11	21
Sr	464	219	519	1130	1038	394	570	612	600	587
Zr	98	83	162	136	401	281	119	118	120	123
Y	20	22	25	19	36	38	22	18	19	19
Nb	5.3	5.3	17.8	6.4	77.0	24.5	7.0	6.4	7.3	7.9
Ga	19	22	22	18	19	21	18	20	23	20
Cu	48	59	39	49	62	23	58	72	62	67
Zn	83	96	96	69	122	89	79	78	75	76

(Table 2, continued)

Sample no.	CTGH-3614	CTGH-3724	CTGH-3916	CTGH-3992	CTGH-4097	CTGH-4487	CTGH-4549	CTGH-4566	CTGH-4703	CTGH-4779
<u>Unnormalized results (wt. %):</u>										
SiO ₂	56.67	56.26	56.82	57.77	57.47	57.47	56.92	57.01	57.03	57.80
Al ₂ O ₃	18.43	18.56	18.70	18.24	18.28	18.15	17.79	17.78	17.67	17.70
TiO ₂	1.065	1.085	1.079	1.038	1.057	1.127	1.170	1.161	1.161	1.136
FeO*	7.17	7.11	7.15	6.96	6.74	7.27	7.33	7.27	7.14	7.17
MnO	0.181	0.155	0.119	0.119	0.118	0.128	0.131	0.128	0.128	0.132
CaO	8.19	8.22	8.23	7.68	7.88	7.90	7.74	7.67	7.61	7.38
MgO	4.11	4.24	4.16	3.78	3.79	4.24	3.93	3.85	4.01	3.91
K ₂ O	0.75	0.58	0.59	0.77	0.74	0.74	0.97	0.84	1.27	1.60
Na ₂ O	4.03	4.05	4.17	4.31	4.30	4.07	4.16	4.33	4.01	4.09
P ₂ O ₅	<u>0.224</u>	<u>0.228</u>	<u>0.237</u>	<u>0.258</u>	<u>0.261</u>	<u>0.332</u>	<u>0.409</u>	<u>0.409</u>	<u>0.405</u>	<u>0.400</u>
Total	100.82	100.49	101.26	100.93	100.64	101.43	100.55	100.45	100.43	101.32
<u>Normalized results (wt. %):</u>										
SiO ₂	55.81	55.59	55.72	56.85	56.73	56.26	56.20	56.35	56.38	56.65
Al ₂ O ₃	18.15	18.34	18.34	17.95	18.04	17.77	17.56	17.57	17.47	17.35
TiO ₂	1.05	1.07	1.06	1.02	1.04	1.10	1.16	1.15	1.15	1.11
Fe ₂ O ₃ *	7.77	7.73	7.71	7.53	7.32	7.83	7.96	7.90	7.76	7.73
MnO	0.18	0.15	0.12	0.12	0.12	0.13	0.13	0.13	0.13	0.13
CaO	8.07	8.12	8.07	7.56	7.78	7.73	7.64	7.58	7.52	7.23
MgO	4.05	4.19	4.08	3.72	3.74	4.15	3.88	3.81	3.96	3.83
K ₂ O	0.74	0.57	0.58	0.76	0.73	0.72	0.96	0.83	1.26	1.57
Na ₂ O	3.97	4.00	4.09	4.24	4.24	3.98	4.11	4.28	3.96	4.01
P ₂ O ₅	0.22	0.23	0.23	0.25	0.26	0.32	0.40	0.40	0.40	0.39
<u>Trace elements (ppm):</u>										
Ni	23	20	24	19	20	24	25	23	26	26
Cr	50	45	49	38	45	29	37	37	43	48
Sc	24	29	29	23	23	24	24	25	24	23
V	187	198	186	180	174	161	178	161	152	159
Ba	291	331	346	364	356	405	453	504	483	485
Rb	19	13	17	23	24	21	25	28	24	34
Sr	582	592	603	593	593	583	702	703	691	685
Zr	128	129	128	137	137	158	178	178	175	175
Y	19	19	19	19	20	23	23	23	22	22
Nb	7.6	7.6	7.1	9.2	8.4	11.6	12.8	13.9	12.2	13.4
Ga	22	20	20	17	22	20	17	21	22	20
Cu	71	57	66	43	53	37	57	47	52	44
Zn	77	76	76	72	76	81	83	79	81	81

Conrey and Sherrod

Drill hole stratigraphy and geochemistry

Table 3. Potassium-argon ages of CTGH-1 drill core.

Sample number	Rock type	Material dated ¹	K ₂ O (wt. %) ³	⁴⁰ Ar _{rad} (10 ⁻¹¹ moles/gm) ³	Percent ⁴⁰ Ar _{rad}	Calculated age (Ma) ²
CTGH-1956	Basaltic andesite	Plagioclase concentrate	(1.392)	(0.5845)		2.91±0.08
			1.406	0.5788	70	
			1.380	0.5840	70	
			1.391	0.5860	70	
				0.5893	71	
CTGH-3152	Basaltic andesite	Plagioclase concentrate	(0.615)	(0.4388)		4.95±0.23
			0.607	0.4310	20	
			0.624	0.4405	19	
			0.613	0.4699	20	
			0.616	0.4138	18	
CTGH-3195	Basaltic andesite	Plagioclase concentrate	(0.801)	(0.5949)		5.15±0.25
			0.793	0.6011	16	
			0.799	0.5918	17	
			0.812	0.5917	17	
CTGH-4633	Basaltic andesite	Plagioclase concentrate	(1.295)	(0.8664)		4.64±0.12
			1.279	0.8492	42	
			1.274	0.8728	43	
			1.335	0.8786	43	
				0.8650	43	
CTGH-4740	Basaltic andesite	Plagioclase concentrate	(1.379)	(0.9232)		4.65±0.12
			1.379	0.9252	39	
			1.370	0.9250	39	
			1.388	0.9254	39	
			1.375	0.9171	39	

Notes:

¹ Sample preparation and analytical work were done at University of Arizona, Paul E. Damon and Mohammed Shafiqullah, principal investigators.

² K-Ar ages were calculated using the constants for the radioactive decay and abundance of ⁴⁰K recommended by the International Union of Geological Sciences Subcommittee on Geochronology (Steiger and Jager, 1977). These constants are:

$\lambda_e = 0.580 \times 10^{-10} \text{ yr}^{-1}$, $\lambda_b = 4.962 \times 10^{-10} \text{ yr}^{-1}$, and $^{40}\text{K}/\text{K}_{\text{total}} = 1.167 \times 10^{-4} \text{ mol/mol}$.

³ Value in parentheses is arithmetic mean used in age calculation.

More isotopic ages would be necessary to fully understand the age-depth relations in the upper part of the hole. In particular, the contact between volcanic rocks of the High Cascades and underlying units is arbitrarily drawn at the top of a series of andesite and dacite lava flows (260-339 m). A K-Ar age of 2.91±0.08 Ma from basaltic andesite at 596 m indicates that by that depth the drill was in the basaltic andesite of Collawash Mountain, as defined by surface mapping (Sherrod and Conrey, this volume).

The crystal-lithic lapilli tuff and welded tuff at 788-810 m in the CTGH-1 hole probably correlate with EWEB-6 andesite and dacite in the bottom of the EWEB-6 hole (depth 171-460 m). These rocks are Pliocene in age, on the basis of K-Ar ages from bracketing units in CTGH-1: 2.91 Ma at 596 m and 4.95 Ma at 961 m.

The 653-m-thick sequence of basalt and basaltic andesite from the bottom of the CTGH-1 drill hole (810-1,463 m) probably represents the lava erupted from two or more shield volcanoes. The interval from about 903 to 1,369 m

comprises rocks very similar in thin section and major-element chemistry (Table 2). The analyzed samples show increasing P₂O₅ and Zr with depth, a pattern also found at several basaltic andesite volcanoes near Mount Jefferson (R.M. Conrey, unpublished data). Another underlying shield volcano is probably indicated by the abrupt increase in Sr at about 1,387 m and the virtually constant Sr from 1,387 to 1,458 m (near the base of hole).

The 560-m thickness represented by these lower two volcanoes is not unusual; several sequences of upper Miocene and Pliocene lava flows exposed in the Cascade Range of Oregon are as thick or thicker. According to the K-Ar ages, these rocks are early Pliocene in age, but the lowest core is undated and could include rocks of late Miocene age. Therefore the sequence is probably Pliocene to late Miocene in age.

There is an abrupt change in the secondary zeolite minerals of CTGH-1 at about 885 m (Bargar, this volume). This depth is 75 m below the top of the basaltic andesite

sequence that forms the base of the core. Above 885 m, phillipsite, thomsonite, analcime, and chabazite are common; below 885-m depth, those minerals are virtually absent, and the core is characterized by heulandite-group minerals (heulandite and clinoptilolite). This contrast presumably results from changes in fluid chemistry with increasing depth of burial and is not due to a marked stratigraphic discontinuity.

Some chemically distinct units were recognized in the core. For example, samples 693 (211 m) and 708A (216 m) are probably from the same unit, as are samples 1974 (602 m) and 2005 (611 m). The latter unit contains fairly high concentrations of Sr and oscillatory-zoned clinopyroxene phenocrysts, an association also found near Mount Jefferson in the southeast corner of the Breitenbush-Austin Hot Springs area (R.M. Conrey, unpublished data).

A 120-m-thick basalt sill was drilled from 621 to 683 m. In thin section, the rocks are coarse grained, contain interstitial fayalite and sanidine, and show pervasive shearing and alteration. There is geochemical evidence for minor reverse offset: samples 2099 (640 m) and 2174 (663 m) are chemically and petrographically similar, as are samples 2047 (624 m) and 2135 (651 m). Another thinner sill (sample 2301, 701-m-depth), probably an offshoot of the thick sill, is also pervasively sheared.

Olivine analcinite in CTGH drill core: A flow of olivine analcinite about 10 m thick was encountered at about 785 m in the CTGH-1 drill hole (sample 2576, Table 2). Forsteritic olivine phenocrysts in the flow contain inclusions of Cr-Al spinel; titanite phenocrysts are spectacularly oscillatory-zoned from uncolored skeletal Ca-rich cores to deep lilac, Ti- and Al-rich rims. The groundmass is a very fine-grained intergrowth of titanite, analcime, Ti-rich magnetite, andesine, biotite, sanidine, and apatite. These mineral identifications are substantiated by electron microprobe analyses (R.M. Conrey, unpublished data).

Olivine analcinite is most commonly found in alkaline basalt provinces and rarely in a volcanic arc setting. The rock is remarkable for its high concentrations of Nb, Rb, Sr, Zr, TiO_2 , and P_2O_5 , in conjunction with high MgO, Cr, and Ni (Table 2).

Sunoco Energy Development Company (SUNEDCO) drill hole (58–28, total depth 2,457 m)

The SUNEDCO hole 58–28, located about 3 km south-east of Breitenbush Hot Springs at an elevation of 899 m (Kelly bushing elevation, D.L. Olmstead, personal communication, 1988), was rotary-drilled in the autumn of 1981 to a total depth of 2,457 m. The drill cuttings were logged by A.F. Waibel, whose unpublished drill log is the basis for the

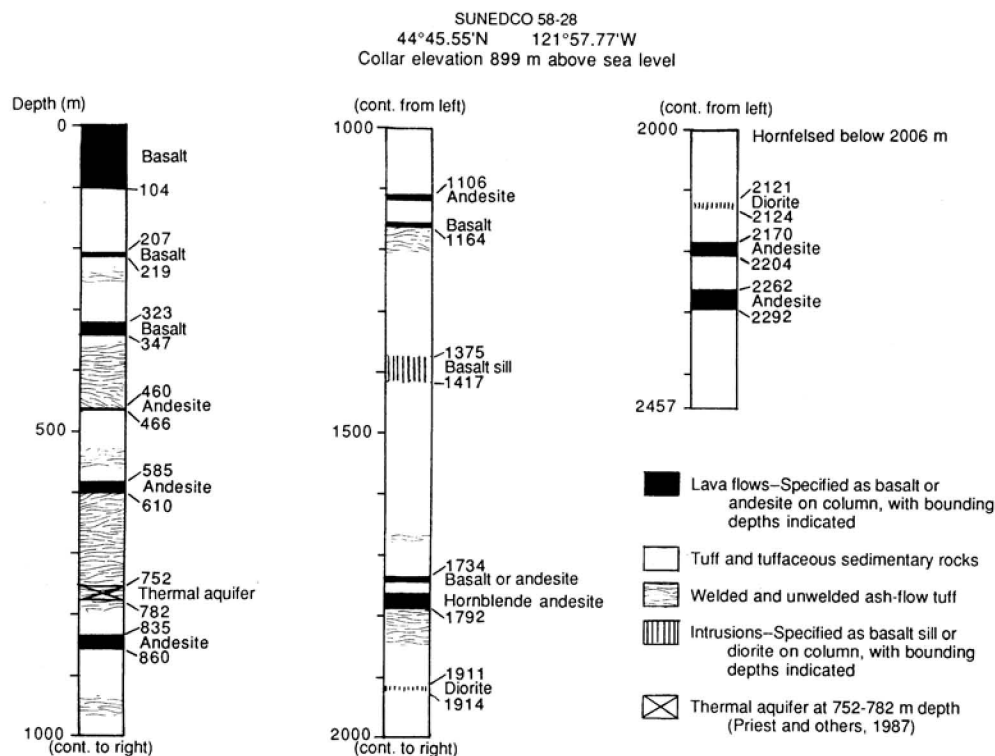


Figure 2. Generalized lithologic log of SUNEDCO 58–28, adapted from A.F. Waibel (unpublished data).

Drill hole stratigraphy and geochemistry

following generalized description of lithology and alteration. Figure 2 shows a generalized lithologic column for SUNEDCO 58-28.

The hole was started in and drilled through about 100 m of middle Miocene lava of Outerson Mountain. The rest of the drilling was in rocks characteristic of the Breitenbush Formation: tuff and tuffaceous volcanoclastic rocks with fewer lava flows and intrusions. Lava flows account for about 10 percent (250 m) of the Breitenbush Formation encountered in drilling and range in composition from basalt to andesite. Intrusions include a 42-m-thick sequence of equigranular basalt or basaltic andesite (1,375-1,417 m) and fine-grained quartz diorite, which forms two thin bodies (sills or dikes) at 1,911-1,914 m and 2,121-2,124 m.

Alteration generally increases with depth for samples from the SUNEDCO hole. Montmorillonite occurs commonly, beginning at a depth of 250 m. Celadonite, chlorite, smectite, and laumontite appear between 375 and 810 m and persist to the bottom of the hole. Epidote was first noted at 814 m, secondary potassium feldspar at 1,046 m, and secondary albite at 1,155 m. Phyllic alteration (fine-grained micaceous clays) becomes pervasive at about 1,800 m.

Intrusions and probably faults have localized alteration in some cases. Tuff beneath the basalt sill (below 1,417 m) is so completely recrystallized to fine-grained secondary minerals that its original texture is destroyed for as much as 10 m below the contact. Recrystallization, probably the result of burial metamorphism, intrusion, and high geothermal gradients, has also affected most rocks from 1,900 m to the bottom of the hole (2,457 m). The quartz diorite sills occur in this interval.

The chemical changes associated with phyllic alteration of two siliceous tuffs from the lower part of SUNEDCO 58-28 (Table 1) include relative increases in silica (78-80 percent SiO_2) and decreases in soda (1-2 percent Na_2O). These tuffs are chemically similar to xenoliths (presumably tuffaceous wallrock) disgorged by late Miocene and Pliocene pyroclastic eruptions during Deschutes Formation volcanism (Conrey, 1985; R.M. Conrey, unpublished data). The sodium loss, which in the xenoliths is accompanied by nearly complete loss of chlorine, may explain the source of sodium (and chlorine) in upwelling thermal waters of Breitenbush and Austin Hot Springs. In contrast, Ingebritsen and others (1988) called upon substantially deeper hydrologic circulation through marine rocks to account for the Na-Cl-component waters found at the hot springs.

CHEMICAL CHARACTERISTICS OF ROCKS EXPOSED AT THE SURFACE IN THE BREITENBUSH HOT SPRINGS QUADRANGLE

Chemically, the rocks of the Breitenbush Hot Springs quadrangle can be divided into four major sequences, originally recognized by White (1980a). As described below, the sequences can be thought of as two pairs, each with an older

Ti- and Rb-rich sequence succeeded by a younger Ti- and Rb-poor sequence. The earlier pair contains (1) the Breitenbush Formation of White (1980a, b) and interbedded lava of Scorpion Mountain, and (2) succeeding lava of Outerson Mountain and andesite and dacite of Rhododendron Ridge. These units range in age from roughly 25-18 Ma and 13-9 Ma, respectively, (Sherrod and Conrey, this volume). The younger pair contains (1) the basaltic andesite of Collawash Mountain and interbedded andesite and dacite of the Clackamas River, and (2) succeeding volcanic rocks of the High Cascades. These units range in age from roughly 6-2.5 Ma and <2.5 Ma respectively.

We have focused on the abundance of TiO_2 and Rb because they are representative of much of the rock chemistry. For example, at a given concentration of SiO_2 , Rb is generally proportional to K_2O and Ba, whereas TiO_2 is proportional to Fe_2O_3 , Zr, and Nb. Tentatively, these elements (TiO_2 and Rb) allow us to discriminate rocks from different age sequences when comparing andesite, dacite, and rhyodacite. Discrimination of basaltic andesite and basalt is not possible with these elements. Analytical methods are described at the end of this chapter.

Breitenbush Formation and lava of Scorpion Mountain

The most striking chemical features of the Breitenbush Formation and lava of Scorpion Mountain are the low contents of Sr, MgO, Cr, and Ni, and the high Rb, TiO_2 , and Fe_2O_3 contents, characteristic of rocks of this age (Oligocene and early Miocene; 25-18 Ma) in the Cascade Range (White, 1980a, b). Relatively few analyses of rocks of this sequence are available from the Breitenbush Hot Springs quadrangle, and only three new analyses of samples from this unit were obtained (BR-M4, -M5, and -M6; Appendix 1). In order to better compare sequences, all available Cascade Range analyses for rocks of similar age from latitudes 44° - 45°N were compiled. In Figures 3 and 5, Harker plots show the very high contents of TiO_2 and Rb. Note the fan shape of the TiO_2 - SiO_2 plot, with a very wide range in TiO_2 values at low values of SiO_2 . This feature is also found in rocks of late Miocene and Pliocene age (Figure 3).

Lava of Outerson Mountain and andesite and dacite of Rhododendron Ridge

The most notable chemical feature of this sequence is the much more restricted range in TiO_2 and Rb compared with underlying rocks of the Breitenbush Formation and Scorpion Mountain lava. Harker diagrams for these elements are displayed in Figures 3 and 5. The data for these figures were compiled from analyses of rocks (44° - 45°N) ranging in age from 18-7 Ma, a wider age range than is found for similar rocks in the Breitenbush Hot Springs quadrangle. Relatively few analyses of these rocks are available from the quadrangle, and none were obtained for this report. All analyses of andesites in the age range 13-9 Ma in the quadrangle contain <1 percent TiO_2 (White, 1980a).

Conrey and Sherrod

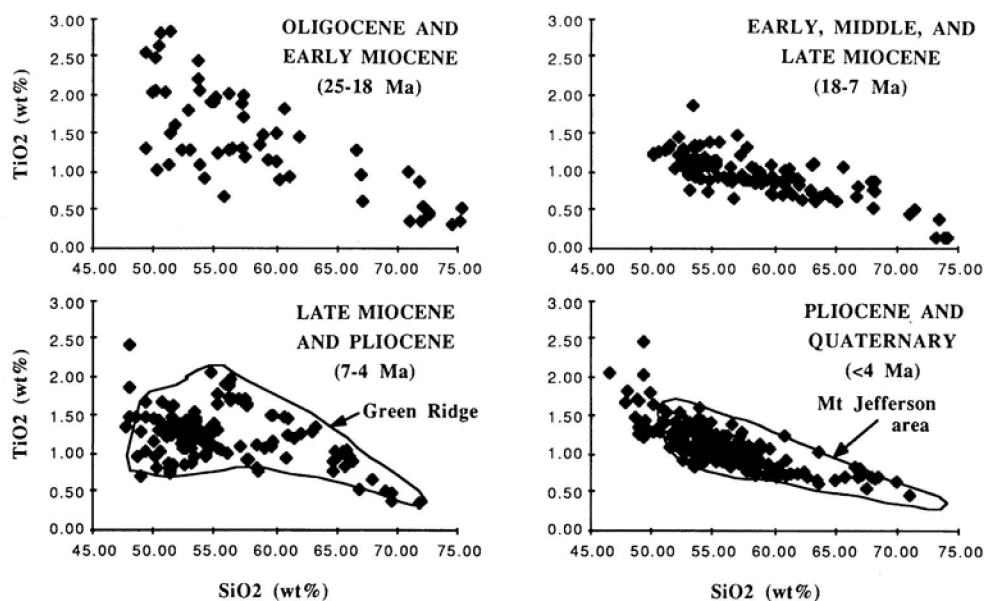


Figure 3. TiO_2 versus SiO_2 for rocks of four age groups in the Cascade Range, 44° - 45°N . Bracketing ages slightly different than ages of rock units in Breitenbush Hot Springs quadrangle (Sherrod and Conrey, this volume). Outlined field "Green Ridge" summarizes 270 analyses not shown individually; "Mt. Jefferson area" summarizes 640 analyses (R.M. Conrey, unpublished data, 1988). Sources: Avramenko (1981), Davie (1980), Flaherty (1981), Lux (1981), Priest and Vogt (1983), Verplanck (1985), White (1980a, 1980b), Yogodzinski (1985), and this volume.

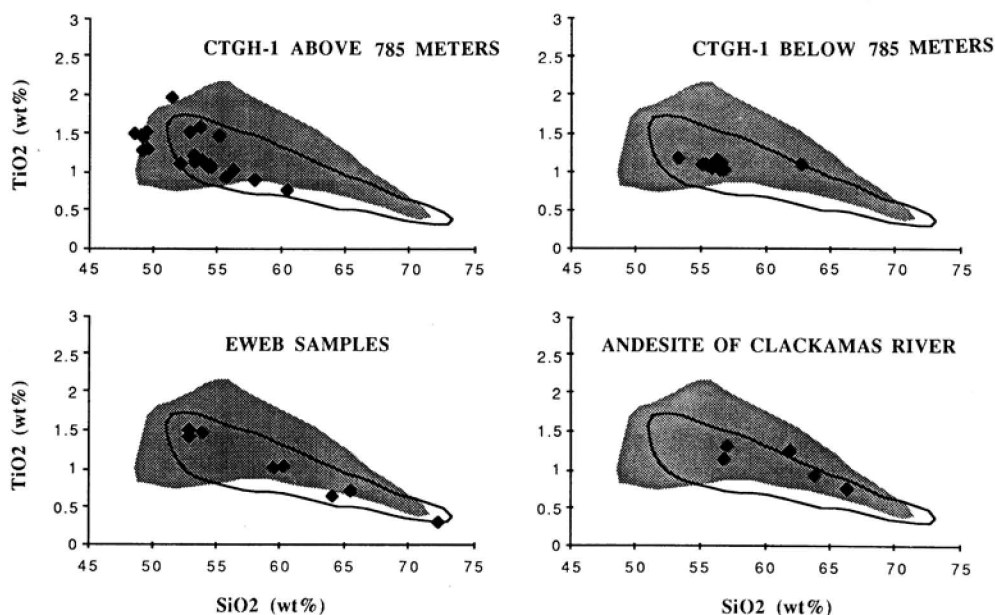


Figure 4. TiO_2 versus SiO_2 for samples from Breitenbush Hot Springs quadrangle. Pattern represents 270 analyses from Green Ridge and outline represents 640 analyses from Mount Jefferson area as explained in Figure 3. Sources: this volume and unpublished data.

Drill hole stratigraphy and geochemistry

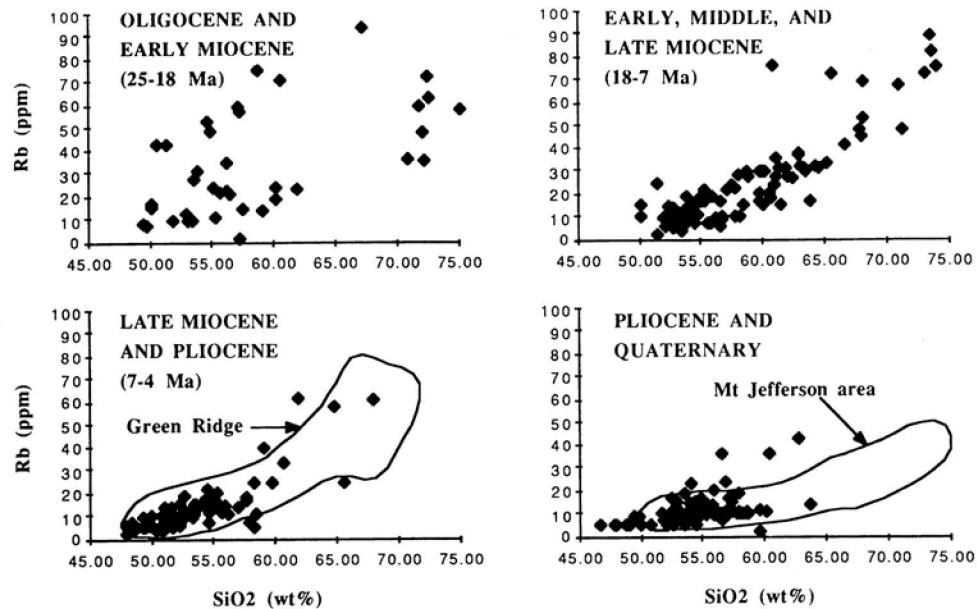


Figure 5. Rb versus SiO_2 for rocks of four age groups in Cascade Range, 44° - 45°N . See Figure 3 for sources of data and explanation of labeled outlines.

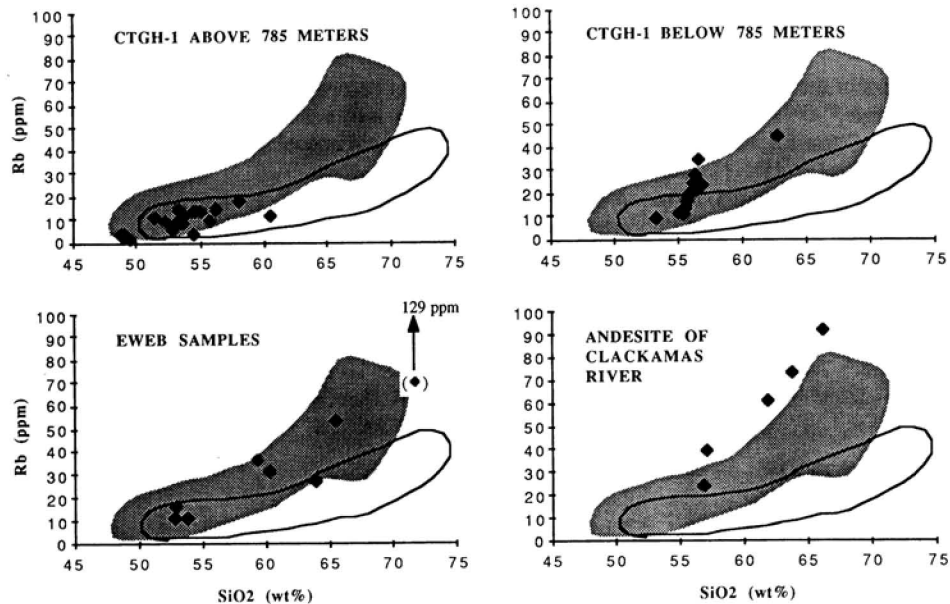


Figure 6. Rb versus SiO_2 for samples from Breitenbush Hot Springs quadrangle. See Figure 4 for explanation of patterned and outlined fields. Sources: this volume and unpublished data.

Basaltic andesite of Collawash Mountain and andesite and dacite of Clackamas River

Several samples from these units were analyzed; the results are compiled with other data from latitudes 44°–45°N in Figures 3 and 5. The largest amount of data for this age range is available from Green Ridge, a major, north-south-trending fault block exposing upper Miocene and Pliocene volcanic rocks and located approximately 40 km southeast of the Breitenbush Hot Springs quadrangle. On Figures 3 and 5, the 270 Green Ridge analyses are shown outlined (R. M. Conrey, unpublished data). The TiO_2 - SiO_2 plot for these rocks resembles that of the Scorpion Mountain lava, with widely ranging TiO_2 contents in basalt, basaltic andesite, and andesite. The Rb - SiO_2 plot resembles that of middle and upper Miocene Outerson Mountain lava and the andesite and dacite of Rhododendron Ridge. A notable feature of the basaltic andesite of Collawash Mountain and the andesite and dacite of the Clackamas River is the paucity of hornblende in the dacite and rhyodacite.

Volcanic rocks of the High Cascades

The volcanic rocks of the High Cascades in the southernmost part of the Breitenbush Hot Springs quadrangle south of Olallie Butte contain a significant proportion of andesite and dacite and only minor basaltic andesite and basalt. These rocks are at the northern edge of a large, long-lived field of andesite, dacite and rhyodacite geographically centered at Park Butte in the Mount Jefferson Wilderness south of the quadrangle (R. M. Conrey, unpublished data). In contrast, in the Breitenbush Hot Springs quadrangle from Olallie Butte northward, the High Cascades sequence is largely basaltic andesite, with very little andesite and no dacite. Most of the new analyses made for this report are from volcanic rocks of the High Cascades in the southern part of the quadrangle.

Compilation of data for volcanic rocks of the High Cascades from latitudes 44°–45°N (with the exception of the Three Sisters area) (Figures 3 and 5) shows some contrasts with the preceding upper Miocene and Pliocene sequence. Both Rb and TiO_2 are lower in the andesite-dacite range. The field of Mount Jefferson-area samples (shown outlined) is based on 640 XRF analyses (R. M. Conrey, unpublished data), including 108 samples from the Breitenbush Hot Springs quadrangle. Mount Jefferson-area dacite and rhyodacite contain ubiquitous hornblende phenocrysts.

ANALYTICAL METHODS

X-ray Fluorescence

Samples were obtained from drill holes (EWEB-3, -4, -5, and -6, CTGH-1, and SUNEDCO 58–28) and surface samples. All of the new major- and trace-element data were obtained using the Li-tetraborate fusion method with a flux:rock ratio of 2:1. Fused beads were analyzed on an automated Rigaku machine at Washington State University.

Duplicate samples from some outcrops were analyzed to check analytical precision: paired samples BHS-24 and BR-150, and RCMJ-554 and BR-136 in Appendix 1; and CTGH-1662 and CTGH-1662D in Table 2. Sample CTGH-1662D was not cleaned prior to analysis in order to test for contamination of the core by drilling mud. To test machine precision during a single run, the same bead was analyzed twice: compare BR-44 and BR-44R.

The analyses reported here may be closely compared and contrasted because they were obtained by the same method on the same machine. On Figures 5 and 6, however, it was necessary to use data obtained using different methods (for example, pressed powder pellets for trace elements via XRF, and AAS and INAA methods for major and trace elements). Thus, there is a possibility of significant inter-laboratory variation.

Potassium-argon

Potassium-argon ages from drill core samples (Table 3) and several samples from surface exposures (Table 1 in Sherrod and Conrey, this volume) were obtained from the Geochronology Laboratory at the University of Arizona, under the direction of Paul E. Damon and Mohammed Shafiqullah. Each sample was prepared by immersing the crushed whole rock in heavy liquid with specific gravity 2.9 g/cm^3 to remove the heavy (chiefly ferromagnesian) minerals, then in liquid with specific gravity 2.5 to remove light material, chiefly glass and zeolites. Plagioclase formed most of the remaining sample. The sample was treated in dilute nitric acid (10 percent HNO_3) for 1–2 minutes (or until fizzing stopped) to remove calcite and some clays, then stirred in dilute hydrofluoric acid (2.5 percent HF) for 10 minutes to remove clinging glass. The resulting plagioclase concentrate, which ranges from perhaps 50 to 80 percent pure, was fused and the gas analyzed on a mass spectrometer using conventional techniques.

ACKNOWLEDGMENTS

Financial support for Conrey's chemical analyses came in part from U.S. Department of Energy Grant No. DE-FG07-84 ID 12526. Potassium-argon ages were determined by P.E. Damon and Mohammed Shafiqullah at the University of Arizona, Tucson, Ariz.

REFERENCES CITED

- Avramenko, Walter, 1981, Volcanism and structure in the vicinity of Echo Mountain, central Oregon Cascade Range: Eugene, Oreg., University of Oregon master's thesis, 156 p.

Drill hole stratigraphy and geochemistry

- Bargar, K.E., 1988 (this volume), Secondary mineralogy of core from geothermal drill hole CTGH-1, Cascade Range, Oregon, *in* Sherrod, D.R., ed., Geology and geothermal resources of the Breitenbush-Austin Hot Springs area, Clackamas and Marion Counties, Oregon: Oregon Department of Geology and Mineral Industries Open-File Report O-88-5, in press.
- Conrey, R.M., 1985, Volcanic stratigraphy of the Deschutes Formation, Green Ridge to Fly Creek, north-central Oregon: Corvallis, Ore., Oregon State University master's thesis, 349 p.
- Davie, E.I., 1980, The geology and petrology of Three Fingered Jack, a High Cascade volcano in central Oregon: Eugene, Ore., University of Oregon master's thesis, 137 p.
- Flaherty, G.M., 1981, The Western Cascade-High Cascade transition in the McKenzie Bridge area, central Oregon Cascade Range: Eugene, Ore., University of Oregon master's thesis, 178 p.
- Hammond, P.E., Geyer, K.M., and Anderson, J.L., 1982, Preliminary geologic map and cross-sections of the upper Clackamas and North Santiam Rivers area, northern Oregon Cascade Range: Portland, Ore., Portland State University Department of Earth Sciences, scale 1:62,500.
- Ingebritsen, S.E., Mariner, R.H., and Sherrod, D.R., 1988, Heat flow and hydrothermal circulation in the Cascade Range, north-central Oregon: EOS, v. 69, no. 16, p. 471.
- Keith, T.E.C., and Boden, J.R., 1980a, Volcanic stratigraphy and alteration mineralogy of drill cuttings from EWEB 3 drill hole, Clackamas County, Oregon: U.S. Geological Survey Open-File Report 80-877, 19 p.
- 1980b, Volcanic stratigraphy and alteration mineralogy of drill cuttings from EWEB 4 drill hole, Clackamas County, Oregon: U.S. Geological Survey Open-File Report 80-891, 8 p.
- 1981a, Volcanic stratigraphy and alteration mineralogy of drill cuttings from EWEB 5 drill hole, Clackamas County, Oregon: U.S. Geological Survey Open-File Report 81-91, 18 p.
- 1981b, Volcanic stratigraphy and alteration mineralogy of drill cuttings from EWEB 6 drill hole, Clackamas County, Oregon: U.S. Geological Survey Open-File Report 81-168, 15 p.
- Lux, D.R., 1981, Geochronology, geochemistry, and petrogenesis of basaltic rocks from the Western Cascades, Oregon: Columbus, Ohio, Ohio State University doctoral dissertation, 171 p.
- Priest, G.R., and Vogt, B.F. eds., 1983, Geology and geothermal resources of the central Oregon Cascade Range: Oregon Department of Geology and Mineral Industries Special Paper 15, 123 p.
- Priest, G.R., Woller, N.M., and Ferns, M.L., 1987, Geologic map of the Breitenbush River area, Linn and Marion Counties, Oregon: Oregon Department of Geology and Mineral Industries Geological Map Series GMS-46, scale 1:62,500.
- Sherrod, D.R., and Conrey, R.M., 1988 (this volume), Geologic setting of the Breitenbush-Austin Hot Springs area, Cascade Range, north-central Oregon, *in* Sherrod, D.R., ed., Geology and geothermal resources of the Breitenbush-Austin Hot Springs area, Clackamas and Marion Counties, Oregon: Oregon Department of Geology and Mineral Industries Open-File Report O-88-5, in press.
- Steiger, R.H., and Jager, E., 1977, Subcommission on geochronology: Convention on the use of decay constants in geo- and cosmochemistry: Earth and Planetary Science Letters, v. 36, p. 359-362.
- Sutter, J.F., 1978, K/Ar ages of Cenozoic volcanic rocks from the Oregon Cascades west of 121° 30': Isochron/West, no. 21, p. 15-21.
- Verplanck, E.P., 1985, Temporal variations in volume and geochemistry of volcanism in the Western Cascades, Oregon: Oregon State University master's thesis, 107 p.
- White, C.M., 1980a, Geology of the Breitenbush Hot Springs quadrangle, Oregon: Oregon Department of Geology and Mineral Industries Special Paper 9, 26 p.
- 1980b, Geology and geochemistry of volcanic rocks in the Detroit area, Western Cascade Range, Oregon: Eugene, Ore., University of Oregon doctoral dissertation, 177 p.
- Yogodzinski, G.M., 1985, The Deschutes Formation - High Cascade transition in the Whitewater River area, Jefferson County, Oregon: Corvallis, Ore., Oregon State University master's thesis, 165 p.
- Youngquist, Walter, 1980, Geothermal gradient drilling, north-central Cascades of Oregon, 1979: Oregon Department of Geology and Mineral Industries Open-File Report O-80-12, 47 p.

Chapter 3

Regional patterns of hydrothermal alteration in the Breitenbush-Austin Hot Springs area of the Cascade Range, Oregon

by Terry E.C. Keith, U.S. Geological Survey, Menlo Park, Calif. 94025

ABSTRACT

Alteration in the Breitenbush-Austin Hot Springs area is broadly zoned outward from the core of the Breitenbush anticline. Oligocene to middle Miocene rocks exhibit multiple fracturing and shearing episodes. Hydrothermal fluids with temperatures locally greater than 200 °C deposited quartz, chalcedony, smectite, mixed-layer clays, zeolites, epidote, hematite, and calcite. Alteration in the SUNEDCO 58-28 hole, which was drilled on the east flank of the Breitenbush anticline, increases downsection in a pattern similar to the increasing alteration down-structure from the flanks to the core of the Breitenbush anticline. Hydrothermal minerals in most of the SUNEDCO 58-28 drill hole indicate temperatures much hotter than present and must be relicts of an older geothermal system. From these observations, the main regional alteration occurred before folding 18-12 Ma. A 116-°C aquifer at 780 m in SUNEDCO 58-28 represents the modern geothermal system.

Alteration in upper Miocene and Pliocene rocks consists of smectite and minor amounts of zeolite minerals, most of which characteristically form at temperatures below 100 °C. Near-surface alteration at Breitenbush, Austin, and Bagby Hot Springs is localized adjacent to fractures.

The most important factor controlling the amount of alteration in the rock is fracture permeability. Temperature and fluid chemistry are important where fluids have gained access to the rocks. The best guide to interpreting the alteration is the secondary mineralogy of volcanoclastic and pyroclastic rocks, flow breccia, and vesiculated or fractured

lavas; interbedded massive lava flows are only slightly altered.

INTRODUCTION

Hydrothermal alteration is diverse in the Breitenbush-Austin Hot Springs area (Figure 1) and includes zeolite-clay, propylitic, and phyllic alteration. The alteration mineral assemblages were produced by several processes such as geothermal activity; contact effects of plutons, dikes, and lava flows; and probably deep burial in the thick volcanic pile. Conditions of temperature and fluid chemistry controlled the mineral assemblages that were formed, whereas the extent to which the rocks were altered depended upon their primary and secondary permeability and crystallinity. For example, glass-rich ash-flow and air-fall tuff was more readily altered than holocrystalline rocks. These are the significant factors that control alteration in the Breitenbush-Austin Hot Springs area and can be extrapolated to other volcanic rocks in the Cascade Range of Oregon and southern Washington.

The purpose of studying alteration patterns in the Breitenbush-Austin Hot Springs area is to interpret ancient and modern geothermal systems by characterizing their hydrothermal mineral assemblages, paragenetic sequences, and relationships to structural and stratigraphic controls. With knowledge gained from the present alteration studies, the tectonic setting and geophysical signatures of the altered rocks can be determined and the lessons applied to poorly exposed or deeply buried geothermal systems.

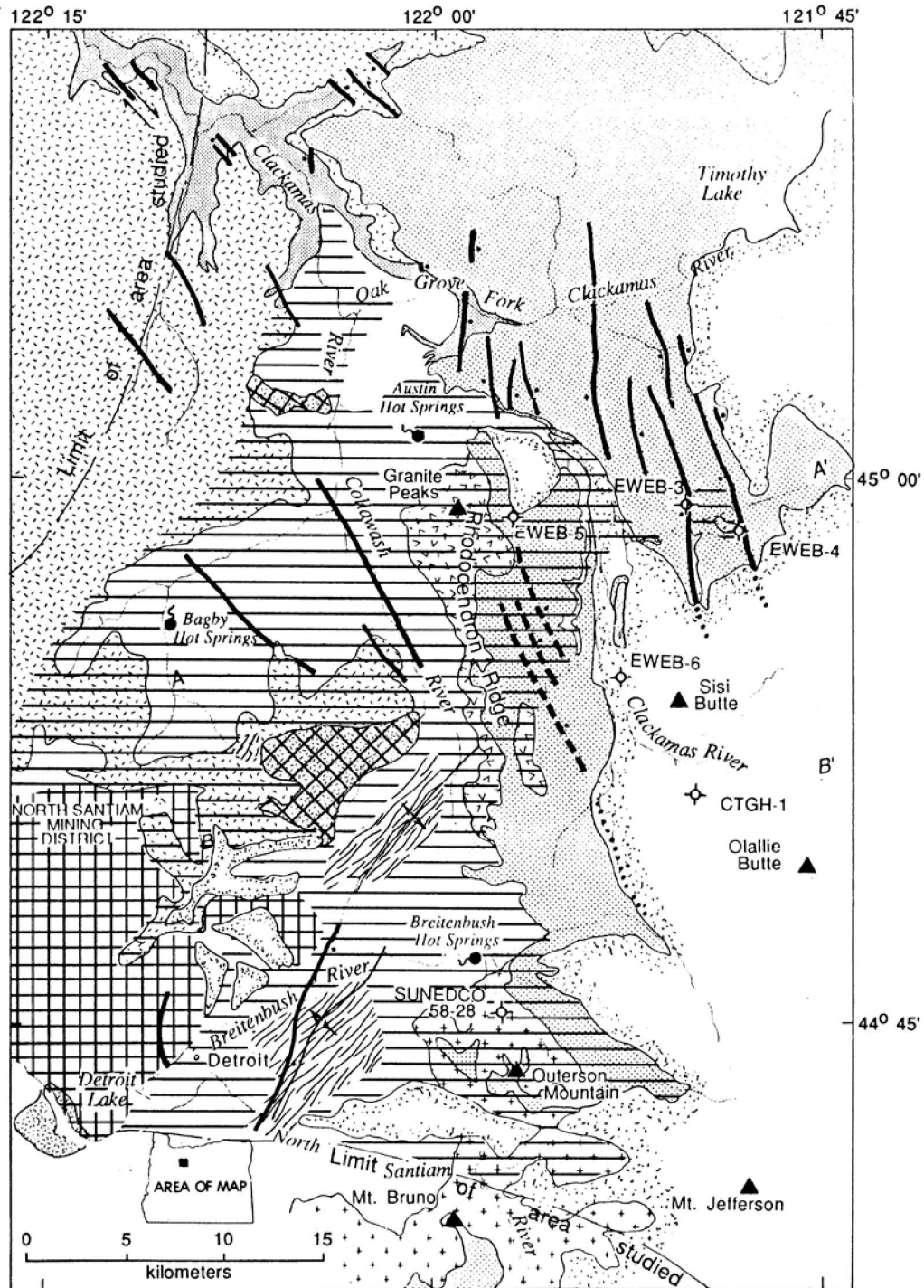

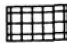




Figure 1. Reconnaissance map showing pattern of regional hydrothermal alteration in the Breitenbush-Austin Hot Springs area. Level of reconnaissance is lower in southern half compared to northern half of map. Geologic base map (shown screened) from Sherrod and Conrey (this volume).

Regional patterns of hydrothermal alteration

Alteration mineral assemblages (bold patterns)

-  Zeolite-clay—Characterized by a variety of zeolites and abundant smectite, mixed-layer clays, celadonite, and local calcite
-  Propylitic—Characterized by chlorite, illite, mixed-layer illite-smectite, mixed-layer smectite-chlorite, hematite, pyrite, quartz, calcite, and local epidote. Mostly found associated with intrusive rocks
-  Phyllic—Characterized by quartz, chalcedony, illite, sericite, hydrothermal K-feldspar, calcite, local epidote. Chiefly localized in major structural zones and in contact and brecciated zones of intrusive rocks
-  Hydrothermal alteration in plutonic rocks—Mostly clay and sericite. Locally consists of quartz, chalcedony, K-feldspar, \pm epidote. Isolated fractures and brecciated mineralized zones contain biotite, tourmaline, and sulfides in addition to previously named minerals

Lithologic and structural symbols (screened patterns)

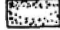


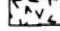

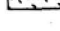










-  Volcanic rocks of the High Cascades subprovince (Pleistocene and Pliocene)—Includes rocks of similar age locally erupted in Western Cascades subprovince or that form intracanyon lava flows there
-  Andesite and dacite of the Clackamas River (Pliocene)
-  Basaltic andesite of Collawash Mountain (Pliocene and Miocene)—Includes rocks mapped as lava of Three Pyramids and younger lava by Priest and others (1987) and by Black and others (1987) south of Outerson Mountain
-  Andesite and dacite of Rhododendron Ridge (Miocene)
-  Intrusive rocks (Miocene)
-  Rhododendron Formation of Hammond and others (1982) (Miocene)
-  Lava of Outerson Mountain (Miocene)—Includes several time-equivalent units mapped by Priest and others (1987) and Black and others (1987) south of Outerson Mountain
-  Columbia River Basalt Group (Miocene)—Grande Ronde and Wanapum Basalt exposed along the Clackamas River
-  Breitenbush Formation (Miocene and Oligocene)—Includes lava of Scorpion Mountain
-  Contact
-  Fault—Short-dashed where inferred, dotted where buried. Ball-and-bar on downthrown side; arrows indicate relative strike-displacement
-  Anticline—Dotted where buried and inferred
-  Form lines on bedding in Breitenbush Formation (on cross section)
-  Line of cross section
-  Drill site
-  Hot springs

Figure 1, continued. Explanation of patterns for alteration mineral assemblages (bold), and lithology and structure (screened).

DISTRIBUTION OF ALTERATION

Regional alteration

Alteration is broadly zoned in the Breitenbush-Austin Hot Springs area (Figure 1). Generally, the most intense alteration is in the core of the northeast-trending Breitenbush anticline, where Oligocene and lower Miocene rocks have been pervasively altered to quartz and K-feldspar, with more or less illite, chlorite, and calcite. Outward from the anticlinal axis, a lower-grade assemblage is characterized by zeolites (mainly clinoptilolite and mordenite), smectite, mixed-layer smectite-chlorite, and mixed layer smectite-illite and celadonite. Superimposed on this zonation is the localized control exerted by structures such as faults and joints.

Lava flows are less altered than adjacent volcaniclastic rocks at most locales, probably owing to the greater instability of glassy material in the clastic strata. Some massive lava flows are only slightly altered, especially at the highest stratigraphic and structural levels. For example, the lower Miocene lava of Scorpion Mountain (White, 1980) is only slightly altered; alteration consists of mixed-layer smectite-chlorite or smectite replacement of mafic phenocrysts (especially olivine) and interstitial glass and deposition of clays and (or) hematite and goethite along fractures and grain boundaries. Zeolites (laumontite, analcime, stilbite, heulandite), clays, epidote, hematite, quartz, and calcite occur locally in highly fractured and sheared lower Miocene lava.

Relatively unaltered middle and upper Miocene volcanic rocks fringe the east, north, and west flanks of the Breitenbush anticline. Replacement minerals and open-space fillings in vesicular and fractured lava flows and breccia consist of smectite, zeolites (commonly chabazite, thomsonite, mesolite, scolecite, stilbite, and analcime), and calcite. In contrast, massive lava and densely welded tuff have no recognizable alteration.

Pliocene and Quaternary volcanic rocks are located chiefly along the eastern margin of the study area (Sherrod and Conrey, this volume). Pliocene rocks are only locally altered; Quaternary rocks are unaltered except for vapor-phase oxidation and fumarolic alteration in near-vent breccia. Small white to clear silica deposits (opal and cristobalite) occur in vents where a wet steam phase was present following eruptions.

Hot springs

Lava flows at Breitenbush and Austin Hot Springs are relatively unaltered except adjacent to fractures, where interstitial glass and mafic phenocrysts are altered to smectite. At Breitenbush Hot Springs the fractures are coated first with a layer of smectite, then silica (chalcedony), and finally calcite. Deposits consisting of amorphous silica and (or) calcite surround many small hot-spring orifices. Orifice deposits at Austin Hot Springs consist of amorphous silica. There are no surficial deposits at Bagby Hot Springs.

Tertiary plutons

Alteration and locally epithermal mineralization are associated with intrusive rocks in the western and central part of the area, where several small Tertiary plutons are exposed (Callaghan and Buddington, 1938; Hammond and others, 1982; Walker and others, 1985; Cummings and others, 1987; Priest and others, 1987). The alteration minerals locally indicate temperatures above 200 °C, on the basis of the assemblage epidote, quartz, hematite, calcite, sericite, and chlorite (Figure 2) and breccias that contain tourmaline, K-feldspar, and biotite. More commonly, however, the alteration indicates relatively low temperatures (less than 200 °C). The minerals probably formed during hydrothermal convection at the interface between the top of a surmised north-south-trending plutonic system and overlying volcanic rocks.

Structural controls

Major faults and folds in the southern part of the map area have fractured, brecciated zones that are cemented by multiple stages of quartz deposition along with chalcedony, calcite, illite, smectite, pyrite, and hematite. This area exposes the oldest rocks in the map area, which were buried beneath a volcanic pile at least 1-2 km thick by middle Miocene time (cross section of Priest and others, 1987). Subordinate faults and shear zones in mafic volcanic rocks throughout the map area are commonly highly altered to zeolites (laumontite, analcime, stilbite, heulandite), smectite, mixed-layer smectite-chlorite, and calcite. The major altered zones most likely represent fracture-controlled fossil geothermal systems.

SUMMARY OF DRILL HOLE ALTERATION

Cuttings from the EWEB drill holes (Keith and Boden, 1980a, b; 1981a, b) and core from CTGH-1 (Bargar, this volume) have been studied for alteration. Virtually no hydrothermal alteration was found in EWEB-3, -4, and -6, but minor zeolitic alteration (heulandite) was encountered below 46 m in EWEB-5 (Figure 2). Low-temperature smectite-zeolite alteration was prevalent in the 1,463-m-deep CTGH-1 hole, with a relatively abrupt change in zeolite assemblages at about 885 m (Bargar, this volume).

Hydrothermal minerals in the 2,457-m-deep SUNEDCO 58-28 drill hole (A.F. Waibel, unpublished data, 1982) formed in a setting much hotter than the present maximum temperature of 150 °C reported by Blackwell and Baker (this volume). Similarly, hydrothermal minerals in the zone of a 116-°C thermal aquifer at 752-782 m (Blackwell and Steele, 1987) are relicts from an older, hotter environment. Epidote first occurs at 640 m; whereas laumontite, illite, calcite, and quartz with sporadic epidote occur from about 795 m to 1,518 m. Epidote was not present below 1,518 m, but the other minerals were prevalent along with chlorite, heulandite(?), and locally, albite, hematite, and pyrite. Illite and chalcedony were identified below

Regional patterns of hydrothermal alteration

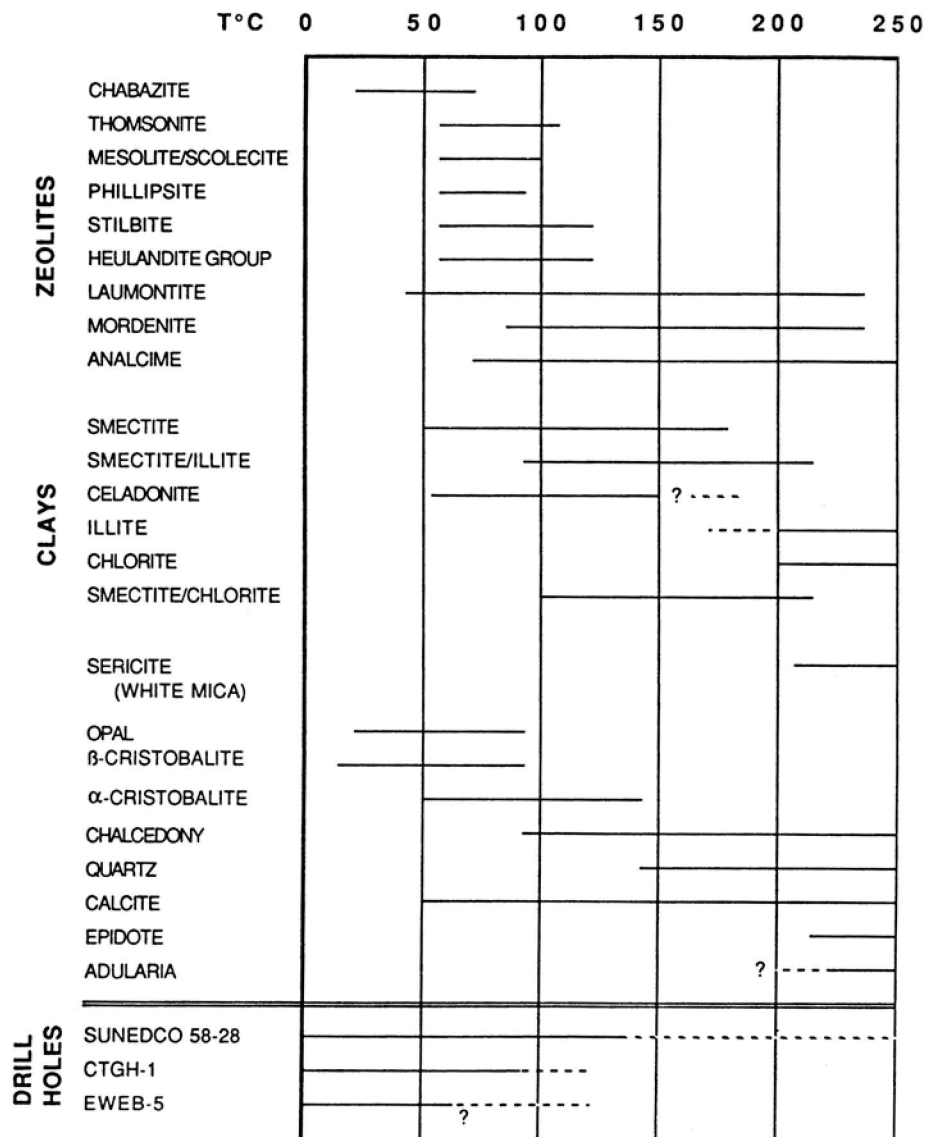


Figure 2. Selected hydrothermal minerals found in the Breitenbush-Austin Hot Springs area, plotted against temperatures of occurrence in well-defined active geothermal systems; dashed lines indicate uncertain temperature range. Shown at bottom of figure are inferred maximum temperature ranges for three drill holes in Breitenbush-Austin Hot Springs area; present maximum temperature (measured) is indicated by solid part of line, whereas past maximum temperature (inferred from alteration mineralogy) is indicated by dashed line. Drill hole data for SUNEDCO 58-28 from A.F. Waibel and T.E.C. Keith (unpublished); for CTGH-1 from Bargar (this volume); for EWB-5 from Keith and Boden, 1981a. Main sources of mineralogical information for zeolites and clays from Kristmannsdóttir and Tómasson (1978), McCulloh and others (1981), and Keith and Staples (1985); for clay minerals from Srodoń and Eberl (1984) and Horton (1985); for celadonite from Keith and others (1978) and Odom (1984); for epidote from Bird and others (1984); for adularia from Browne and Ellis (1970).

about 1,800 m, where there is substantial recrystallization of ash-flow tuff to quartz, K-feldspar, and illite (phyllitic alteration). Unfortunately, since only cuttings are available from the rotary-drilled SUNEDCO 58-28 hole, there is virtually no textural information for interpreting superimposed alteration stages.

DISCUSSION

Secondary minerals and mineral assemblages can be keys to interpreting the alteration history in the area. In Figure 2, secondary minerals found in the map area are plotted by temperature range, using information from active geothermal areas where they are being actively deposited (see figure caption for references).

Many zeolite minerals are metastable phases that formed at low temperatures, but a few are stable to about 200 °C (Figure 2). Clay minerals are also important as a guide to temperatures. To be diagnostic, however, the clay mineral structure must be determined by some method such as X-ray diffraction or differential thermal analysis, and not by color and other field techniques, which are inadequate to specify the structural state. Clay minerals have more overlap than zeolites, but they commonly occur where zeolites are unstable because of other stability factors. For example, zeolites are favored by slightly alkaline conditions, and they do not form in high $p_{(\text{CO}_2)}$ environments. The stability of mordenite and celadonite appear to be more chemically dependent. Mordenite occurs in greater abundance and at higher temperatures in siliceous rocks; celadonite, though it has the illite structure, forms at lower temperature where abundant K and Fe are available.

Alteration in the Breitenbush-Austin Hot Springs area was clearly controlled by permeability, with fractures creating sufficient permeability for the circulation of hydrothermal fluids. The controls of fluid temperature and composition were important once fluid penetrated the rock. Volcaniclastic rock, ash-flow tuff, flow breccia, and fractured and vesicular lava flows show more effects of alteration than do interbedded massive lava flows. The glassy components of volcanic rocks altered more readily than crystalline components, and poorly welded glassy tuffs altered more readily than densely welded tuffs. Epiclastic volcanic rocks, in contrast to pyroclastic rocks, apparently contained less glass and did not alter as readily under the low-temperature hydrothermal conditions characteristic of much of the Breitenbush-Austin Hot Springs area. The only alteration found in most massive lava flows is the change of interstitial glass and mafic phenocrysts (especially olivine) to clays.

Low-temperature zeolite-smectite alteration encountered in most of the geothermal holes drilled in upper Miocene and Pliocene rocks in the Breitenbush-Austin Hot Springs area could be developing at present conditions. Secondary minerals identified in EWEB-3, -4, -5, and -6,

and in the CTGH-1 core indicate that past temperatures were no hotter than present measured temperatures.

ACKNOWLEDGMENTS

This work was funded by the Geothermal Research Program of the U.S. Geological Survey.

REFERENCES CITED

- Bargar, K.E., 1988 (this volume), Secondary mineralogy of core from geothermal drill hole CTGH-1, Cascade Range, Oregon, *in* Sherrod, D.R., ed., Geology and geothermal resources of the Breitenbush-Austin Hot Springs area, Clackamas and Marion Counties, Oregon: Oregon Department of Geology and Mineral Industries Open-File Report O-88-5, in press.
- Bird, D.K., Schiffman, P., Elders, W.A., Williams, A.E., and McDowell, S.D., 1984, Calc-silicate mineralization in active geothermal systems: *Economic Geology*, v. 79, p. 671-695.
- Black, G.L., Woller, N.M., and Ferns, M.L., 1987, Geologic map of the Crescent Mountain area, Linn County, Oregon: Oregon Department of Geology and Mineral Industries Geological Map Series GMS-47, scale 1:62,500.
- Blackwell, D.D., and Baker, S. L., 1988 (this volume), Thermal analysis of the Austin and Breitenbush geothermal systems, Western Cascades, Oregon, *in* Sherrod, D.R., ed., Geology and geothermal resources of the Breitenbush-Austin Hot Springs area, Clackamas and Marion Counties, Oregon: Oregon Department of Geology and Mineral Industries Open-File Report O-88-5, in press.
- Blackwell, D.D., and Steele, J.L., 1987, Geothermal data from deep holes in the Oregon Cascade Range: *Geothermal Resources Council Transactions*, v. 11, p. 317-322.
- Browne, P.R.L., and Ellis, A.J., 1970, The Ohaki-Broadlands hydrothermal area, New Zealand: Mineralogy and related geochemistry: *American Journal of Science*, v. 269, p. 97-131.
- Callaghan, Eugene, and Buddington, A.F., 1938, Metalliferous mineral deposits of the Cascade Range in Oregon: *U.S. Geological Survey Bulletin* 893, 141 p.
- Cummings, M.L., Mestrovich, J.K., Pollock, J.M., and Thompson, G.D., 1987, Geothermal systems in the Cascade Range in Oregon: insights from a fossil system, North Santiam mining area, Western Cascades: *Geothermal Resources Council Transactions*, v. 11, p. 235-241.

Regional patterns of hydrothermal alteration

- Hammond, P.E., Geyer, K.M., and Anderson, J.L., 1982, Preliminary geologic map and cross-sections of the upper Clackamas and North Santiam Rivers area, northern Oregon Cascade Range: Portland, Oreg., Portland State University Department of Earth Sciences, scale 1:62,500.
- Horton, D.G., 1985, Mixed-layer illite/smectite as a paleotemperature indicator in the Amethyst vein system, Creede district, Colorado, U.S.A.: *Contributions to Mineralogy and Petrology*, v. 91, p. 171-179.
- Keith, T.E.C., and Boden, J.R., 1980a, Volcanic stratigraphy and alteration mineralogy of drill cuttings from EWEB 3 drill hole, Clackamas County, Oregon: U.S. Geological Survey Open-File Report 80-877, 19 p.
- 1980b, Volcanic stratigraphy and alteration mineralogy of drill cuttings from EWEB 4 drill hole, Clackamas County, Oregon: U.S. Geological Survey Open-File Report 80-891, 8 p.
- 1981a, Volcanic stratigraphy and alteration mineralogy of drill cuttings from EWEB 5 drill hole, Clackamas County, Oregon: U.S. Geological Survey Open-File Report 81-91, 18 p.
- 1981b, Volcanic stratigraphy and alteration mineralogy of drill cuttings from EWEB 6 drill hole, Clackamas County, Oregon: U.S. Geological Survey Open-File Report 81-168, 15 p.
- Keith, T.E.C., and Staples, L.W., 1985, Zeolites in Eocene basaltic pillow lavas of the Siletz River Volcanics, central Coast Range, Oregon: *Clays and Clay Minerals*, v. 33, p. 133-144.
- Keith, T.E.C., White, D.E., and Beeson, M.H., 1978, Hydrothermal alteration and self-sealing in Y-7 and Y-8 drill holes in northern part of Upper Geyser Basin, Yellowstone National Park, Wyoming: U.S. Geological Survey Professional Paper 1054-A, 26 p.
- Kristmannsdóttir, Hrefna, and Tómasson, Jens, 1978, Zeolite zones in geothermal areas in Iceland, *in* Sand, L.B., and Mumpton, F.A., eds., *Natural Zeolites: Occurrence, Properties, Use*: Pergamon Press, Oxford, p. 277-284.
- McCulloh, T.H., Frizzell, V.A., Jr., Stewart, R.J., and Barnes, I., 1981, Precipitation of laumontite with quartz, thenardite, and gypsum at Sespe Hot Springs, western Transverse Ranges, California: *Clays and Clay Minerals*, v. 29, p. 353-364.
- Odom, I.E., 1984, Glauconite and celadonite, *in* Bailey, S.W., ed., *Micas: Mineralogical Society of America Reviews in Mineralogy*, v. 16, p. 545-572.
- Priest, G.R., Woller, N.M., and Ferns, M.L., 1987, Geologic map of the Breitenbush River area, Linn and Marion Counties, Oregon: Oregon Department of Geology and Mineral Industries Geological Map Series GMS-46, scale 1:62,500.
- Sherrod, D.R., and Conrey, R.M., 1988 (this volume), Geologic setting of the Breitenbush-Austin Hot Springs area, Cascade Range, north-central Oregon, *in* Sherrod, D.R., ed., *Geology and geothermal resources of the Breitenbush-Austin Hot Springs area, Clackamas and Marion Counties, Oregon*: Oregon Department of Geology and Mineral Industries Open-File Report O-88-5, in press.
- Srodon, J., and Eberl, D.D., 1984, Illite, *in* Bailey, S.W., ed., *Micas: Mineralogical Society of America Reviews in Mineralogy*, v. 16, p. 495-544.
- Walker, G.W., MacLeod, N.S., and Blakely, R.J., 1985, Mineral resource potential of the Bull of the Woods Wilderness, Clackamas and Marion Counties, Oregon: U.S. Geological Survey Open-File Report 85-247, 27 p.
- White, C.M., 1980, Geology of the Breitenbush Hot Springs quadrangle, Oregon: Oregon Department of Geology and Mineral Industries Special Paper 9, 26 p.

Chapter 4

Secondary mineralogy of core from geothermal drill hole CTGH-1, Cascade Range, Oregon

by Keith E. Bargar, U.S. Geological Survey, Menlo Park, Calif. 94025

ABSTRACT

Geothermal drill hole CTGH-1, located about 14 km northeast of Breitenbush Hot Springs in the Cascade Range of northwest Oregon, was drilled to a depth of 1,463 m. The maximum reported temperature at the bottom of the drill hole was 96.4 °C. Minor vapor-phase (tridymite and ilmenite) and devitrification (α -cristobalite) mineralization is present in the predominantly andesitic to basaltic drill core. Red to orange iron-oxide-stained tuffaceous rocks are at least partly altered to smectite. Vesicles, fractures, and open spaces between breccia fragments are partly to completely filled by secondary minerals. Initial secondary-mineral deposits consist of Fe- and Mg-rich minerals (hematite, smectite, and celadonite), which were followed by precipitation of K-rich minerals (celadonite, wellsite, phillipsite, and adularia(?)). Later-formed deposits include Na-rich analcime, clinoptilolite, calcite(?), Ca-rich zeolite minerals (chabazite, erionite, heulandite, scolecite, and thomsonite), silica minerals (β -cristobalite, α -cristobalite, chalcedony, and quartz), and mordenite. Native copper, apatite, and wellsite precipitated in localized zones from fluids that contained sufficient Cu, P_2O_5 , and Ba. All of the above minerals are compatible with the present low-temperature conditions.

INTRODUCTION

Geothermal drill hole CTGH-1 is located about 14 km northeast of Breitenbush Hot Springs and 6 km northwest of Olallie Butte, at an elevation of 1,170 m, near the Western Cascades-High Cascades boundary in northwest Oregon. Drilling of the 1,463-m-deep core hole by Thermal Power

Company and Chevron Geothermal on a cost-sharing basis with the U.S. Department of Energy began on June 7, 1986, and was completed September 7, 1986 (University of Utah Research Institute, 1987). The hole was rotary drilled to 161-m depth and then cored to the hole bottom with essentially 100-percent core recovery. The maximum reported temperature at the bottom of the hole was 96.4 °C (Blackwell and Steele, 1987), and the temperature gradient below ~500-m depth was about 83 °C/km (Priest and others, 1987).

Drill core from the CTGH-1 drill hole is stored in the University of Utah Research Institute core library in Salt Lake City, Utah. A total of 307 core samples between the depths of 163 m and 1,463 m, consisting of fracture fillings, vug fillings, or representative samples of stratigraphic intervals, was obtained to identify the alteration minerals in the drill core and to gain a preliminary understanding of the physical and chemical conditions responsible for secondary mineralization of the drill core. The drill core samples were studied using binocular microscope, X-ray diffraction, and scanning electron microscope (SEM) methods.

Detailed stratigraphic and petrographic descriptions of upper Tertiary to Quaternary rocks recovered from the drill hole are discussed elsewhere (Conrey and Sherrod, this volume; Appendix 2). Except for two sections of andesite and dacite lava and tuff, drill core from the CTGH-1 drill hole consists predominantly of basaltic andesite to basalt lava flows, tuff, and breccia (Conrey and Sherrod, this volume). The more silicic rocks contain some vapor-phase tridymite in addition to primary minerals: quartz, plagioclase, magnetite, and pyroxene. Primary minerals of the mafic rocks are mostly plagioclase, pyroxene, magnetite,

olivine, and hornblende (identified in only one sample); α -cristobalite from devitrification occurs in several samples.

Textures of the lava flows range from massive to vesicular; fracturing ranges from moderate to very intense. Most fractures and vesicles contain at least traces of mineralization, and the majority of open spaces are partly to completely filled by secondary minerals.

SECONDARY MINERALIZATION

Drill cuttings above 161-m depth in the drill hole were not sampled for this investigation. From 163- to 622-m depth, the secondary mineralogy consists of smectite, hematite, and rarely, zeolites (chabazite, wellsite, and heulandite) (see Figure 1). Between depths of 622 m and 885 m, smectite and chabazite are the predominant alteration minerals, although significant amounts of analcime and other zeolite minerals (clinoptilolite, heulandite, phillipsite, scolecite, and thomsonite) are present with minor hematite, calcite, and apatite. Below 885-m depth, smectite remains the dominant secondary mineral and is found with celadonite, zeolite minerals (clinoptilolite, erionite, heulandite, and mordenite), and silica minerals (β -cristobalite, α -cristobalite, chalcedony, and quartz); less-abundant hematite and rare goethite, native copper, and adularia were also identified.

Hematite

Red-orange-brown iron-oxide stains are scattered throughout the CTGH-1 drill core (Figure 1) in abundances that range from a pervasive brick-red coloring of an entire specimen to microscopic orange-staining. In most cases, the iron oxide was identified as hematite by X-ray diffraction. However, a few samples appear to contain amorphous iron oxide. Much of the hematite occurs in volcanic breccia, highly vesicular basalt, or tuffaceous deposits, where it probably formed by oxidation of primary magnetite during cooling of the volcanic rocks. A few thin red hematite stains on fracture surfaces or vesicle walls in the lower part of the drill hole appear to be closely associated with later secondary mineral fillings. Similarly, soft orange-red goethite coats a fracture surface at 1,456-m depth. The only other secondary iron oxide mineral identified in the drill core is ilmenite, which occurs as black, metallic hexagonal crystals that are closely associated with vapor-phase tridymite at 440-m depth.

Smectite

Core samples from depths of 163-480 m contain light-brown to orange (locally white or pink) clay that commonly coats the exterior core surfaces and partly to completely fills open spaces in the drill core. Much of this clay is probably residual drilling mud. X-ray diffraction analyses of clays from this part of the drill core mostly show low, broad X-ray peaks that suggest poorly crystalline or even amorphous material. Several analyzed samples probably contain a

mixed-layer illite-smectite consisting predominantly of illite, on the basis of a ~ 10 Å peak that shows very slight expansion after being placed in an atmosphere of ethylene glycol at 60 °C for 1 hour. In geothermal areas, mixed-layer illite-smectite typically forms well above the <20 °C temperatures that were measured in the upper part of the CTGH-1 drill hole (Aumento and Liguori, 1986). Mixed-layer illite-smectite was not found below 403-m depth in the drill core; wherever the mineral was found in X-ray analyses of open-space fillings, it was presumed to be drilling mud residue. Most of the X-ray diffraction analyses of clays from this interval also showed a ~ 15 Å peak that expanded to ~ 17 Å after exposure to ethylene glycol, which is typical for smectite. Smectite was determined to be a component of several samples of drilling mud where it occurs alone or in association with the mixed-layer illite-smectite. In Figure 1, a few smectite samples between depths of 163 m and 480 m are classified as secondary based on the mode of occurrence. It is possible that additional secondary smectite exists in samples from this zone, but any occurrences are masked by drilling mud contamination.

Below 480-m depth, smectite (various colors but predominantly green) occurs in virtually every sampled interval as fracture coatings, vesicle wall linings, between breccia fragments, or as groundmass alteration (particularly in tuffaceous rocks). Characteristically, secondary smectite from drill hole CTGH-1 has a basal spacing of ~ 14 - 15 Å (although basal spacings as low as ~ 12 Å were noted in a few samples) that expands to ~ 17 Å with glycolation and collapses to ~ 10 Å after overnight heating at 450 °C. Measurements of the 060 X-ray peak for 12 selected clay samples from the core ranged from 1.50 Å (montmorillonite, commonly a Ca- or Na-rich smectite) to 1.52 Å (nontronite, an Fe-rich smectite) and 1.53 Å (saponite, a Mg-rich smectite) (Starkey and others, 1984) with apparent random distribution of dioctahedral (montmorillonite and nontronite) and trioctahedral (saponite) smectite species (Brindley and Brown, 1980). Semiquantitative chemical analyses of smectite were obtained using an X-ray energy dispersive spectrometer (EDS) on the scanning electron microscope (SEM). Samples from 564 m, 764 m, and 861 m contain (in addition to Si and Al) Fe > Ca > Mg; the two shallower samples also contain minor amounts of K and Ti. Using EDS, low concentrations of Na are difficult to detect, but Na is possibly present in clay from 764-m depth. The 060 peaks for these clays are too indistinct for accurate measurement on routine X-ray diffractograms. Because Fe is the predominant cation, however, these three clays are most likely dioctahedral nontronite, although trioctahedral saponite with high Fe content has been reported (Weaver and Pollard, 1973).

Celadonite

The micaceous mineral celadonite occurs intermittently below 1,130-m depth, normally as a soft, blue-green clay-like material deposited as horizontal layers (later than

Secondary mineralogy in CTGH-1 drill core

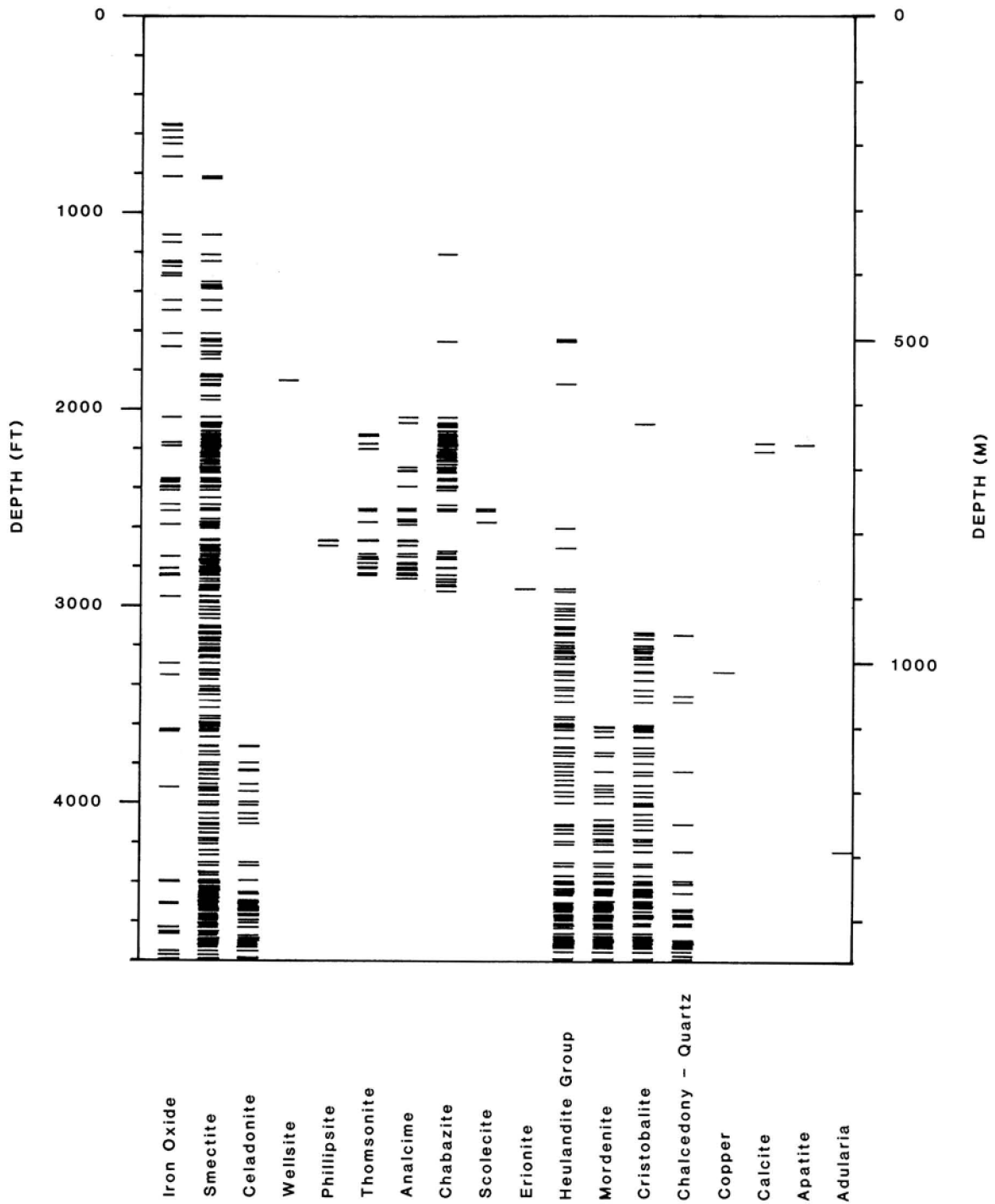


Figure 1. Distribution of secondary minerals with depth in drill hole CTGH-1.

green smectite) in cavities and fractures. In a few vesicles, the blue-green clayey layers are sandwiched between horizontal beds of medium- and dark-green smectite. At 1,133-m depth, celadonite that produces a low, broad 10-Å X-ray peak formed earlier than a heulandite-group mineral (probably clinoptilolite) and β -cristobalite. Later-formed emerald-green micaceous celadonite, characterized by a high, sharp 10-Å X-ray peak, is sprinkled on top of the β -cristobalite. A semiquantitative EDS analysis of soft blue-green celadonite from 1,133-m depth shows, in addition to Si and Al, very abundant Fe and K, and very minor Mg, Ti, Ca, and possibly Na.

Zeolite minerals

In the interval from 163 m to 622 m, the only secondary minerals other than hematite and smectite are rare occurrences of chabazite, heulandite, and wellsite. The first two of these zeolite minerals will be discussed later. Wellsite, an intermediate zeolite mineral in the phillipsite-harmotome group, was identified only in vesicles of basalt from 564-m depth. It forms randomly oriented, elongate prismatic crystals, clusters of radiating crystals, or closely spaced elongate crystals that are deposited as overlapping radiating hemispherical crystal clusters to produce a botryoidal coating. At 564-m depth, the wellsite crystals are partly coated by later smectite; however, the majority of the light- to dark-green horizontal smectite layers fill the bottoms of the vesicles and are earlier deposits. Two semiquantitative EDS analyses of wellsite show significant Ba and K, and a little Ca in addition to Si and Al. X-ray diffraction analyses of the wellsite are similar to phillipsite and harmotome, but the approximately equal proportions of Ba and K suggest that the mineral is wellsite rather than Ba-poor phillipsite or K-poor harmotome (Cerny and others, 1977).

In the interval from 622- to 885-m depth, zeolites occur with orange to green smectite and local iron-oxide staining (mostly hematite but amorphous iron oxide may be present). These minerals fill vesicles, fractures, and open spaces between volcanic breccia fragments and are dispersed in altered tuffaceous rocks. Phillipsite, an early-formed zeolite mineral in this drill core, was identified only in three samples (at 811, 812, and 821 m). At 821-m depth, colorless phillipsite crystals formed in basalt vesicles, whereas at 812-m depth the phillipsite pervasively coats open spaces in volcanic breccia, forming clusters of closely spaced elongate crystals that appear partly dissolved in scanning electron micrographs. Semiquantitative EDS analyses indicate that both samples have approximately the same chemical composition: Si, Al, and K > Ca.

At 812-m depth, phillipsite is associated with later clusters of colorless thomsonite crystals. The thomsonite crystals are usually tabular or lamellar. At 764-m depth, thomsonite crystals were deposited as irregularly oriented, tabular clusters; whereas at a depth of 767 m, the tapered, tabular thomsonite crystals form somewhat fan-shaped clus-

ters. Three analyzed samples of thomsonite from widely separated intervals have Ca, Si, and Al. Fractures and vesicles in very altered basalt at 663-m depth contain a soft, colorless, botryoidal coating that consists of hemispherical-shaped clusters of closely spaced thomsonite crystals.

The thomsonite crystals at 663-m depth are overlain by later deposits of colorless chabazite crystals. Pseudocubic rhombohedral chabazite (frequently twinned), deposited in association with earlier smectite in many open spaces, is the predominant zeolite mineral in this interval (Figure 1). Semiquantitative EDS analyses of chabazite from 634-m depth indicate Ca, Al, Si, and very minor K.

Scattered open-space deposits of colorless trapezohedral analcime crystals are closely associated with chabazite, although the depositional sequence is undetermined; in SEM, analcime was observed to have formed later than thomsonite and phillipsite. Semiquantitative analyses for analcime indicate Si, Al, Na, K, and Ca. The abundance of Ca indicates that the mineral is not a pure analcime end-member of the analcime-wairakite solid solution series and probably should be considered a "calcian" analcime (Gottardi and Galli, 1985).

Fracture fillings in drill core between 764- to 785-m depth contain radiating clusters of colorless acicular scolecite crystals that were seen in SEM to be deposited later than thomsonite, chabazite, and analcime at 767-m depth. Semiquantitative analyses by EDS indicate that the chemical constituents are Ca, Al, and Si, and the mineral is identified as scolecite rather than structurally similar Na-rich natrolite or Na+Ca mesolite (Gottardi and Galli, 1985).

An abrupt change in secondary mineralogy occurs at 885-m depth in the CTGH-1 drill hole. Except for one occurrence of chabazite at 892-m depth, the zeolite minerals discussed above are absent, and the interval is characterized by heulandite-group zeolites: heulandite and clinoptilolite. Abundant mordenite and minor erionite are also present in this part of the drill core. Early-formed reddish hematite staining is sporadically distributed through the interval. Later-formed smectite is the dominant open-space filling. Below 1,130-m depth, fracture- and vesicle-filling deposits of blue-green clayey minerals, identified as celadonite in several X-ray diffraction analyses, formed either later than green smectite or are sandwiched between horizontal green smectite layers.

Three samples between the depths of 886 m and 888 m contain acicular or columnar erionite crystals that were deposited later than green smectite. In the SEM, these columns consist of bundles of fibrous crystals. Locally the erionite crystal clusters show hexagonal cross sections and are seen to have formed earlier than associated blocky heulandite crystals at 887-m depth. An EDS analysis of erionite indicates Ca, K, Al, and Si.

Heulandite and clinoptilolite, two heulandite-group zeolite minerals, are present in the lower part of the CTGH-1 drill core. The two minerals have virtually the same

Secondary mineralogy in CTGH-1 drill core

structure and are therefore indistinguishable in X-ray diffraction analyses. Mumpton (1960) discriminated between clinoptilolite and heulandite on the basis of overnight heating at 450 °C. If the 020 X-ray peak at ~ 9.0 Å is unchanged after heating, the mineral is identified as clinoptilolite, whereas heulandite is characterized by destruction of the 020 peak. However, Gottardi and Galli (1985) favor nomenclature based on the chemical composition, as suggested by earlier workers (Mason and Sand, 1960). In this classification, heulandite should contain more Ca+Sr+Ba than Na+K, and for clinoptilolite, Na+K are dominant.

Samples containing a heulandite-group mineral, collected from 14 depth intervals, were heated overnight at 450 °C. Above 892-m depth, only one sample showed no change in peak position or intensity after heating, and the mineral is probably clinoptilolite. In the remaining samples above 892-m depth, the 020 X-ray peak was destroyed, so the mineral should be heulandite according to Mumpton's (1960) classification. Below 892-m depth, none of the heated samples showed a change in the 020 peak after heating, so presumably clinoptilolite is the only heulandite-group zeolite present.

In the distribution diagram of Figure 1, the heulandite-group minerals were combined because semiquantitative EDS analyses from CTGH-1 samples do not completely support the heulandite-clinoptilolite distinction suggested by Mumpton (1960). In heulandite from 887-m depth, Ca is undoubtedly more abundant than Na+K, as would be suggested by the heating test. Below 892-m depth, heating tests showed only the presence of clinoptilolite; however, Na+K are clearly dominant over Ca only at a depth of 983 m. In four other samples below this depth, Ca appears to be dominant over Na+K, although the difficulty in detecting Na by EDS analyses makes the distinction between clinoptilolite and heulandite unreliable when significant Ca is present.

In drill hole CTGH-1, heulandite-group zeolites, deposited in vesicles, in fractures, and between breccia fragments, formed later than hematite, smectite, celadonite, and erionite but are earlier than α -cristobalite, β -cristobalite, or mordenite in scanning electron micrographs. In SEM photographs, minor smectite appears to be deposited later than some open-space heulandite group minerals. The crystal morphology of the heulandite group minerals in drill core CTGH-1 ranges from a tabular tombstone-like habit at 1,341-m depth to a more blocky habit in samples from shallower depths.

White cottonlike mats of interwoven long thin fibrous crystals or small tufts of fibrous mordenite crystals appear to be the latest mineral deposited in many open spaces below 1,099-m depth in drill core from the CTGH-1 hole. At 1,260-m depth, an EDS analysis of mordenite showed only Ca, Al, and Si.

Silica minerals

Silica minerals (α -cristobalite, β -cristobalite, chalcedony, and quartz) from the CTGH-1 drill hole occur as open-

space deposits that formed later than most other minerals except for mordenite and minor smectite. Between depths of 956 m and 1,372 m, silica forms colorless, frosted, or bluish botryoidal deposits identified as β -cristobalite in several X-ray diffraction analyses. Deposits of β -cristobalite alternate with similar-appearing botryoidal α -cristobalite between 1,061-m and 1,372-m depth. Below 1,372-m depth, α -cristobalite is the predominant silica phase. In the SEM, β -cristobalite has a smooth, noncrystalline appearance, whereas α -cristobalite usually consists of spherical clusters of blocky crystals. However, the two minerals are best distinguished by X-ray diffraction. β -cristobalite has a broad major peak between 4.07 Å and 4.11 Å and a single minor peak near 2.50 Å; α -cristobalite has a sharp major peak between 4.04 Å and 4.07 Å and several other minor peaks. In Figure 1, α -cristobalite and β -cristobalite were combined because the presence of the two minerals was only spot checked by X-ray diffraction, and no attempt was made to determine their precise distribution.

Tiny, colorless, euhedral quartz crystals occur in vesicles from seven drill core samples. Many other open-space-filling white, colorless, yellow, or green massive silica deposits gave an X-ray diffraction pattern indicative of quartz but when viewed in refractive index liquids were observed to have a fibrous structure and are chalcedony. Chalcedony, a cryptocrystalline variety of quartz, can be distinguished from quartz in thin section or in immersion media. No attempt was made, however, to distinguish between the massive quartz and chalcedony deposits on Figure 1. Another complication arises from a few X-ray diffraction analyses of botryoidal silica that showed the presence of chalcedony in addition to α - or β -cristobalite.

Other minerals

The only other secondary minerals in this drill core are calcite, apatite, adularia, and native copper. Native copper was identified (by EDS in SEM studies) in two samples from near 1,015-m depth as an open-space deposit that formed earlier than botryoidal β -cristobalite and white smectite. The other minerals, whose mode of occurrence is unknown, were identified only in X-ray diffraction analyses from depths of 663 m and 675 m (calcite), 665 m (apatite), and 1,293 m (adularia).

DISCUSSION

Drill core from the CTGH-1 drill hole is predominantly andesitic to basaltic in composition. Early-formed vapor-phase tridymite and possibly ilmenite are present in dacitic rocks from 260-m to 339-m depth. Minor scattered α -cristobalite, formed by devitrification, is present in a few pieces of drill core. Some mafic minerals and what was probably the glassy groundmass of several drill core samples are altered to iron oxide (mostly hematite but also amorphous iron oxide) and smectite. Vesicles, fractures, and open spaces between breccia fragments are partly to com-

pletely filled by secondary minerals that include iron oxide minerals (hematite and goethite), smectite, celadonite, zeolite minerals (analcime, chabazite, clinoptilolite, erionite, heulandite, mordenite, phillipsite, scolecite, thomsonite, and wellsite), silica minerals (α -cristobalite, β -cristobalite, chalcedony, and quartz), native copper, apatite, calcite, and adularia.

Iron oxide (primarily hematite), which probably formed by the oxidation of magnetite during the cooling of lava flows, is the earliest-formed significant secondary mineral in the CTGH-1 drill core. Locally, iron- and magnesium-rich green smectite (nontronite and saponite) was deposited later than reddish iron oxide in fractures or vesicles. More than one generation of smectite was deposited in the drill hole, and some vesicles were observed to contain multiple horizontal layers consisting of different shades of green smectite. Smectite color is quite variable in the CTGH-1 drill core, and many colors (white, pink, brown, orange, and red) other than green were observed. Differences in X-ray basal spacing and position of 060 peaks suggest that some of the later smectite deposits may contain Ca, Na, or K as exchangeable cations rather than Fe and Mg.

Blue-green clay identified as celadonite was deposited later than green smectite in many open spaces and is sandwiched between horizontal green smectite in a few vesicles. Celadonite, containing abundant Fe and K, also occurs as an emerald-green micaceous deposit that is later than smectite, blue-green clayey celadonite, clinoptilolite, and β -cristobalite at 1,133-m depth.

Several zeolite minerals were deposited later than the above Fe, Mg, and K minerals. The first zeolite minerals to be deposited appear to be K-rich wellsite and phillipsite. Wellsite occurs in the upper zeolite zone along with the Ca-rich minerals heulandite and chabazite (exact order of deposition is uncertain). In the middle zeolite zone, Na-rich analcime and Ca-rich thomsonite, chabazite, and scolecite were deposited later than phillipsite. The lower zeolite zone contains Ca- and K-rich erionite along with later-formed clinoptilolite, heulandite, and Ca-rich mordenite. Silica minerals apparently were deposited later than the zeolites (except for mordenite). Beta-cristobalite and α -cristobalite alternate in open-space fillings of the lower zeolite zone. Chalcedony and quartz crystals appear to be deposited later than either cristobalite mineral in several vesicles and fractures of this lower zone. The order of deposition for apatite, calcite, and adularia is unknown because they were detected as only minor components in X-ray diffraction analyses. Native copper was deposited in a few open spaces and formed earlier than β -cristobalite and white smectite.

The paragenetic sequence of secondary minerals from this drill core suggests that rock/water interaction, initially through alteration of basaltic glass and mafic minerals, provided sufficient Fe and Mg to form the early-deposited secondary minerals. During later mineralization, K, Na, Ca, and Si were more prevalent in the fluids, and the minerals

that formed were mostly zeolites and silica minerals. Smectite and most of the zeolite minerals (Kristmannsdóttir and Tómasson, 1978) are compatible with the present low temperatures found in the drill hole. Apparently the silica minerals are compatible with temperatures below 100 °C and have been reported at similar temperatures in core from several holes drilled in the Columbia River Basalt Group (CRBG) in the Pasco Basin of south-central Washington (Benson and Teague, 1982). In fact, nearly all of the secondary minerals identified in drill hole CTGH-1 and their distribution within the drill core are remarkably similar to secondary mineral assemblages reported in the Pasco Basin drill holes by Benson and Teague (1982). The CRBG alteration minerals are attributed to formation at temperatures less than 100 °C and are characterized as diagenetic.

The secondary mineral assemblage of the CTGH-1 drill core is also similar to hydrothermal alteration mineralogy of upper Tertiary volcanic rocks in the Breitenbush-Austin Hot Springs area (Keith, this volume). Even though the depth of burial at the bottom of the CTGH-1 drill hole is nearly 1.5 km, the current high heat flow of the area (Blackwell and Baker, this volume) and the nearby hot springs suggest that low-temperature hydrothermal alteration probably played a larger role than diagenesis in creating the alteration mineralogy of the CTGH-1 drill core.

ACKNOWLEDGMENTS

The author thanks P.M. Wright of the University of Utah Research Institute (UURI) for making the drill core available for this study. R.O. Oscarson assisted in the scanning electron microscopy. R.C. Erd and L.C. Calk provided helpful reviews and constructive criticisms of the manuscript. This work was funded in part by the Geothermal Research Program of the U.S. Geological Survey.

REFERENCES CITED

- Aumento, F., and Liguori, P.E., 1986, Conceptual reservoir models through geoscientific investigations: *Geothermics*, v. 15, p. 799-806.
- Benson, L.V., and Teague, L.S., 1982, Diagenesis of basalts from the Pasco Basin, Washington-I. Distribution and composition of secondary mineral phases: *Journal of Sedimentary Petrology*, v. 52, p. 595-613.
- Blackwell, D.D., and Baker, S.L., 1988 (this volume), Thermal analysis of the Austin and Breitenbush geothermal systems, Western Cascades, Oregon, in Sherrod, D.R., ed., *Geology and geothermal resources of the Breitenbush-Austin Hot Springs area, Clackamas and Marion Counties, Oregon*: Oregon Department of Geology and Mineral Industries Open-File Report O-88-5, in press.

Secondary mineralogy in CTGH-1 drill core

- Blackwell, D.D., and Steele, J.L., 1987, Geothermal data from deep holes in the Oregon Cascade Range: Geothermal Resources Council Transactions, v. 11, p. 317-322.
- Brindley, G.W., and Brown, G., 1980, Crystal structures of clay minerals and their X-ray identification: Mineralogical Society Monograph No. 5, Mineralogical Society, London, 495 p.
- Cerny, P., Rinaldi, R., and Surdam, R.C., 1977, Wellsite and its status in the phillipsite-harmotome group: Neues Jahrbuch fur Mineralogie Abhandlungen, v. 128, p. 312-330.
- Conrey, R.M., and Sherrod, D.R., 1988 (this volume), Stratigraphy of drill holes and geochemistry of surface rocks, Breitenbush Hot Springs 15-minute quadrangle, Cascade Range, Oregon, *in* Sherrod, D.R., ed., Geology and geothermal resources of the Breitenbush-Austin Hot Springs area, Clackamas and Marion Counties, Oregon: Oregon Department of Geology and Mineral Industries Open-File Report O-88-5, in press.
- Gottardi, G., and Galli, E., 1985, Natural Zeolites: Minerals and Rocks, v. 18, Springer-Verlag, Germany, 409 p.
- Keith, T.E.C., 1988 (this volume), Regional patterns of hydrothermal alteration, Breitenbush-Austin Hot Springs area, Cascade Range, Oregon, *in* Sherrod, D.R., ed., Geology and geothermal resources of the Breitenbush-Austin Hot Springs area, Clackamas and Marion Counties, Oregon: Oregon Department of Geology and Mineral Industries Open-File Report O-88-5, in press.
- Kristmannsdóttir, Hrefna, and Tómasson, Jens, 1978, Zeolite zones in geothermal areas in Iceland, *in* Sand, L.B., and Mumpton, F.A., eds., Natural Zeolites: Occurrence, Properties, Use: Pergamon Press, Oxford, p. 277-284.
- Mason, B., and Sand, L.B., 1960, Clinoptilolite from Patagonia, the relationship between clinoptilolite and heulandite: American Mineralogist, v. 45, p. 341-350.
- Mumpton, F.A., 1960, Clinoptilolite redefined: American Mineralogist, v. 45, p. 351-369.
- Priest, G.R., Woller, N.M., Blackwell, D.D., and Gannet, M.W., 1987, Geothermal exploration in Oregon, 1986: Oregon Geology, v. 49, p. 67-73.
- Starkey, H.C., Blackmon, P.D., and Hauff, P.L., 1984, The routine mineralogical analysis of clay-bearing samples: U.S. Geological Survey Bulletin 1563, 32 p.
- University of Utah Research Institute, 1987, Cascades geothermal program, U.S. Department of Energy: Cascades Newsletter, no. 3, 3 p.
- Weaver, C.E., and Pollard, L.D., 1973, The chemistry of clay minerals: Developments in Sedimentology, v. 15, Elsevier Scientific Publishing Company, The Netherlands, 213 p.

Chapter 5

Thermal analysis of the Austin and Breitenbush geothermal systems, Western Cascades, Oregon

*by David D. Blackwell and Sydney L. Baker, Department of Geological Sciences,
Southern Methodist University, Dallas, Texas 75275*

ABSTRACT

Geothermal gradient and heat-flow data from twelve 150-m-deep, two 300-450-m-deep, and one 2,500-m-deep industry exploration holes in the area near Breitenbush and Austin Hot Springs are presented. These data are combined with previously published thermal data to analyze the geothermal systems. Distinct local geothermal gradient and heat-flow anomalies are associated with each system and can be distinguished from the regional background values of 65 ± 5 °C/km and 100 ± 10 mW/m². These anomalies are dominated by steep horizontal gradients that suggest that the systems are dominated by flow along steep fracture systems, at least to depths of 1-2 km. In the Breitenbush area, however, one component of the system may be an aquifer near the top of the Breitenbush Formation. An age of about 25,000 yr for flow in the aquifer is the best-fitting model for the temperature-depth curve in drill-hole SUNEDCO 58-28, which penetrated the aquifer between depths of 752 and 782 m. This model assumes a porosity of 15-20 percent and a velocity of flow on the order of 4-10 m/yr. The results of the deep-well geothermal gradient profile and heat-flow analysis suggest that the Breitenbush system is superficial and that temperatures of 150 °C will occur only east of the thermal manifestations and at depths in excess of 2 km. The results from the deep well also support the interpretation that the high regional heat flow and geothermal gradient at the Western Cascades-High Cascades boundary are related to midcrustal sources and not to upper crustal groundwater flow—unless the major portion of such flow is at depths of 3 km or more and at temperatures in excess of 200 °C.

INTRODUCTION

This report summarizes the thermal data in the vicinity of Austin and Breitenbush Hot Springs, two of several hot springs that occur near the boundary between the Western and High Cascades in Oregon. Both hot springs are situated east of the major thermal transition between the High Cascades and the Western Cascades described by Blackwell and others (1982); thus the regional heat flow is about 100 mW/m², and the regional gradient averages 65 °C/km. To date, published thermal data for this area are limited. Blackwell and others (1982) presented two measurements that bracket Austin Hot Springs and two measurements in the general vicinity of Breitenbush Hot Springs: one measurement made approximately 2 km to the east and one located approximately 5 km to the west of the hot springs. In addition, several values in the general region were discussed.

More recently, thermal data became available from the 2,457-m-deep Sunoco Energy Development Company (SUNEDCO) exploration hole 58-28, located approximately 4 km southeast of Breitenbush Hot Springs (Priest, 1985). The temperature-depth curve, which probably represents near-equilibrium temperatures, was logged in 1982 by Southern Methodist University (SMU) Geothermal Laboratory under contract to SUNEDCO approximately eight months after the hole was completed.

When SUNEDCO left the geothermal business, they donated part of their exploration data to SMU. Consequently, this report presents an extensive new data set for 14 holes in the Breitenbush Hot Springs area. These data have already been made available in the form of tempera-

In 1986, under a cost-sharing program with the U.S. Department of Energy (DOE), a 1,463-m-deep hole (CTGH-1) was drilled by Thermal Power Company approximately 14 km northeast of Breitenbush Hot Springs. The thermal results from that hole have been discussed by Blackwell and Steele (1987). In 1980, several holes were drilled at Breitenbush Hot Springs by resort owner Alex Beamer and logged by Oregon Department of Geology and Mineral Industries personnel. Thus, in the Breitenbush area alone, thermal data now exist for a total of sixteen 150-m-deep holes, one 300-m-deep hole, one 1,500-m-deep hole, one 2,500-m-deep hole, and the three holes at the hot springs, an unprecedented amount of data for a Western Cascades geothermal area.

Blackwell and others (1982) presented a series of models for the controls on the fluid circulation of the Western Cascades geothermal systems. The models developed in this paper will be compared to those hypothetical models in the concluding portion of this report.

Thermal data

The locations of the holes near Breitenbush Hot Springs are shown in Figure 1, and the thermal data for the

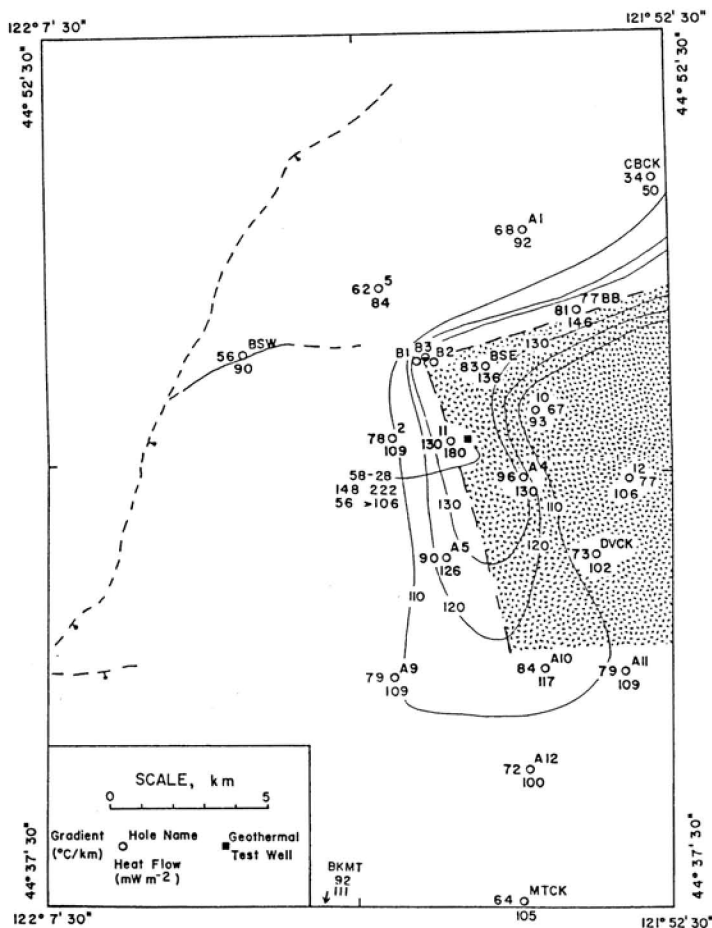


Figure 1. Map showing heat-flow sites, geothermal gradients, and heat flow in vicinity of Breitenbush Hot Springs, Oregon. Contour interval (solid lines) is 10 mW/m². Faults (dashed lines) on west half of figure from Priest and others (1987). Pattern indicates extent of geothermal aquifer as inferred from heat flow and geothermal gradient data.

holes are listed in Table 1. Temperature-depth plots illustrating most of the SUNEDCO shallow-hole data are shown in Figure 2, whereas all of the deep holes (greater than 150 m deep) are plotted in Figure 3. In addition, the OMF-7 hole at Mount Hood (Steele and others, 1982), 45-50 km northeast of Austin Hot Springs, is plotted to show a deep measurement that may approximate the background temperatures to be expected in the Breitenbush-Austin part of the Cascade Range. The three holes at the hot springs are plotted in Figure 4. All of these holes, with the exception of CTGH-1 and four holes drilled by the Eugene Water and Electric Board (EWEB) (Youngquist, 1980; Conrey and Sherrod, this volume), were sited with the explicit purpose of avoiding Pliocene and Pleistocene volcanic rocks, which are susceptible to water flow and which generally yield low-quality thermal data at depths less than 200-300 m. Because of this selectivity, the quality of the temperature-gradient data is quite high. Most of the temperature-depth curves show reasonably long linear segments, which can be confidently interpreted in terms of the average thermal gradient for each hole. The primary exceptions to this generally conductive pattern are the CTGH-1 hole, which shows an isothermal section to approximately 400 m depth, and EWEB-3, -4, and -5, which are isothermal to total depth (Blackwell and others, 1982). Of all the holes, CTGH-1 is located at the highest elevation and passes through the thickest section of young volcanic rocks.

Linear temperature-depth curves are measured below a depth of 30-40 m in all of the 150-m-deep holes except BR2, and even in this shallow well, the interval from 40 to 80 m has a reasonably linear curve. The holes at high elevation are distinct on the temperature-depth plot (Figure 2) because of the lower surface temperature and slightly lower observed gradients. In the plots shown in Figure 2, the holes in the valleys with normal gradient are similar to the holes in the thermally anomalous region (with the exception of BR11). The close correspondence of the observed temperature-depth arrays to those predicted on the basis of heat conduction theory alone is evidence that rocks of the Breitenbush Formation generally have low permeability.

Many of the holes in the Western Cascades are in or near valley bottoms, so corrections for the steep topography characteristic of this region decrease the observed gradients by 20-30 percent (see Blackwell and others, 1980, for a more detailed discussion). A two-dimensional correction has been applied to the holes, although topography is not two-dimensional in many cases. A more extensive and complicated three-dimensional correction is beyond the scope of this study.

In view of the consistent results, however, it is unlikely that the three-dimensional corrections would increase precision, particularly because lithologic and (or) thermal conductivity information are unavailable for most of the exploration holes and because locations are uncertain

for several of the critical sites. Some conductivity measurements were made on cuttings from the 300-m-deep hole BRET77BB (J. Combs, unpublished data, 1978); consequently the heat-flow value is more accurate for that hole.

An attempt was made to estimate thermal conductivity on the basis of geologic units exposed near each hole. However, the formations cannot be characterized with measurements currently available. Fortunately, the variation in thermal conductivity associated with typical near-surface rocks in the Cascade Range is quite small. Thermal conductivity ranges from approximately 1.2 to 1.6 W/m/K in the upper part of the Breitenbush Formation in SUNEDCO 58-28 (Blackwell and Steele, 1987) and in the post-18-Ma volcanic rocks of the area (see Blackwell and others, 1982). As an approximation, therefore, the thermal conductivity has been assumed to be 1.4 ± 0.2 W/m/K, with an error of about ± 15 percent. In the thermal data shown in Table 1, estimated values of thermal conductivity are given in parentheses.

A lithologic log and thermal conductivity measurements on cuttings are available for the 2.5-km-deep SUNEDCO 58-28 hole (A.F. Waibel and D.D. Blackwell, unpublished data). Also, extensive thermal conductivity information is available on core samples from the CTGH-1 well. The heat flow for these holes has been calculated and is briefly discussed by Blackwell and Steele (1987).

The SUNEDCO 58-28 hole has a complicated temperature-depth curve. The shape of the curve is explained by transient heating associated with lateral flow of hot water in a confined aquifer, as is common in geothermal systems (see Ziagos and Blackwell, 1985). The temperature-depth curve for SUNEDCO 58-28 has a peculiar jog of about 5 °C at 800 m, almost exactly the inferred aquifer position. Flow from that horizon was never tested because an intermediate string of casing was set at 799 m. Diment and others (1985) noted a similar offset in the temperature-depth curve for a well in the shallow aquifer in Long Valley (well Chance 1). They attributed the offset to a disturbance caused by the end of the casing in the aquifer. When SUNEDCO 58-28 was logged (eight months after completion of drilling), the mud in the hole was very viscous, and the probe moved down very slowly, finally sticking at 1,600 m. The distribution of mud in the hole also may have created temperature offset. Additional aspects of the SUNEDCO 58-28 temperature-depth curve will be discussed in detail in a subsequent section of the report.

Heat-flow results

The temperature gradients show a systematic pattern after corrections for topography. They are highest in two linear zones intersecting at Breitenbush Hot Springs (Figure 1). One of these zones extends east-west along the Breitenbush River and is collinear with a fault to the east mapped by Priest and others (1987). The second zone, which trends north-south and is 3-5 km wide, includes

Table 1. Geothermal data for Breitenbush-Austin Hot Springs area, Cascade Range, Oregon

Twn./Rng. section ¹	Tectonic province ²	Lat. (N)	Long. (W)	Hole no. Date logged	Collar elev. (m)	Depth ³ (m)	Thermal conductivity ⁴ (W/m/K)	No. ⁵	Uncorrected gradient ⁶ (°C/km)	Corrected gradient ⁶ (°C/km)	Corrected heat flow (mW/m ²)	Quality of data ⁷	Lithologic summary of drilled strata
6S/7E 21CD	WH	45°01.77'	121°57.74'	RDH-AHSE 6/29/77	603	10-40	1.47±0.07	4	231.6±8.7	162.8	240	G	Basalt, andesite, tuff
6S/7E 29ABA	WH	45°01.50'	121°58.40'	77AHS 3/23/78	573	0-460	1.67±0.13		174.0	140.0	231	G	Basalt, tuff, pyroclastics
6S/7E 30BBC	WH	45°01.33'	122°00.55'	AHS-H1 6/05/86	524	0-20	--	0	2250.0	--	--	G	do.
				do.		20-297	(1.4)	0	258	205	301	G	do.
6S/7E 30BB	WH	45°01.33'	122°00.54'	RDHCRAHS 9/30/76	512	95-130	1.65±0.08	9	240.7±2.0	169.5	280	G	Basalt, tuff, silicic lava
6S/6E 34CD	WH	44°59.95'	122°03.76'	RDHCRCR 9/30/76	487	10-150	1.64±0.04	9	81.8±0.5	65.0	106	A	Diorite sill, basalt
7S/8E 5DD	HC	44°59.01'	121°50.83'	EWEB-3 10/30/79	975	70-185	1.58±0.04	10	4.5±0.8	--	--	X	Basalt
7S/7E 4DD	HC	44°58.99'	121°57.01'	EWEB-5 11/13/79	1273	165-190	1.62±0.04	10	--	--	--	X	Basalt
7S/8E 10AD	HC	44°58.53'	121°48.43'	EWEB-4 10/18/79	1140	110-137	1.45±0.10	10	--	--	--	X	Basalt
7S/5E 22AA	WH	44°57.12'	122°10.39'	CR-BHS 9/30/76	655	20-90	1.46±0.05	7	84.3±1.0	66.8	97	B	Basalt, claystone
8S/8E 6DD	HC	44°54.35'	121°52.89'	EWEB-6 4/29/80	860	150-460	1.49±0.13	20	71.5±1.1	63.3	95	B	Basalt, andesite
8S/8E 28	HC	44°51.10'	121°49.90'	CTGH-1 8/06/87	1146	500-1465	1.38±0.06	7	81.7	79.8	110	A	Basaltic andesite
8S/8E 31C	HC	44°50.02'	121°52.86'	RDH-CBCK 9/28/79	1072	70-98	1.47±0.08	3	37.8±1.4	34.0	50	C	Basaltic andesite
8S/5E 31CC	WC	44°49.87'	122°14.78'	CDRCK 10/26/77	705	35-345	1.80±0.33		32.3±0.5	28.6	51	A	Volcanics
9S/7E 3CA	WH	44°49.10'	121°56.10'	BRA1 9/30/81	1219	30-138	(1.38)	0	63.5±0.5	67.5	(92)	C	Weathered volcanics
9S/7E 7DDB	HC	44°48.10'	121°59.50'	BR5 9/30/81	957	50-150	(1.38)	0	55.4±0.3	61.7	(84)	C	Altered tuff
9S/7E 14ACA	WH	44°47.74'	121°54.75'	BRET77BB 3/11/78		80-360	1.80±0.09		100.8±0.5	81.4	146	G	Basalt, tuff

Notes at end of table

Table 1, (continued).

Twn./Rng. section ¹	Tectonic province ²	Lat. (N)	Long. (W)	Hole no. Date logged	Collar elev. (m)	Depth ³ (m)	Thermal conductivity ⁴ (W/m/K)	No. ⁵	Uncorrected gradient ⁶ (°C/km)	Corrected gradient ⁶ (°C/km)	Corrected heat flow (mW/m ²)	Quality of data ⁷	Lithologic summary of drilled strata
9S/7E 20AA	WH	44°46.93'	121°58.35'	BEAMER3 4/29/80	677	5-35	1.27±0.13	6	1097.0	1097.0	1393	G	Tuff, clay, basalt
				do.		0-310	1.55±0.13	18	<277.2	<261.0	<404	G	do.
9S/7E 20AC	WH	44°46.87'	121°58.62'	BEAMER1 4/29/80	682	0-150	(1.46)	0	600.0	521.7	764	G	Tuff, clay, basalt
9S/7E 20AD	WH	44°46.83'	121°58.27'	BEAMER2 4/29/80	680	6-74	1.27±0.13	5	407.3±40.3	339.4	430	G	Tuff, clay, basalt
9S/7E 21AD	WH	44°46.73'	121°57.11'	RDH-BHSE 9/30/76	725	30-90	1.18	7	109.7±2.4	97.5	115	G	Tuff, basalt, claystone
				do.		90-150	1.65	5	92.9±1.4	82.6	136	G	do.
9S/7E 27ADA	WH	44°45.99'	121°55.70'	BR10 9/30/81	828	30-153	(1.38)	0	94.9±0.7	67.3	93	C	Andesite, basalt, tuff
9S/7E 29CCB	WH	44°45.60'	121°59.20'	BR2 9/30/81	939	70-84	(1.38)	0	83.4±3.7	78.0	109	C	Basalt, tuff
9S/7E 28CDA	WH	44°45.55'	121°57.55'	SUNEDCO 58-28 8/12/82	823	250-856	1.51	5	148.0	148.0	222	G	Oligocene and Miocene tuff
				do.		0-2457	1.88	13	56.0	56.0	105	B	do.
9S/7E 28CCD	WH	44°45.50'	121°57.85'	BR11 9/16/80	878	120-153	(1.38)	0	146.0±3.8	130.0	180	G	Soft gray clay
				do.		60-110	(1.38)	0	189.8±1.1	172.5	238	G	do.
9S/7E 34DBB	WH	44°44.95'	121°56.20'	BRA4 9/30/81	939	20-150	(1.38)	0	103.6±0.2	96.2	130	G	Basalt, basaltic andesite
9S/7E 36BAD	HC	44°44.80'	121°53.60'	BR12 10/02/81	895	50-154	(1.38)	0	86.7±0.5	77.3	107	C	Altered basalt, andesite
10S/5E 3DCC	WH	44°43.69'	122°10.76'	FS-DRSWW 6/26/78	518	10-170	(1.17)	0	52.0	43.0	51	C	Western Cascades volcanics
10S/7E 9BBC	HC	44°43.55'	121°57.95'	BRA5 9/30/81	1329	115-152	(1.38)	0	68.6±0.6	92.6	126	G	Basalt, basaltic andesite
				do.		10-110	(1.38)	0	69.9±2.4	99.9	138	G	do.

Notes at end of table

Table 1, (continued).

Twn./Rng. section ¹	Tectonic province ²	Lat. (N)	Long. (W)	Hole no. Date logged	Collar elev. (m)	Depth ³ (m)	Thermal conductivity ⁴ (W/m/K)	No. ⁵	Uncorrected gradient ⁶ (°C/km)	Corrected gradient ⁶ (°C/km)	Corrected heat flow (mW/m ²)	Quality of data ⁷	Lithologic summary of drilled strata
10S/7E 11AA	HC	44°43.44'	121°54.37'	RDH-DVCK 11/05/79	1194	70-150	1.40±0.04	10	83.5±1.6	72.6	102	B	Volcanics
10S/7E 23BCB	HC	44°41.60'	121°55.55'	BRA10 9/30/81	817	85-152	(1.38)	0	115.6±0.5	84.2	117	C	Basalt, basaltic andesite
10S/7E 24ACB	HC	44°41.60'	121°53.65'	BRA11 10/01/81	975	50-145	(1.38)	0	87.4±0.4	78.9	109	C	Andesite, dacite
10S/7E 20CBB	WH	44°41.45'	121°59.20'	BRA9 9/30/81	640	75-153	(1.38)	0	104.3±0.9	78.4	108	C	Welded and unwelded tuff
10S/7E 34ACA	HC	44°39.90'	121°55.95'	BRA12 9/30/81	780	50-150	(1.38)	0	84.8±0.4	71.8	100	C	Andesite, basaltic andesite
11S/7E 10D	HC	44°37.58'	121°56.11'	RDH-MTCK 10/07/80	762	0-108	1.64±0.13	4	68.4±3.7	64.0	105	D	Basaltic andesite, mudflows
11S/6E 22DBD	WH	44°36.01'	122°03.39'	BUCK MTN 10/08/80	1333	28-76	1.21±0.08	3	54.9±5.2	63.6	77	D	Andesite, clay
				do.		66-76	1.21±0.08	3	79.0±2.9	91.6	111	C	do.

Notes:

- ¹ Cadastral (township, range, section). Letters after section number indicate location of well in section as shown in Figure T-1 at right.
- ² WH = Western Cascades-High Cascades boundary; HC = High Cascades; WC = Western Cascades.
- ³ Indicates depth range across which geothermal gradient was measured.
- ⁴ Parentheses around the thermal conductivity values indicate estimate from surrounding well or wells. Hyphens indicate no measurements made or calculated. ± is standard error.
- ⁵ Number of thermal conductivity measurements made.
- ⁶ Hyphens indicate no measurement or calculation. ± is standard error.
- ⁷ Quality: A, 100-m linear gradient and several core conductivity values, estimated error ±5%; B, linear gradient, estimated error ±10%; C, disturbed gradient, uncertain thermal conductivity, estimated error ±25%; D, gradient ±10%, heat flow error unknown; G, geothermal system; X, gradient disturbed by regional groundwater flow.

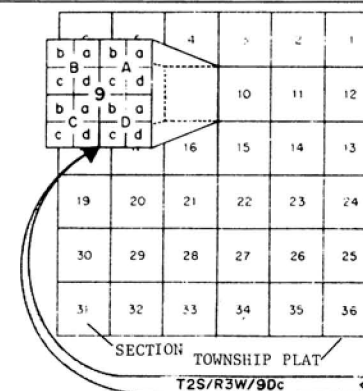


Figure T-1 (see note 1 in this table)

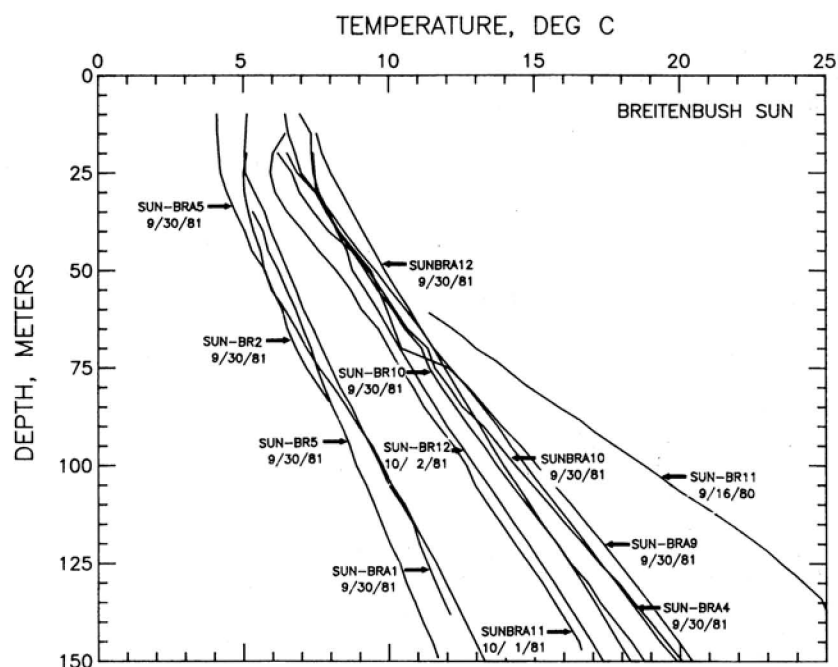


Figure 2. Temperature-depth plots for several SUNEDCO 150-m-deep gradient test holes. Temperatures were measured every 5 m.

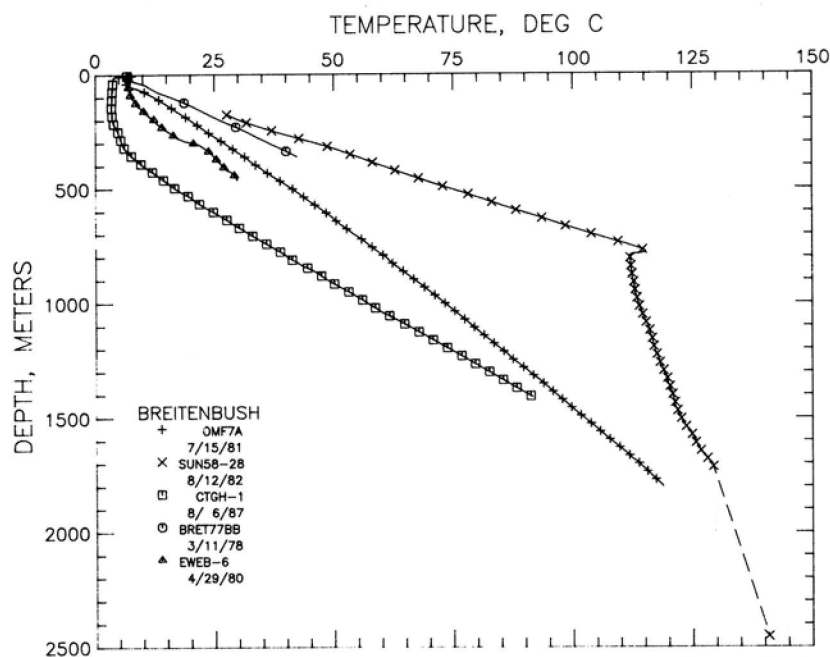


Figure 3. Temperature-depth plots for holes deeper than 150 m in the vicinity of Breitenbush Hot Springs. Only selected points are shown for each hole. Included for comparison are the OMF-7a data from a 1,837-m-deep hole drilled at Old Maid Flat near Mount Hood. Dashed line connects last point on equilibrium-temperature log to nonequilibrium bottom-hole temperature measurement.

holes SUNEDCO 58–28, BRA5, and perhaps BRA10. Details of the pattern are uncertain because of uncertain locations (and consequently, terrain corrections) for two critical holes: BR10 and BR12. On Figure 1, both holes are plotted in their most likely positions (resulting in low gradients). For example, the location of BR12 is shown in a valley bottom, where the terrain-corrected gradient is 77 °C/km and heat flow is 106 mW/m², and is not plotted on a hillside (as shown by Priest and others, 1987), where the corresponding values would be 105 °C/km and 142 mW/m². Similarly, an alternative but unlikely location for BR10 is about 2 km east of its position as plotted in Figure 1 (approximately 0.5 km northwest of SUNEDCO 58–28), in which case its corrected gradient would be 92 °C/km and corrected heat flow would be 126 mW/m².

Holes BR10, BR12, DVCK, BRA10, BRA11, and BRA12 all have slightly higher gradients than the regional average (65±5 °C/km). However, since thermal conductivity values are not available for the BR wells, the actual heat-flow values could be either equal to or above the regional average. In either case, the geothermal gradient appears to be higher east of the north-south-trending zone of high heat flow than west of it. Regardless, an area of 30–50 km² at the east margin of the Western Cascades has anomalous thermal conditions. Within this region, typical temperature gradients are on the order of 100 °C/km, and typical heat-flow values average approximately 135 mW/m². The

values are 30–50 percent above the regional background, indicating that a significant thermal anomaly associated with Breitenbush Hot Springs actually encompasses an area much larger than the hot springs themselves.

The highest temperatures that have been measured are approximately 111 °C in one well at the hot springs and approximately 116 °C at a depth of 800 m in SUNEDCO 58–28, although 137 °C was recorded by a maximum-reading thermometer during the drilling of the well (A.F. Waibel, unpublished data). The geochemistry of the hot springs suggests that the temperature of water in the system might be as high as 195 °C (Brook and others, 1979).

The shape of the temperature-depth curve in SUNEDCO 58–28 is peculiar (Figure 5). The temperature increases rapidly with a temperature gradient of 148 °C/km to a temperature of 116 °C at 800 m. Below this depth, the temperature gradient is almost zero, with a gradual increase to about 20 °C/km at 1,600 m. The bottom part of the hole had filled with mud, so the logging tool did not penetrate to the bottom of the hole. The only bottom-hole temperature data available are a series of maximum-temperature-reading runs. The maximum temperature was at least 141 °C 25 hours after the hole had been completed.

The data do not allow a simple extrapolation to equilibrium, but a bottom-hole temperature in the range of 145–150 °C is conservative. In this case, the temperature gradient asymptote in the bottom part of the hole would be

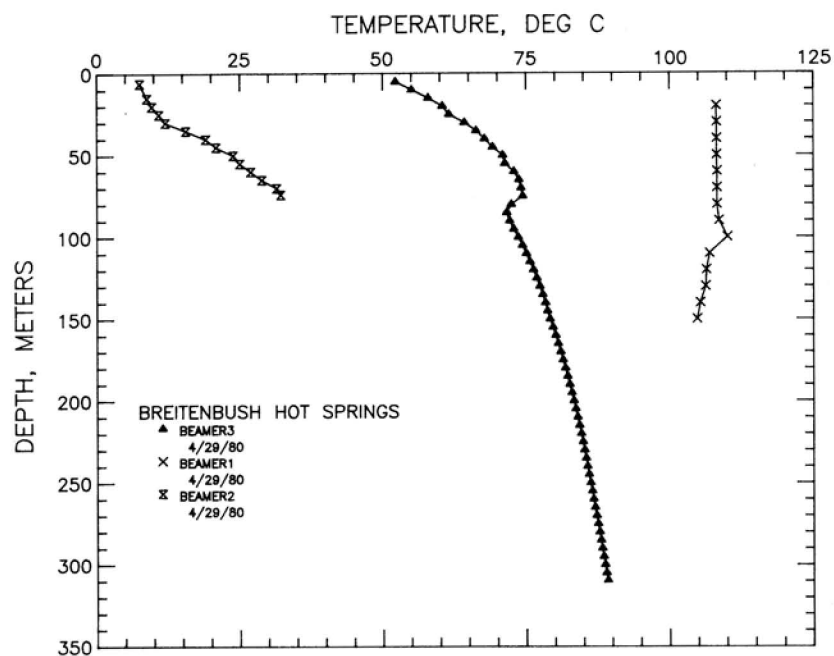


Figure 4. Temperature-depth plots for wells at Breitenbush Hot Springs.

40-50 °C/km, as shown by the dashed portion of the temperature-depth curve in Figure 5. The inferred background temperature is very close to that observed in the Old Maid Flat hole (OMF-7A; see Figure 3), a 1,837-m-deep geothermal-gradient hole drilled at Old Maid Flat, about 10 km west of Mount Hood and 45-50 km northeast of Austin Hot Springs. The temperature gradient would be expected to decrease with depth, because SUNEDCO 58-28 is drilled in a topographically low area relative to surrounding terrain (negative topographic effect). In addition, thermal conductivity increases 50 percent or more downhole (even if the temperature effect on the thermal conductivity is included), so that the geothermal gradient should decrease significantly between the surface and 2.5 km even if no disturbing influences were present. The 25-°C values of bulk thermal conductivity in the bottom part of the hole are 3.3 W/m/K. These values have been reduced to estimated *in situ* values of 2.3 W/m/K below 800 m to account for the change in thermal conductivity that results from increasing temperature and decreasing porosity. Using this value and a gradient of 45 °C/km, the heat flow in the bottom part of SUNEDCO 58-28 would be approximately 106 mW/m². Therefore, the bottom-hole temperature, the inferred geothermal gradient, and the heat flow in the bottom part of the well are values that would be expected to occur on a regional basis.

On the other hand, the heat flow value of 222 mW/m² observed above 800 m (Blackwell and Steele, 1987) and temperatures at 800 m in SUNEDCO 58-28 are definitely anomalous with respect to the regional values and are explained by geothermal fluid in an aquifer located at about 780-800 m that has introduced a transient temperature anomaly. This aquifer has been correlated by A.F. Waibel (personal communication, 1985) with a quartz-rich tuff in the Breitenbush Formation on the basis of mapping by Priest and others (1987) and is shown on their cross section A-A'. The tuff dips approximately 10° eastward and crops out in the Breitenbush Hot Springs area. It appears, therefore, that the high temperatures in the well and at the springs might be associated with geothermal fluid in an aquifer that intersects the surface in the topographically low area near the springs. On Figure 1, the area bounded by the dashed lines and shown by pattern coincides with the area thermally disturbed by this geothermal aquifer. The northern and western boundaries of flow are delineated, but the eastern and southern boundaries are undefined.

If the flow is in a stratigraphically controlled aquifer, the situation is analogous to overturns of temperature described from wells in the caldera of Long Valley, Calif. (Blackwell, 1985). At Long Valley, the surface manifestations, which are scattered over a distance of approximately 10 km, are associated with an extremely rapid fluid flow in

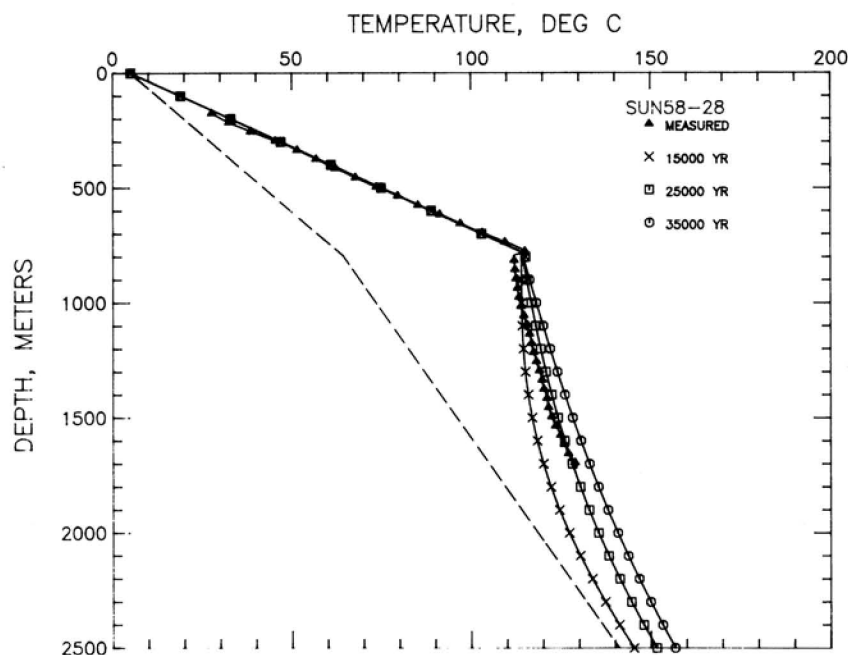


Figure 5. Comparison of calculated and measured temperatures in SUNEDCO 58-28. Curves were calculated using the model of Ziagos and Blackwell (1985) with aquifer parameters summarized in Table 2b and for times indicated on the figure. Dashed line represents inferred background temperatures that would occur in the absence of the transient thermal anomaly.

Table 2. (A) Thermal characteristics of hot springs and (B) parameters for modeling flow in Breitenbush

A.			
	Breitenbush	Austin	Bagby
Flow Volume (l/s)	57 (5.7x10 ⁴)	16 (1.6x10 ⁴)	17 (1.7x10 ³)
Spring Temperature	92	91	58
Reservoir Temperature* (°C)	195	104	100
(Sulfate Geothermometer)*	181		
Total Heat Loss (T ₀ = 10 °C) (W)	4.4x10 ⁷	6.3x10 ⁶ (11.4x10 ⁶)	6.4x10 ⁵
Convective Heat Loss (W)	2.2x10 ⁷	5.4x10 ⁶	3.4x10 ⁵
Conductive Heat Loss (W)	2.2x10 ⁷	0.9x10 ⁶ (6.0x10 ⁶)	3.0x10 ⁵
Area to Generate Heat (km ²)	440	63-114	3
Area of Anomalous Heat Flow (km ²)	110-220	6 (40)	?
B.			
Aquifer Thickness (m)			30
Aquifer Width	4 km with 15% porosity gives flow velocity of (m/yr)		9.9
	6 km with 25% porosity gives flow velocity of (m/yr)		4.0
Average Thermal Conductivity	0-800 m (W/m/K)		1.53
	800-2500 m (W/m/K)		2.30
Flow Parameter [†]	$\alpha = Kr/VMC$		0.38-0.25

* Reservoir temperatures from Brook and others, 1979

† Kr is rock thermal conductivity, V is fluid velocity, M is mass per area of fluid in aquifer, and C is fluid heat capacity.)

very shallow aquifer (on the order of 50-200 m deep). Water in the aquifer is moving on the order of 100 m/yr, (quite high for ground-water flow). In many wells at Long Valley, temperatures are 50-100 °C higher in shallow parts of wells than in deep sections, and one well shows two separate temperature spikes. The hot water, initially at 200-250 °C, cools in a predictable way eastward until it finally exits in a number of hot springs at temperatures of 100 °C or less. Deep drilling has shown that the area of thermal manifestations at Long Valley, Calif., is not underlain at depth by a high-temperature region.

The setting at the Breitenbush Hot Springs could be considered analogous to Long Valley, although at Breitenbush the aquifer is much deeper and is confined by about 800 m of low-permeability rocks. Given the fact that high-temperature fluids probably underlie an area 30-50 km² near Breitenbush Hot Springs, an important question to be answered is: what are the temperatures on the aquifer at various locations? That question will be addressed in the following section.

Analysis of the Breitenbush geothermal system

Unlike the Long Valley situation, there is only a limited amount of information available for the geothermal aquifer at Breitenbush Hot Springs. A discharge rate of 3,400 l/min has been estimated for Breitenbush Hot Springs (Brook and others, 1979). The water exits at 90 °C but reaches over 110 °C at shallow depth (Figure 4). Geochemical thermometers suggest temperatures as high

as 195 °C somewhere within the geothermal system. If it is assumed that the geochemically defined temperature represents the initial temperature of the aquifer, then the total heat lost by the system, approximately 3 x 10⁷ W, is defined as the product of fluid-loss rate at the hot springs multiplied by the heat that would be lost in cooling the water from 195 °C to ambient temperature. This heat-loss value is typical of many medium-sized geothermal systems such as Leach Hot Springs in Nevada (Welch and others, 1981) and Roosevelt Hot Springs in Utah (Ward and others, 1978).

The general characteristics of the Breitenbush aquifer are very poorly known. By making some assumptions, however, a simple model of the aquifer can be constructed. The aquifer is assumed to be 30 m thick on the basis of the temperature-depth curve. Assuming (1) a porosity of 15-20 percent and (2) a uniform water flow throughout the approximately 4-6 km width of the aquifer (although obviously it must be concentrated near the exit point at the hot springs), then the velocity of flow in the aquifer is on the order of 4-10 m/yr.

Using the known thermal parameters listed in Table 1 and the assumed parameters for the geothermal aquifer described above and summarized in Table 2, the aquifer temperatures were modeled by the technique of Ziagos and Blackwell (1985) as applied by Blackwell (1985) to the Long Valley geothermal system. The model was modified to include a two-layer thermal conductivity distribution as actually observed in SUNEDCO 58-28 (see Table 2). The

results are shown in Figure 5, which compares modeled temperature-depth curves to the observed temperature-depth curve. The best-fitting model requires a mean background gradient of 54 °C/km and an age of about 25,000 yr for flow through the aquifer. Because of the uncertain bottom-hole temperature, a perfect match to the observed temperatures was not attempted.

AUSTIN HOT SPRINGS

In addition to the data from Breitenbush Hot Springs, Table 1 lists a 450-m-deep hole drilled near Austin Hot Springs by SUNEDCO (77AHS), a hole drilled in 1986 by land owner George Heidgerkin (AHS-H1), and three shallow holes already available in the literature (Blackwell and others, 1982); the geothermal gradients are plotted in Figure 6. The Heidgerkin well was artesian when logged, so the high apparent surface temperature of the hole is not real. The bottom-hole temperature, 81.8 °C at 285 m, is remarkably similar to the bottom-hole temperature of 83.1 °C at 451 m in well 77AHS (J. Combs, unpublished data, 1978), and both are consistent with the gradients in shallow holes AHSE and CR-AHS. The location of these holes and additional background data from Blackwell and others (1982) are shown on Figure 7. This figure is at the same scale and covers the same area as the summary geologic map in Sherrod and Conrey (this volume).

Unfortunately, the same detailed coverage of geothermal gradient test holes that exists for the Breitenbush area is not available for the Austin area; furthermore, no detailed geology is available for Austin. It is significant that two wells 2.5 and 3 km east of the hot springs indicate heat flow and water temperatures as high as those observed in a well at the springs. The extent of the thermal anomaly is substantial, even if confined to the Clackamas River canyon.

The heat-loss rate at Austin is 2.2×10^7 W, based on a surface temperature of 10 °C, observed flow rate of 950 l/min, and an inferred reservoir temperature of 104 °C. The sulfate geothermometer suggests temperatures as high as 181 °C (Brook and others, 1979), requiring a heat loss rate of 4.1×10^7 W, a heat loss rate comparable to that at Breitenbush Hot Springs (see Table 2). With a spring temperature of 91 °C at Austin, the convective heat loss is 1.9×10^7 W, so that the apparent conductive heat loss is between 0.3×10^7 and 2.2×10^7 W. Given the measured surface heat flow of 250 mW/m² (150 mW/m² above background), a minimum area of 20-146 km² must be involved in the surface loss of heat from the system. The range in values is a function of the uncertain reservoir temperature.

Austin and, even more so, Bagby Hot Springs represent a westward limit of distance (about 30 km) from the axis of the High Cascades (Cascade Range crest) for significant hot-spring discharge. Similarly, the back-

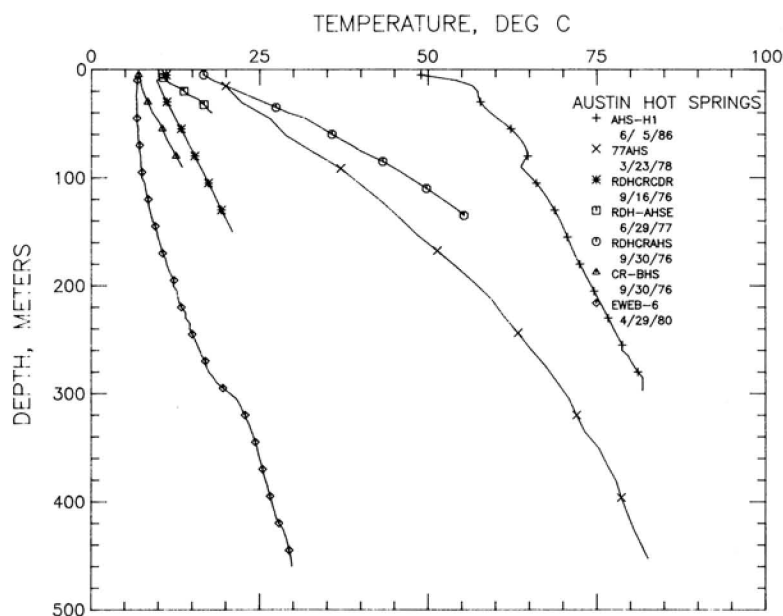


Figure 6. Temperature-depth plots for holes in the vicinity of Austin Hot Springs.

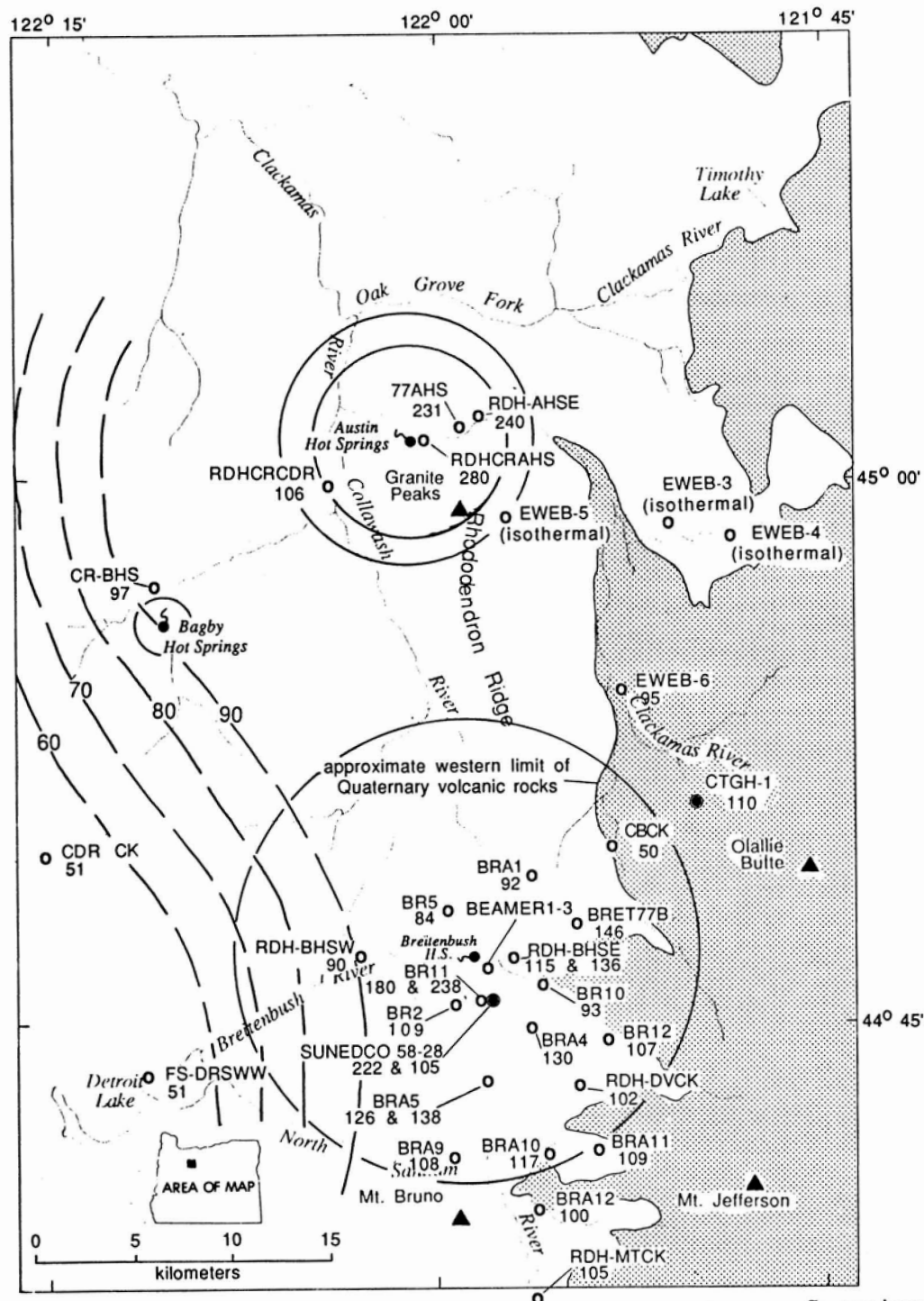


Figure 7. Map showing heat-flow sites and heat flow in Breitenbush-Austin Hot Springs area. Contour interval (dashed line) is 10 mW/m². Circles around hot springs show area required to match heat loss at hot springs, assuming a uniform heat flow of 100 mW/m² within the circle; two circles at Austin Hot Springs correspond to alternative heat-loss values listed in Table 2. Pattern indicates volcanic rocks of High Cascades (Sherrod and Conrey, this volume), which are mainly of Quaternary age in this area.

ground thermal data show a westward bulge of the 95-105 mW/m² contour into the Western Cascades. At Austin Hot Springs, this bulge coincides with an area possessing shallow depth (6-9 km below sea level) to the geophysically defined base of the magnetic layer, which in this area may represent the depth to the Curie point (Foote, 1985; R.W. Couch, personal communication, 1987). This westward deflection is geographically coincident with the north-northwest-trending zone of faults along Rhododendron Ridge and the Clackamas River. The coincidence of geophysical and geothermal anomalies is evidence for a deep source of the Cascade Range thermal anomaly, rather than an upper crustal source such as regional water flow.

DISCUSSION AND CONCLUSIONS

One of the often frustrating problems in determining heat flow in active volcanic terranes is the high permeability that characterizes surficial rocks, as in the High Cascades. Yet in the Western Cascades, the volcanic rocks are generally impermeable except along discrete fractures or beds, and geothermal gradients measured below 20-100 m are generally conductive. In the CTGH-1 hole, the transition from the near-surface convective regime to the conductive regime occurs over a depth range of 350-550 m. Bargar (this volume) notes that smectite occurs ubiquitously below 480 m. He further notes that most of the original void space is partly to completely filled by secondary minerals and concludes that most of the alteration is associated with temperatures less than 100 °C.

Keith (this volume), following work by A.F. Waibel (unpublished data), found that the rocks of the Breitenbush Formation in SUNEDCO 58-28 have been exposed to temperatures much higher than those that presently exist, up to 200-250 °C below 640-800 m. Effects of the modern thermal aquifer are not discernable in the alteration analysis. Regionally, alteration is extensive in the Breitenbush Formation, so most of the alteration is apparently related to post-early Miocene relatively deep burial of the section with subsequent unroofing of the altered and deformed rocks by erosion between 18 and 12 Ma (Sherrod and Conrey, this volume).

The results of these observations emphasize the conclusion that the transition from surface volcanic rocks with very high permeability to rocks with low permeability coincides in depth with hydrothermal alteration associated with fluids at temperatures of 50 °C or higher. This alteration is probably more a function of depth of burial than age, but age is a useful site criteria in the Cascade Range nonetheless. In the Breitenbush-Austin Hot Springs area, rocks 6-10 Ma or older have been buried to a depth of 500-2,000 m (and exposed to temperatures and fluids at 50 °C or higher) and seem generally impermeable. Rocks 6-2 Ma appear to have been buried only hundreds of meters

and generally give low heat-flow values (<50 percent of regional values) in 150-m-deep holes. Rocks that have never been buried deeper than 500-1,000 m (generally less than 2 Ma) seldom have a geothermal gradient in holes 150 m deep. A strict observation of this characteristic assignment of rock properties by selecting only old or visibly altered young rocks as sites for 150-m-deep gradient tests has resulted in highly successful drilling programs in the Cascade Range (Blackwell and others, 1978, 1982, the SUNEDCO holes). However, sites that meet these criteria in the High Cascades subprovince are rare.

Because the loss of permeability appears to be associated with alteration above 50 °C with the characteristic alteration suite described by Bargar (this volume), this depth should be detectable using electrical exploration techniques. Wright and Nielson (1986) pointed out the correspondence of units of low electrical resistivity with units that have smectite alteration in a deep hole (N-1) at Newberry volcano, a large Pleistocene volcano centered about 35 km south of Bend, Oreg. (for example, MacLeod and Sherrod, 1988). Therefore, in volcanic terrain, the transition from near-surface ground-water convective regimes (5-75 °C) to low permeability conductive regimes (50 °C and greater, past or present) should be characterized by a marked decrease in resistivity. One consideration in siting the CTGH-1 hole was the presence of a large area of low electrical resistivity at depth (J.L. Iovenetti, personal communication, 1986). This electrical resistivity anomaly may be related to the pervasive alteration and vug-filling noted in the CTGH-1 core.

The thermal characteristics of the hot springs, including heat-loss values, flow rates, surface temperatures, and possible reservoir temperatures, are listed in Table 2. From these data, the convective, total, and (by difference) conductive heat loss values for each hot springs system can be determined. The most uncertain values are the reservoir temperatures because there are not enough drilling data to understand the implications of the various geochemically inferred reservoir temperatures in the Cascade Range. Conventional SiO₂ or Na-K-Ca values are given in Table 2 (Brook and others, 1979).

At Austin and Bagby Hot Springs, the resulting total heat losses are modest; at Breitenbush, the heat loss is an order of magnitude greater. If the sulfate geothermometer is used (Mariner, 1985), then Austin and Breitenbush heat-loss values are comparable. The large area of high temperatures at shallow depths along the Clackamas River suggests that the higher loss value may be more appropriate. The heat-loss values can be normalized by the area required to generate the observed heat loss if all the regional heat flow (100 mW/m²) is tapped and if there is no local heat concentration such as around a shallow young intrusive center. This area is shown diagrammatically by the circles on Figure 7 around each hot spring. The heat loss at Bagby is insignificant and is probably related to flow within a few

kilometers of the hot springs. Austin and Breitenbush represent the heat that might be extracted from a cross section of the Cascade Range about 10 km long if the width is 40-50 km (assuming no magmatic heat input). These convective systems at least locally may represent a significant component of the total heat loss.

The extensive data in the Breitenbush Hot Springs area allow characterization of both the regional geothermal setting and the local thermal anomaly associated with the hot springs. An area of approximately 30-50 km² has heat flow as much as 40-50 percent above regional background values and average geothermal gradients of about 100 °C/km. The fluid feeding the hot springs may flow through a gently east-dipping aquifer in the Breitenbush Formation, as indicated by the area shown by the pattern in Figure 1. If the temperature in the aquifer reaches the values indicated by geochemistry within the area of Figure 1, the aquifer must dip so that it lies at a depth of 2-4 km along the east side of the area.

If the holes along the east side of the area represent regional values of geothermal gradient and heat flow not increased by the effect of the aquifer, then the thermally anomalous area forms a sideways L-shape, suggesting that the hot springs lie at the intersection of two fracture zones with geothermal flow. A deep-seated fracture system does not seem consistent with the results of SUNEDCO 58-28, however, which has the temperature-depth shape associated with transient geothermal fluid flow in a shallow aquifer. Deep flow along the east-west fault that projects through the hot springs (Figure 1) with shallow flow to the south along a stratigraphic horizon or at shallow depths

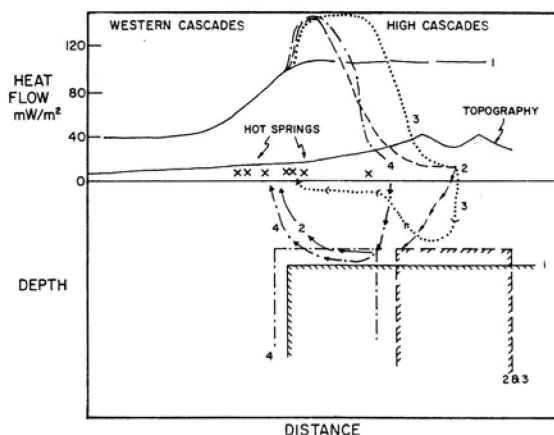


Figure 8. Several models of the relationship of hot springs to the heat-flow transition observed near the Western Cascades-High Cascades boundary (Blackwell and others, 1982). Curve 1 corresponds to the conductive anomaly and Curve 3 is the closest match to fluid circulating from High Cascades to the Breitenbush Hot Springs system.

along a fracture system would be consistent with the data. The connection of the aquifer to the source of hot water at depth remains questionable but may be associated with fracture permeability related to intrusive feeders for Quaternary volcanoes (nearby Mount Jefferson, for example) along the crest of the Cascade Range or structurally induced permeability (fault or fracture zones) in the High Cascades.

Blackwell and others (1982) presented a series of models for the hot springs in the Western Cascades (see Figure 8). The Breitenbush area is apparently an example of Case 3 because the permeability associated with the system seems to be primarily controlled by stratigraphy. Future exploration of the other hot springs in the Western Cascades may find other types of flow systems.

The results described in this paper reinforce the conclusions of Blackwell and others (1978, 1982) about the regional and local thermal regimes. Significant but regionally limited thermal anomalies are associated with both Austin and Breitenbush Hot Springs. On the other hand, geothermal gradients average 65 °C/km, and heat-flow values average 100 mW/m² where measured in 150-m-deep holes elsewhere in relatively impermeable rocks (that is, in units generally older than 9 Ma), regardless of the location of the data points with respect to topography (on ridges or in valleys) or with respect to proximity to the High Cascades. For example, holes CTGH-1 and RDH-BHSW, within 5 and 30 km of the Cascade crest, respectively (Figure 7), have identical heat-flow values within the error of the determinations. Furthermore, the deeper drill holes (OMF-7A and SUNEDCO 58-28) are consistent with the continuation of such high gradients and heat-flow values to depths of 2-2.5 km where temperatures reach 125-150 °C.

Recently, Ingebritsen and others (1988) have revived the hypothesis that the thermal pattern in the Western Cascades is due to systematic water flow from the High Cascades. This hypothesis was our working hypothesis tested in the initial drilling project in 1976 and illustrated by Figure 8 in Blackwell and others (1978) and retested in 1979 and 1980 (Blackwell and others, 1982). The hypothesis was discarded because of accumulated evidence against it, and instead the models illustrated in Figure 8 (this paper) were suggested. The new data presented here, because they outline anomalous heat-flow areas with respect to the 100 mW/m² regional background, are not consistent with a model that generates the 100 mW/m² background heat flow by regional fluid circulation, with the hot springs representing only the surficial evidence of this regional system.

ACKNOWLEDGMENTS

John Knox and Edward Western were responsible for permission to use the SUNEDCO exploration results. This work was supported by USDOE Grant No. DF-FG07-86ID 12623 to SMU and by subcontracted funds from USDOE

Grant No. DE-FG07-84 ID 12526 to the Oregon Department of Geology and Mineral Industries. Shari Kelley helped program the aquifer-flow analysis. George Priest and Gerald Black (Oregon Department of Geology and Mineral Industries) made constructive comments on drafts of the manuscript.

REFERENCES CITED

- Bargar, K.E., 1988 (this volume), Secondary mineralogy of core from geothermal drill hole CTGH-1, Cascade Range, Oregon, *in* Sherrod, D.R., ed., Geology and geothermal resources of the Breitenbush-Austin Hot Springs area, Clackamas and Marion Counties, Oregon: Oregon Department of Geology and Mineral Industries Open-File Report O-88-5, in press.
- Blackwell, D.D., 1985, A transient model of the geothermal system of the Long Valley caldera, California: *Journal of Geophysical Research*, v. 90, p. 11229-11241.
- Blackwell, D.D., Black, G.L., and Priest, G.R., 1986, Geothermal-gradient data for Oregon (1982-1984): Oregon Department of Geology and Mineral Industries Open-file Report O-86-2, 107 p.
- Blackwell, D.D., Hull, D.A., Bowen, R.G., and Steele, J.L., 1978, Heat flow of Oregon: Oregon Department of Geology and Mineral Industries Special Paper 4, 42 p.
- Blackwell, D.D., Bowen, R.G., Hull, D.A., Riccio, J., and Steele, J.L., 1982, Heat flow, arc volcanism, and subduction in northern Oregon, *Journal of Geophysical Research*, v. 87, no. B10, p. 8735-8754.
- Blackwell, D.D., Steele, J.L., and Brott, C.A., 1980, The terrain effect on terrestrial heat flow: *Journal of Geophysical Research*, v. 85, p. 4757-4772.
- Blackwell, D.D., and Steele, J.L., 1987, Geothermal data from deep holes in the Oregon Cascade Range: *Geothermal Resources Council Transactions*, v. 11, p. 317-322.
- Brook, C.A., Mariner, R.H., Mabey, D.R., Swanson, J.R., Guffanti, Marianne, and Muffler, L.J.P., 1979, Hydrothermal convection systems with reservoir temperatures $\geq 90^{\circ}\text{C}$, *in* Muffler, L.J.P., ed., Assessment of geothermal resources of the United States—1978: U.S. Geological Survey Circular 790, p. 18-85.
- Conrey, R.M., and Sherrod, D.R., 1988 (this volume), Stratigraphy of drill holes and geochemistry of surface rocks, Breitenbush Hot Springs 15-minute quadrangle, Cascade Range, Oregon, *in* Sherrod, D.R., ed., Geology and geothermal resources of the Breitenbush-Austin Hot Springs area, Clackamas and Marion Counties, Oregon: Oregon Department of Geology and Mineral Industries Open-File Report O-88-5, in press.
- Diment, W.H., Urban, T.C., and Nathenson, Manuel, 1985, Temperature variation with time in a perennially boiling well in the Long Valley caldera, Mono County, California; Observations in Chance No. 1 (1976-1983): *Geothermal Resources Council Transactions*, v. 9, no. 1, p. 417-422.
- Footo, R.W., 1985, Curie-point isotherm mapping and interpretation from aeromagnetic measurements in the northern Oregon Cascades: Corvallis, Oreg., Oregon State University master's thesis, 115 p.
- Ingebritsen, S.E., Mariner, R.H., and Sherrod, D.R., 1988, Heat flow and hydrothermal circulation in the Cascade Range, north-central Oregon [abs.]: *EOS*, v. 69, p. 470.
- Keith, T.E.C., 1988 (this volume), Regional patterns of hydrothermal alteration in the Breitenbush-Austin Hot Springs area, Cascade Range, Oregon, *in* Sherrod, D.R., ed., Geology and geothermal resources of the Breitenbush-Austin Hot Springs area, Clackamas and Marion Counties, Oregon: Oregon Department of Geology and Mineral Industries Open-File Report O-88-5, in press.
- MacLeod, N.S., and Sherrod, D.R., 1988, Geologic evidence for a magma chamber beneath Newberry Volcano, Oregon: *Journal of Geophysical Research*, in press.
- Mariner, R.H., 1985, Geochemical features of Cascades hydrothermal systems, *in* Guffanti, Marianne, and Muffler, L.J.P., eds., Proceedings of the workshop on geothermal resources of the Cascade Range: U.S. Geological Survey Open-File Report 85-521, p. 59-62.
- Priest, G.R., 1985, Geothermal exploration in Oregon, 1984: *Oregon Geology*, v. 47, no. 6, p. 63-66.
- Priest, G.R., Woller, N.M., and Ferns, M.L., 1987, Geologic map of the Breitenbush River area, Linn and Marion Counties, Oregon: Oregon Department of Geology and Mineral Industries Geological Map Series GMS-46, scale 1:62,500.
- Sherrod, D.R., and Conrey, R.M., 1988 (this volume), Geologic setting of the Breitenbush-Austin Hot Springs area, Cascade Range, north-central Oregon, *in* Sherrod, D.R., ed., Geology and geothermal resources of the Breitenbush-Austin Hot Springs area, Clackamas and Marion Counties, Oregon: Oregon Department of Geology and Mineral Industries Open-File Report O-88-5, in press.
- Steele, J.L., Blackwell, D.D., and Robison, J., 1982, Heat flow in the vicinity of the Mount Hood volcano, Oregon, *in* Priest, G.R., and Vogt, B.F., eds., Geology and geothermal resources of the Mount Hood area: Oregon Department of Geology and Mineral Industries Special Paper 14, p. 31-42.
- Ward, S.H., Parry, W.T., Nash, W.P., Sill, W.R., Cook, K.C., Smith, R.B., and Chapman, D.S., 1978, A sum-

- mary of the geology, geochemistry and geophysics of the Roosevelt Hot Springs thermal area, Utah: *Geophysics*, v. 43, p.1515-1542.
- Welch, A.H., Sorey, M.C., and Olmsted, F.H., 1981, The hydrothermal system in southern Grass Valley, Pershing County, Nevada: U.S. Geological Survey Open-File Rept. 81-915, 193 pp.
- Wright, P.M., and Nielson, D.L., 1986, Electrical anomalies at Newberry volcano, Oregon: Comparison with alteration mineralogy in Geo corehole N-1: *Geothermal Resources Council Transactions*, v. 10, p. 247-252.
- Youngquist, Walter, 1980, Geothermal gradient drilling, north-central Cascades of Oregon, 1979: Oregon Department of Geology and Mineral Industries Open-File Report O-80-12, 47 p.
- Ziagos, J.P., and Blackwell, D.D., 1985, A model for the transient temperature effects of horizontal fluid flow in geothermal systems: *Journal of Volcanology and Geothermal Research*, v. 27, p. 371-397.

Chapter 6

Geologic and geothermal summary of the Breitenbush-Austin Hot Springs area, Clackamas and Marion Counties, Oregon

by David R. Sherrod, U.S. Geological Survey, Menlo Park, Calif. 94025

ABSTRACT

Several contributions are used here to derive a geologic cross section showing topography, stratigraphy, structure, isotherms, heat flow, gravity, and hydrology. The data suggests an igneous-related hydrothermal system, with heat flow of 100 mW/m² beneath the High Cascades and 40 mW/m² in the Western Cascades west of Austin and Breitenbush Hot Springs. Heat flow in the Western Cascades east of the hot springs is increased by convective anomalies resulting from the migration of heated ground water in fracture zones (Austin Hot Springs) and along the top of impermeable barriers in altered Oligocene and lower Miocene volcaniclastic rocks (Breitenbush Hot Springs).

This model differs from interpretations that extend the igneous-related heat source from the High Cascades into the Western Cascades and thus narrows the area of prime interest for geothermal exploration. Though not fully tested, it is compatible with the information presently available.

CROSS SECTION

I have prepared a cross section (Figure 1) in order to summarize the geologic and geophysical data presented in the papers of this volume. The cross section runs from the Breitenbush River in the Western Cascades subprovince to the Whitewater River east of the Cascade Range crest. The topographic profile shows relief of 1,478 m, ranging from

about 610 m at the Breitenbush River to 2,088 m at Park Butte, which is the eroded neck of a late Quaternary andesite volcano in the High Cascades 5 km north of Mount Jefferson. The physiographic boundary between Western and High Cascades is at the South Fork of the Breitenbush River on this cross section.

Stratigraphy and structure

The oldest geologic unit exposed at the surface or penetrated by any drill hole is the Oligocene and lower Miocene Breitenbush Formation of White (1980a), a sequence of mainly volcaniclastic strata (unit Tb on Figure 1). Bedding on the cross section shows the axis of the Breitenbush anticline, which formed in middle Miocene time (Sherrod and Conrey, this volume). Grouped with the Breitenbush Formation is the lower Miocene lava of Scorpion Mountain (White, 1980a; not shown separately).

The three generalized units (Figure 1) above the Breitenbush Formation contain mainly lava flows: (1) unit Tv, which includes middle and upper Miocene lava of Outerson Mountain (Priest and others, 1987), Rhododendron Formation of Hammond and others (1982), and andesite and dacite of Rhododendron Ridge (Sherrod and Conrey, this volume); (2) unit Tbc, upper Miocene and Pliocene basaltic andesite of Collawash Mountain (Priest and others, 1987; Sherrod and Conrey, this volume); and (3) unit QTv, volcanic rocks of the High Cascades (Sherrod and Conrey, this volume). The position of these contacts at depth east of the South Fork of the Breitenbush River is virtually unknown. Drill hole

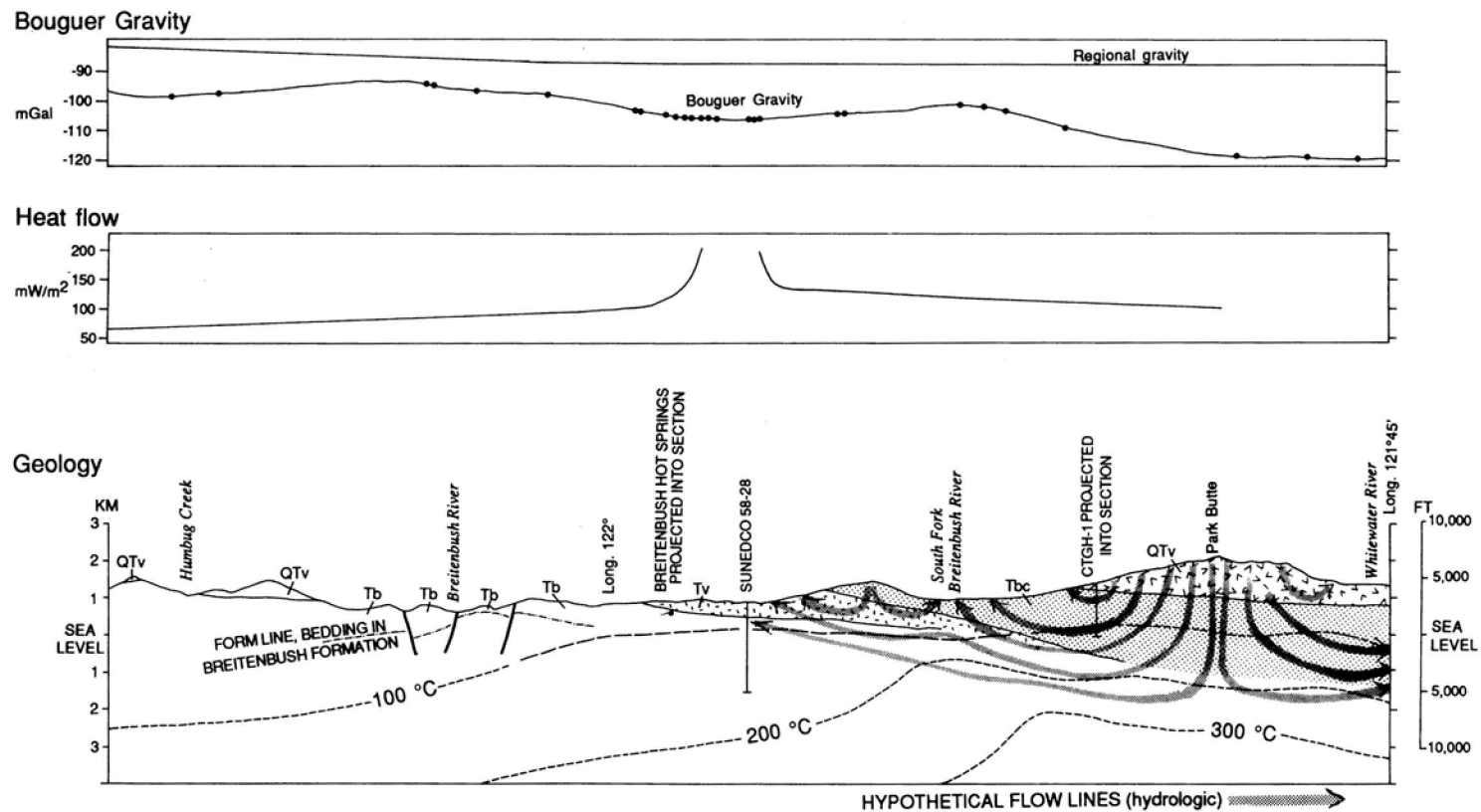


Figure 1. Geologic, gravity, and thermal cross sections of the Breitenbush-Austin Hot Springs area, Cascade Range, Oregon. See text for explanation and discussion.

Geologic and geothermal summary

CTGH-1, located 6 km west of the Cascade crest and 15 km north of the cross section, is projected to show the relative thickness of units QTV and Tbc intercepted at the CTGH-1 drill site. Breitenbush Hot Springs is projected onto the section from 2 km north-northeast.

The volcanic rocks of the High Cascades at the latitude of the cross section comprise mainly andesite, dacite, and rhyodacite that range in age from about 2.5 Ma to <0.3 Ma on the east side of the cross section (Sherrod and Conrey, this volume; L.B.G. Pickthorn, unpublished data); the latest eruptions from Mount Jefferson (5 km south) occurred about 76,000 yrs ago (A.M. Sarna-Wojcicki and W.E. Scott, personal communication; data summarized in Sherrod and Conrey, this volume). The intrusive equivalents of upper Pleistocene andesite, dacite, and rhyodacite are presumably the heat source for upwelling water at Breitenbush Hot Springs, at Austin Hot Springs, and in SUNEDCO 58-28. Unit QTV mapped on the west side of the cross section corresponds to 1-2 Ma volcanic rocks erupted from a vent near Battle Axe Mountain (White, 1980b), one of the few Quaternary volcanoes found in the Western Cascades of Oregon.

Isotherms

Isotherms (short-dashed) shown at the west end of the section (Western Cascades) correspond to a geothermal gradient of 40 °C/km, whereas at the east end (High Cascades) they indicate a gradient of 60 °C/km (for example, Blackwell and Steele, 1983). The position of the 100-°C isotherm from the Breitenbush River to the South Fork of the Breitenbush River (shown long-dashed) was contoured by Ingebritsen and others (1988), on the basis of numerous shallow geothermal-gradient test holes. The 200- and 300-°C isotherm is shown perturbed by the thermal aquifer that feeds Breitenbush Hot Springs and that was intercepted in the SUNEDCO 58-28 hole (Blackwell and Baker, this volume; Priest and others, 1987). The isotope geochemistry (sulfate-water) of Breitenbush Hot Springs suggests reservoir temperatures as great as 195 °C (Brook and others, 1979).

Heat flow

A profile of the heat flow contoured by Blackwell and Baker (this volume) is shown above the cross section. The contours are abruptly domed by the convective disturbance responsible for Breitenbush Hot Springs and the thermal aquifer in SUNEDCO 58-28.

Gravity

Regional and complete Bouguer gravity anomaly profiles accompany the cross section (Braman, 1981, and Couch and others, 1981, respectively). To indicate control, dots on the Bouguer gravity profile show gravity stations located within 2.5 km of and projected onto the cross-section line (Couch and others, 1982). The regional gravity has a

gently southeast-decreasing gradient of about 0.7-0.8 mGal/km on the west half of the profile and a virtually flat gradient on the east, where the cross section parallels the grain of a gradient that decreases about 0.3-0.4 mGal/km to the south-southwest (Braman, 1981).

The complete Bouguer profile shows a broad gravity high on the west that may correspond to the Breitenbush anticline as mapped by Priest and others (1987). The Breitenbush anticline has virtually no gravity expression elsewhere in the Western Cascades, however, allowing the interpretation that the gravity high is unrelated to the anticline. At the east end of the section, the complete Bouguer profile decreases about 3 mGal/km down an east-dipping slope that is well defined for 10 km either side of the cross section (Couch and others, 1981). This east-dipping gradient may correspond to a narrow fault zone that displaces rocks down to the east and that is now completely buried by Pliocene and younger rocks. It is on line with the structural trend defined by contours at the top of the Breitenbush Formation 5 km north (Sherrod and Conrey, this volume, their Figure 3) where there is weak expression in the gravity data. Perhaps the contrasting gravity signature north of the cross section results from distributive faulting along a broad zone instead of a narrow fault zone.

However, even the steep east-side gradient may be an artifact of the gravity interpretation. The anomaly disappears when modeled with a reduction density of 2.43 g/cm³, which was the density used by Couch and others (1982) for the residual gravity map. In contrast, a reduction density of 2.67 g/cm³ was used for the complete Bouguer gravity anomaly map (Couch and others, 1981) and consequently for this cross section.

Hydrology

Oxygen and deuterium isotopes indicate that water discharging at Breitenbush Hot Springs originates as precipitation near the range crest in the High Cascades (Mariner and others, 1980; Ingebritsen and others, 1988). This water moves downward perhaps 3-4 km through permeable units such as the volcanic rocks of the High Cascades (QTV) and basaltic andesite of Collawash Mountain (Tbc), and through slightly less permeable middle and upper Miocene lava (Tv) as it migrates away from the range crest. Presumably the lateral migration is above a relatively impermeable barrier created by alteration of the volcanoclastic tuffaceous rocks of the Breitenbush Formation (Tb).

Hydrologic flow lines are modified from a theoretical analysis of ground-water flow (Tóth, 1963, particularly his Figure 2i, which shows maximum surficial relief and an impermeable boundary at 3-km depth). These flow lines are purely hypothetical; my purpose is simply to indicate the depths to which topography will drive regional hydrologic flow in permeable rocks. Perhaps less than 10 percent of the total recharge will ever penetrate more than 100 m (Tóth, 1963), and far less will participate in the deepest flow that

finally reaches the hot springs. Considering the magnitude of recharge by snow and rain in the Cascade Range, however, a very small percentage is sufficient to explain flow at hot springs. Investigations to simulate the cross-section hydrology are now underway (S.E. Ingebritsen and D.R. Sherrod, unpublished data).

DISCUSSION AND CONCLUSIONS

Of all the topics discussed above, probably the greatest controversy surrounds the location of deep heat sources. Blackwell and Baker (this volume) discuss this problem, especially in regard to Austin and Bagby Hot Springs, which are not adjacent to potential heat sources in the High Cascades. Indeed, at the latitude of Austin Hot Springs, High Cascades volcanism is almost entirely basaltic andesite in composition and is chiefly older than 0.5 Ma. Reversely polarized rocks (>0.73 Ma) are widespread along the Cascade crest from Austin's latitude north to Mount Hood (D.R. Sherrod, unpublished data).

The cross section must be viewed as a working hypothesis, and I stress several assumptions: contrasts in rock permeability between the Breitenbush Formation (relatively impermeable) and younger rocks (relatively permeable), major sources of heat restricted to intrusions of intermediate and silicic composition beneath the High Cascades, and a relationship between regional ground-water flow and heat discharge. Blackwell and Baker (this volume) explain the thermal setting of Breitenbush Hot Springs in a similar fashion, but differ by interpreting the convective anomaly as superimposed on a regionally limited, significant conductive anomaly in the Western Cascades. Similarly, they view Austin Hot Springs as the result of igneous-related heat sources located in the Western Cascades (see also Blackwell and others, 1982).

Surely hydrology must be a critical parameter in any final interpretation of heat flow in the Cascade Range. The model of regional ground-water flow to explain convective thermal anomalies in the Western Cascades will narrow the area of prime interest for geothermal exploration but result in a better-defined exploration target.

ACKNOWLEDGMENTS

I wish to acknowledge reviews by G.R. Priest (Oregon Department of Geology and Mineral Industries) and S.E. Ingebritsen (U.S. Geological Survey). I am indebted to Ingebritsen and R.M. Conrey for shared field work and harrowing discussions of Cascade Range geology; many of my interpretations stem from collaboration with them.

This work was funded in part by a cooperative agreement between the Oregon Department of Geology and Mineral Industries and the U.S. Geological Survey's Office

of Mineral Resources. Other support came from the Geothermal Research Program of the U.S. Geological Survey and subcontracted funds from U.S. Department of Energy Grant No. DE-FG07-84 ID 12526 (to the Oregon Department of Geology and Mineral Industries).

REFERENCES CITED

- Blackwell, D.D., Bowen, R.G., Hull, D.A., Riccio, Joseph, and Steele, J.L., 1982, Heat flow, arc volcanism, and subduction in northern Oregon: *Journal of Geophysical Research*, v. 87, no. B10, p. 8735-8754.
- Blackwell, D.D., and Steele, J.L., 1983, Geothermal data from deep holes in the Oregon Cascade Range: *Geothermal Resources Council Transactions*, v. 11, p. 317-322.
- Blackwell, D.D., and Baker, S.L., 1988 (this volume), Thermal analysis of the Austin and Breitenbush geothermal systems, Western Cascades, Oregon, in Sherrod, D.R., ed., *Geology and geothermal resources of the Breitenbush-Austin Hot Springs area, Clackamas and Marion Counties, Oregon*: Oregon Department of Geology and Mineral Industries Open-File Report O-88-5, in press.
- Braman, D.E., 1981, Interpretation of gravity anomalies observed in the Cascade Mountain province of northern Oregon: Corvallis, Ore., Oregon State University master's thesis, 144 p.
- Brook, C.A., Mariner, R.H., Mabey, D.R., Swanson, J.R., Guffanti, Marianne, and Muffler, L.J.P., 1979, Hydrothermal convection systems with reservoir temperatures $\geq 90^{\circ}\text{C}$: U.S. Geological Survey Circular 790, p. 18-85.
- Couch, R.W., Pitts, G.S., Braman, D.E., and Gemperle, M., 1981, Free-air gravity anomaly map and complete Bouguer gravity anomaly map, Cascade Mountain Range, northern Oregon: Oregon Department of Geology and Mineral Industries Geological Map Series GMS-15, scale 1:250,000.
- Couch, R.W., Pitts, G.S., Gemperle, M., Veen, C.A., and Braman, D.E., 1982, Residual gravity maps of the northern, central, and southern Cascade Range, Oregon, 121°00' to 122°30'W by 42°00' to 45°45'N: Oregon Department of Geology and Mineral Industries Geological Map Series GMS-26, scale 1:250,000.
- Hammond, P.E., Geyer, K.M., and Anderson, J.L., 1982, Preliminary geologic map and cross sections of the upper Clackamas and North Santiam Rivers area, northern Oregon Cascade Range: Portland, Ore., Portland State University Department of Earth Sciences, scale 1:62,500.
- Ingebritsen, S.E., Mariner, R.H., and Sherrod, D.R., 1988, Heat flow and hydrothermal circulation in the Cascade Range, north-central Oregon: *EOS*, v. 69, no. 16, p. 471.

Geologic and geothermal summary

- Mariner, R.H., Swanson, J.R., Orris, G.J., Presser, T.S., and Evans, W.C., 1980, Chemical and isotopic data for water from thermal springs and wells of Oregon: U.S. Geological Survey Open-File Report 80-737, 50 p.
- Priest, G.R., Woller, N.M., and Ferns, M.L., 1987, Geologic map of the Breitenbush River area, Linn and Marion Counties, Oregon: Oregon Department of Geology and Mineral Industries Geological Map Series GMS-46, scale 1:62,500.
- Sherrod, D.R., and Conrey, R.M., 1988 (this volume), Geologic setting of the Breitenbush-Austin Hot Springs area, Cascade Range, north-central Oregon, *in* Sherrod, D.R., ed., Geology and geothermal resources of the Breitenbush-Austin Hot Springs area, Clackamas and Marion Counties, Oregon: Oregon Department of Geology and Mineral Industries Open-File Report O-88-5, in press.
- Tóth, J., 1963, A theoretical analysis of groundwater flow in small drainage basins: *Journal of Geophysical Research*, v. 68, no. 16, p. 4795-4812.
- White, C.M., 1980a, Geology of the Breitenbush Hot Springs quadrangle, Oregon: Oregon Department of Geology and Mineral Industries Special Paper 9, 26 p.
- 1980b, Geology and geochemistry of volcanic rocks in the Detroit area, Western Cascade Range, Oregon: Eugene, Oreg., University of Oregon doctoral dissertation, 177 p.

APPENDICES

Appendix 1. Chemical analyses of rocks in the Breitenbush Hot Springs 15-minute quadrangle, Cascade Range, northern Oregon.

Sample no.	Lava of Scorpion Mountain			Andesite and dacite of Clackamas River			Basaltic andesite of Collawash Mountain			
	BR-M4	BR-M5	BR-M6	BD-15	BD-16	BD-24	BHS-22†	BR-140	BR-142	BR-141
Unnormalized results (wt. %):										
SiO ₂	57.66	55.50	54.41	67.75	65.44	58.22	60.97	54.52	54.43	56.83
Al ₂ O ₃	17.16	16.71	17.62	16.25	16.71	17.40	16.99	17.77	17.73	17.96
TiO ₂	1.319	1.363	1.646	0.777	0.971	1.347	0.765	1.190	1.184	1.174
FeO*	9.78	9.98	9.19	4.91	5.67	7.66	6.13	8.20	7.99	7.51
MnO	0.222	0.225	0.215	0.090	0.100	0.125	0.122	0.146	0.140	0.134
CaO	6.06	6.43	8.32	3.36	4.25	6.94	6.46	8.10	8.18	7.34
MgO	2.43	2.43	3.13	0.93	1.60	3.56	4.12	5.78	6.16	4.93
K ₂ O	1.36	1.23	1.18	3.03	2.62	1.60	1.25	1.02	0.98	1.01
Na ₂ O	4.49	4.37	3.46	4.39	4.45	4.02	3.99	3.95	3.90	4.02
P ₂ O ₅	0.514	0.511	0.333	0.238	0.286	0.287	0.146	0.301	0.298	0.288
Total	101.00	98.75	99.50	101.73	102.10	101.16	100.94	100.98	100.99	101.20
Normalized results (wt. %):										
SiO ₂	56.54	55.64	54.18	66.28	63.74	57.12	60.04	53.56	53.47	55.74
Al ₂ O ₃	16.83	16.75	17.55	15.90	16.28	17.07	16.73	17.46	17.42	17.62
TiO ₂	1.29	1.37	1.64	0.76	0.95	1.32	0.75	1.17	1.16	1.15
Fe ₂ O ₃ **	10.55	11.01	10.07	5.28	6.08	8.27	6.64	8.86	8.63	8.10
MnO	0.22	0.23	0.21	0.09	0.10	0.12	0.12	0.14	0.14	0.13
CaO	5.94	6.45	8.28	3.29	4.14	6.81	6.36	7.96	8.04	7.20
MgO	2.38	2.44	3.12	0.91	1.56	3.49	4.06	5.68	6.05	4.84
K ₂ O	1.33	1.23	1.18	2.96	2.55	1.57	1.23	1.00	0.96	0.99
Na ₂ O	4.40	4.38	3.45	4.29	4.33	3.94	3.93	3.88	3.83	3.94
P ₂ O ₅	0.50	0.51	0.33	0.23	0.28	0.28	0.14	0.30	0.29	0.28
Trace elements (ppm):										
Ni	1	14	10	9	19	60	109	104	67	
Cr	0	0	36	0	5	37	80	130	137	109
Sc	22	25	32	12	15	22	18	25	24	20
V	50	53	215	53	77	159	138	206	183	146
Ba	478	477	468	676	617	416	352	346	351	311
Rb	36	33	26	92	73	39	28	13	11	14
Sr	415	427	395	318	373	423	503	746	764	547
Zr	164	152	160	274	268	202	106	146	140	173
Y	34	33	29	35	41	29	17	20	19	22
Nb	10.8	11.1	11.7	21.6	20.0	17.3	7.1	11.6	9.0	12.5
Ga	23	21	19	21	22	20	16	18	16	19
Cu	10	7	38	11	20	24	48	60	59	48
Zn	96	88	89	76	79	82	62	74	77	75
Elev.(ft)	3520	3720	3640	2920	2940	3020	2760	3450	3870	4060
Lat.	44°48.55'	44°48.69'	44°48.64'	44°56.4'	44°57.9'	44°56.9'	44°46.59'	44°52.9'	44°52.2'	44°52.55'
Long.	121°58.84'	121°58.59'	121°58.24'	121°53'	121°54.15'	121°52.9'	121°56.97'	121°53.5'	121°54.4'	121°54.15'

† K-Ar age 5.97±0.13 Ma (Sherrod and Conrey, this volume)

Appendix 1. Chemical analyses . . . (continued).

Sample no.	Basaltic andesite of Collawash Mountain									
	BHS-10	BHS-8	BHS-7	BHS-5	BHS-9	BHS-16	BHS-14	BHS-18	BHS-3	BHS-17
Unnormalized results (wt. %):										
SiO ₂	51.12	50.89	53.64	53.24	51.63	52.54	55.38	52.32	53.27	54.09
Al ₂ O ₃	17.77	17.98	20.55	18.19	19.70	18.65	18.22	18.41	17.72	17.22
TiO ₂	0.977	1.034	1.202	1.335	1.328	1.502	1.297	1.161	1.210	1.187
FeO*	9.26	8.86	7.81	9.11	9.38	9.92	8.51	8.42	8.08	8.06
MnO	0.168	0.162	0.132	0.154	0.151	0.164	0.134	0.149	0.142	0.142
CaO	10.05	10.24	9.04	8.54	8.74	8.22	7.79	10.15	10.06	9.65
MgO	8.28	8.99	5.22	6.82	6.02	6.45	5.55	7.48	7.22	7.21
K ₂ O	0.42	0.36	0.55	0.62	0.37	0.51	0.92	0.22	0.50	0.62
Na ₂ O	2.27	2.56	3.30	3.54	3.53	3.54	3.75	2.91	2.93	2.98
P ₂ O ₅	0.119	0.150	0.175	0.236	0.301	0.345	0.323	0.187	0.231	0.216
Total	100.43	101.23	101.62	101.79	101.15	101.84	101.87	101.41	101.36	101.37
Normalized results (wt. %):										
SiO ₂	50.43	49.84	52.38	51.84	50.57	51.09	53.91	51.17	52.14	52.94
Al ₂ O ₃	17.53	17.61	20.07	17.71	19.30	18.14	17.74	18.01	17.34	16.85
TiO ₂	0.96	1.01	1.17	1.30	1.30	1.46	1.26	1.14	1.18	1.16
Fe ₂ O ₃ **	10.05	9.54	8.39	9.76	10.11	10.61	9.11	9.06	8.70	8.68
MnO	0.17	0.16	0.13	0.15	0.15	0.16	0.13	0.15	0.14	0.14
CaO	9.92	10.03	8.83	8.32	8.56	7.99	7.58	9.93	9.85	9.44
MgO	8.17	8.80	5.10	6.64	5.90	6.27	5.40	7.32	7.07	7.06
K ₂ O	0.41	0.35	0.54	0.60	0.36	0.50	0.90	0.22	0.49	0.61
Na ₂ O	2.24	2.51	3.22	3.45	3.46	3.44	3.65	2.85	2.87	2.92
P ₂ O ₅	0.12	0.15	0.17	0.23	0.29	0.34	0.31	0.18	0.23	0.21
Trace elements (ppm):										
Ni	69	129	26	111	77	107	83	54	47	41
Cr	232	326	57	182	102	162	125	159	190	188
Sc	42	36	30	26	27	28	25	31	33	33
V	253	222	201	198	207	198	177	227	216	232
Ba	148	147	236	170	295	311	356	173	272	242
Rb	7	3	4	6	2	3	13	3	4	8
Sr	279	391	601	454	563	475	571	773	842	800
Zr	80	87	106	112	124	135	155	123	134	126
Y	27	20	18	21	22	27	23	21	22	21
Nb	3.8	3.2	5.2	7.0	8.5	10.0	10.9	4.7	6.1	5.1
Ga	16	14	19	20	20	18	21	18	19	17
Cu	56	64	42	57	77	58	57	51	42	49
Zn	65	63	72	79	85	93	85	70	71	67
Elev. (ft)	4230	4300	4330	4440	4290	4090	4000	4260	4520	4260
Lat.	44°46.72'	44°46.71'	44°46.73'	44°46.77'	44°46.71'	44°46.61'	44°46.55'	44°46.73'	44°46.72'	44°46.73'
Long.	121°55.53'	121°55.41'	121°55.32'	121°55.19'	121°55.44'	121°54.63'	121°54.94'	121°54.26'	121°54.59'	121°54.26'

Conroy

Appendix 1. Chemical analyses . . . (continued).

Sample no.	Basaltic andesite of Collawash Mountain						Volcanic rocks of the High Cascades			
	BHS-19	BHS-12	BHS-11	BHS-13	BHS-4B	BHS-6	BHS-15	BR-150	BHS-24†	BR-55
Unnormalized results (wt. %):										
SiO ₂	54.30	54.44	53.21	53.71	53.96	56.88	59.23	59.75	59.91	54.01
Al ₂ O ₃	18.97	18.00	18.76	18.38	18.17	18.20	17.19	17.09	17.11	18.78
TiO ₂	1.388	1.365	1.432	1.433	1.533	1.014	0.947	1.429	1.425	1.200
FeO*	8.33	8.74	8.82	9.28	8.92	7.21	6.50	7.96	7.93	8.32
MnO	0.141	0.146	0.150	0.146	0.156	0.127	0.114	0.118	0.120	0.156
CaO	8.92	8.60	8.65	8.03	8.44	6.42	7.23	6.17	6.17	8.52
MgO	4.75	5.75	5.92	4.81	5.29	5.88	5.63	2.88	2.88	5.43
K ₂ O	0.68	0.84	0.60	0.85	0.83	1.16	1.32	1.25	1.25	0.77
Na ₂ O	3.70	3.63	3.63	3.70	3.61	3.28	3.74	4.65	4.66	3.81
P ₂ O ₅	0.259	0.442	0.459	0.493	0.460	0.228	0.216	0.331	0.330	0.255
Total	101.44	101.95	101.63	100.83	101.37	100.40	102.12	101.63	101.79	101.25
Normalized results (wt. %):										
SiO ₂	53.09	52.94	51.91	52.78	52.77	56.25	57.64	58.34	58.40	52.91
Al ₂ O ₃	18.55	17.51	18.30	18.06	17.77	18.00	16.73	16.69	16.68	18.40
TiO ₂	1.36	1.33	1.40	1.41	1.50	1.00	0.92	1.40	1.39	1.18
Fe ₂ O ₃ **	8.96	9.35	9.46	10.03	9.60	7.84	6.96	8.55	8.50	8.97
MnO	0.14	0.14	0.15	0.14	0.15	0.13	0.11	0.12	0.12	0.15
CaO	8.72	8.36	8.44	7.89	8.25	6.35	7.04	6.02	6.01	8.35
MgO	4.64	5.59	5.77	4.73	5.17	5.81	5.48	2.81	2.81	5.32
K ₂ O	0.66	0.82	0.59	0.84	0.81	1.15	1.28	1.22	1.22	0.75
Na ₂ O	3.62	3.53	3.54	3.64	3.53	3.24	3.64	4.54	4.54	3.73
P ₂ O ₅	0.25	0.43	0.45	0.48	0.45	0.23	0.21	0.32	0.32	0.25
Trace elements (ppm):										
Ni	10	71	75	57	50	73	79	6	5	74
Cr	36	144	148	92	110	134	124	8	7	87
Sc	29	29	27	23	27	20	22	21	22	28
V	234	189	200	200	210	181	161	188	180	197
Ba	250	329	385	398	375	393	385	394	402	295
Rb	10	10	3	7	12	13	22	20	21	8
Sr	809	989	1027	810	492	855	818	457	455	577
Zr	132	169	176	173	170	151	143	161	161	122
Y	23	23	22	26	29	21	19	25	25	20
Nb	6.0	11.9	10.7	15.3	15.2	6.9	7.8	13.4	13.0	6.8
Ga	19	19	20	19	22	20	17	21	18	22
Cu	30	47	53	57	45	56	61	30	36	388
Zn	76	89	94	93	94	70	65	80	79	68
Elev. (ft)	4260	4120	4230	3970	4450	4380	4050	3340	3340	4000
Lat.	44°46.73'	44°46.66'	44°46.73'	44°46.54'	44°46.7'	44°46.76'	44°46.55'	44°46.74'	44°46.74'	44°46.36'
Long.	121°54.26'	121°55.55'	121°55.6'	121°55.33'	121°54.71'	121°55.24'	121°54.77'	121°50.2'	121°50.2'	121°50.54'

† K-Ar age 2.31±0.05 Ma (Sherrod and Conrey, this volume)

Chemical analyses of rocks in Breitenbush Hot Springs quadrangle

Appendix 1. Chemical analyses . . . (continued).

Sample no.	Volcanic rocks of the High Cascades									
	BR-56	BR-57	BR-58	BR-54	BR-59	BR-64	BR-61	BR-80	BR-117	BR-81
Unnormalized results (wt. %):										
SiO ₂	53.97	54.27	54.27	56.04	55.94	56.16	57.44	57.67	56.92	56.59
Al ₂ O ₃	18.38	18.42	18.20	18.92	18.41	18.74	18.57	18.88	18.61	18.66
TiO ₂	1.308	1.334	1.333	1.036	1.016	1.027	1.023	1.100	1.108	1.194
FeO*	8.78	8.72	8.67	7.30	7.30	7.17	7.00	6.90	6.96	7.43
MnO	0.144	0.145	0.135	0.125	0.122	0.121	0.117	0.114	0.120	0.123
CaO	8.39	8.39	8.20	8.06	7.78	8.05	7.66	7.69	7.98	7.78
MgO	5.18	5.16	5.04	5.37	5.55	5.32	4.69	4.09	4.41	4.80
K ₂ O	0.75	0.75	0.79	0.74	0.85	0.80	0.85	0.72	0.78	0.93
Na ₂ O	3.90	3.86	3.90	3.90	3.86	3.87	4.07	4.22	4.17	4.15
P ₂ O ₅	<u>0.286</u>	<u>0.287</u>	<u>0.287</u>	<u>0.184</u>	<u>0.197</u>	<u>0.189</u>	<u>0.196</u>	<u>0.279</u>	<u>0.321</u>	<u>0.338</u>
Total	101.09	101.34	100.83	101.68	101.02	101.45	101.62	101.66	101.38	102.00
Normalized results (wt. %):										
SiO ₂	53.10	53.37	54.72	54.98	54.97	56.14	56.34	55.76	55.08	
Al ₂ O ₃	18.03	18.02	17.90	18.48	18.09	18.34	18.15	18.45	18.23	18.16
TiO ₂	1.28	1.31	1.31	1.01	1.00	1.01	1.00	1.07	1.09	1.16
Fe ₂ O ₃ **	9.47	9.38	9.38	7.84	7.89	7.72	7.53	7.42	7.50	7.96
MnO	0.14	0.14	0.13	0.12	0.12	0.12	0.11	0.11	0.12	0.12
CaO	8.23	8.21	8.06	7.87	7.65	7.88	7.49	7.51	7.82	7.57
MgO	5.08	5.05	4.96	5.24	5.45	5.21	4.58	4.00	4.32	4.67
K ₂ O	0.74	0.73	0.78	0.72	0.84	0.78	0.83	0.70	0.76	0.91
Na ₂ O	3.82	3.78	3.84	3.81	3.79	3.79	3.98	4.12	4.09	4.04
P ₂ O ₅	0.28	0.28	0.28	0.18	0.19	0.18	0.19	0.27	0.31	0.33
Trace elements (ppm):										
Ni	61	58	60	82	91	86	65	50	44	52
Cr	71	71	64	91	105	93	72	55	51	49
Sc	27	22	27	22	23	23	24	23	24	22
V	200	207	203	172	167	164	165	156	166	169
Ba	278	265	290	256	223	235	235	328	320	348
Rb	7	8	10	8	10	10	12	7	8	8
Sr	579	575	566	646	651	623	635	929	908	996
Zr	127	126	132	120	119	117	129	177	174	160
Y	23	21	22	17	17	17	18	21	21	18
Nb	8.4	7.6	8.5	7.4	7.2	6.3	7.2	11.9	11.2	11.6
Ga	18	19	20	20	19	20	18	19	22	22
Cu	59	88	75	60	82	66	54	42	65	50
Zn	79	78	78	71	68	70	69	73	70	79
Elev. (ft)	3660	3580	3880	4080	3960	4020	4360	5860	5570	4800
Lat.	44°46.42'	44°46.45'	44°46.54'	44°46.35'	44°46.53'	44°46.84'	44°46.77'	44°46.14'	44°46.29'	44°51.34'
Long.	121°50.47'	121°50.45'	121°50.59'	121°50.56'	121°50.62'	121°51.23'	121°51.25'	121°45.44'	121°46.25'	121°46.73'

Appendix 1. Chemical analyses . . . (continued).

Sample no.	Volcanic rocks of the High Cascades									
	BR-82	BR-88	BR-86	BR-87	BR-89	BR-98	BR-102	BR-103	BR-96	BR-95
Unnormalized results (wt. %):										
SiO ₂	55.05	54.26	54.92	55.20	62.53	57.30	56.89	56.34	56.18	56.96
Al ₂ O ₃	19.05	18.81	19.05	20.26	18.32	19.15	17.88	17.93	18.03	18.35
TiO ₂	1.054	1.065	1.138	0.984	0.689	0.998	1.254	1.246	1.189	1.122
FeO*	7.35	7.44	6.86	7.32	4.77	6.84	7.91	7.99	8.06	7.44
MnO	0.121	0.127	0.120	0.122	0.082	0.119	0.137	0.139	0.141	0.130
CaO	9.28	9.17	9.05	8.63	6.42	7.04	7.43	7.49	7.62	7.49
MgO	5.00	5.25	5.26	4.81	2.88	3.33	4.45	4.55	4.76	4.21
K ₂ O	0.70	0.69	0.82	0.65	0.95	1.42	1.05	1.01	0.99	0.96
Na ₂ O	3.97	3.83	4.07	3.83	4.44	4.48	4.21	4.16	4.06	4.07
P ₂ O ₅	0.156	0.162	0.208	0.198	0.135	0.288	0.450	0.444	0.426	0.354
Total	101.73	100.80	101.50	102.00	101.22	100.96	101.66	101.30	101.46	101.09
Normalized results (wt. %):										
SiO ₂	53.73	53.43	53.75	53.73	61.49	56.37	55.53	55.18	54.94	55.94
Al ₂ O ₃	18.59	18.52	18.64	19.72	18.02	18.84	17.45	17.56	17.63	18.02
TiO ₂	1.03	1.05	1.11	0.96	0.68	0.98	1.22	1.22	1.16	1.10
Fe ₂ O ₃ **	7.89	8.06	7.38	7.84	5.16	7.40	8.49	8.61	8.67	8.04
MnO	0.12	0.13	0.12	0.12	0.08	0.12	0.13	0.14	0.14	0.13
CaO	9.06	9.03	8.86	8.40	6.31	6.93	7.25	7.34	7.45	7.36
MgO	4.88	5.17	5.15	4.68	2.83	3.28	4.34	4.46	4.65	4.13
K ₂ O	0.68	0.68	0.80	0.63	0.93	1.40	1.02	0.99	0.97	0.94
Na ₂ O	3.87	3.77	3.98	3.73	4.37	4.41	4.11	4.07	3.97	4.00
P ₂ O ₅	0.15	0.16	0.20	0.19	0.13	0.28	0.44	0.43	0.42	0.35
Trace elements (ppm):										
Ni	25	32	36	49	25	17	56	57	62	49
Cr	56	61	71	63	25	18	73	75	88	55
Sc	29	29	25	26	19	21	21	21	24	21
V	189	199	185	162	116	162	163	166	160	177
Ba	169	174	216	221	183	451	397	373	369	357
Rb	7	7	8	7	12	18	15	13	14	11
Sr	697	681	762	657	904	916	603	607	604	649
Zr	107	108	129	113	125	166	191	190	176	152
Y	14	15	17	16	12	16	24	25	23	20
Nb	5.7	5.1	6.6	6.4	4.8	7.3	14.9	14.4	14.1	9.3
Ga	20	21	20	17	18	23	23	20	17	18
Cu	71	40	58	77	88	75	48	29	56	58
Zn	61	66	70	63	56	69	82	86	87	78
Elev. (ft)	4700	4540	4960	5000	4680	5500	5320	5400	5240	5210
Lat.	44°50.05'	44°51.29'	44°49.1'	44°48.71'	44°51.45'	44°46.7'	44°48.35'	44°48.68'	44°47.99'	44°47.91'
Long.	121°47.24'	121°46.23'	121°47.45'	121°47.6'	121°45.64'	121°47.78'	121°48.6'	121°48.53'	121°48.27'	121°47.78'

Appendix 1. Chemical analyses . . . (continued).

Volcanic rocks of the High Cascades										
Sample no.	BR-104	BR-106	BR-108	BR-113	BR-115	BR-114	BR-121	BR-122	BR-127	BR-99
Unnormalized results (wt. %):										
SiO ₂	56.46	55.16	56.89	51.73	50.93	60.98	62.09	69.65	62.36	55.01
Al ₂ O ₃	20.15	19.19	18.14	17.07	16.60	18.97	18.38	16.90	17.73	17.60
TiO ₂	0.823	1.083	1.244	1.624	1.571	0.768	0.719	0.496	1.112	1.471
FeO*	6.45	7.79	7.81	8.90	8.68	5.86	5.57	3.50	6.10	8.03
MnO	0.114	0.141	0.138	0.155	0.151	0.106	0.102	0.076	0.101	0.139
CaO	8.09	8.30	7.68	9.20	9.50	6.48	6.01	3.70	5.57	7.66
MgO	4.73	5.13	4.74	7.90	8.59	3.33	3.01	1.28	1.94	4.78
K ₂ O	0.77	0.76	1.00	0.85	0.71	1.05	1.15	1.80	1.33	1.21
Na ₂ O	3.98	3.84	4.22	3.60	3.40	4.39	4.44	4.89	4.93	4.07
P ₂ O ₅	0.180	0.277	0.445	0.402	0.315	0.104	0.097	0.130	0.236	0.479
Total	101.75	101.67	102.31	101.43	100.45	102.04	101.57	102.42	101.41	100.45
Normalized results (wt. %):										
SiO ₂	55.14	53.84	55.19	50.56	50.27	59.42	60.80	67.77	61.13	54.33
Al ₂ O ₃	19.68	18.73	17.60	16.68	16.38	18.48	18.00	16.44	17.38	17.38
TiO ₂	0.80	1.06	1.21	1.59	1.55	0.75	0.70	0.48	1.09	1.45
Fe ₂ O ₃ **	6.93	8.36	8.33	9.57	9.42	6.28	6.00	3.75	6.58	8.72
MnO	0.11	0.14	0.13	0.15	0.15	0.10	0.10	0.07	0.10	0.14
CaO	7.90	8.10	7.45	8.99	9.38	6.31	5.88	3.60	5.46	7.57
MgO	4.62	5.01	4.60	7.72	8.48	3.24	2.95	1.25	1.90	4.72
K ₂ O	0.75	0.74	0.97	0.83	0.70	1.02	1.13	1.75	1.30	1.20
Na ₂ O	3.89	3.75	4.09	3.52	3.36	4.28	4.35	4.76	4.83	4.02
P ₂ O ₅	0.18	0.27	0.43	0.39	0.31	0.10	0.09	0.13	0.23	0.47
Trace elements (ppm):										
Ni	63	72	60	129	159	24	28	13	9	60
Cr	41	94	78	255	304	22	20	0	0	77
Sc	24	23	23	29	30	17	16	10	17	23
V	141	189	161	203	213	133	105	68	148	147
Ba	209	370	378	241	182	230	243	429	389	441
Rb	8	9	14	10	9	14	17	23	19	13
Sr	632	637	639	624	578	600	568	440	474	841
Zr	124	144	183	161	143	103	106	128	151	203
Y	16	23	23	24	20	14	14	14	19	24
Nb	6.7	8.8	13.6	19.0	16.4	5.1	4.5	7.7	9.7	18.4
Ga	22	18	19	19	18	18	18	18	23	22
Cu	76	69	73	57	127	41	37	31	42	55
Zn	62	77	79	68	72	53	52	49	62	89
Elev. (ft)	5240	4940	4540	4950	5460	4880	5400	5450	5250	5660
Lat.	44°48.4'	44°49.09'	44°48.82'	44°48.03'	44°46.92'	44°47.99'	44°46.05'	44°45.73'	44°46.6'	44°46.86'
Long.	121°48.93'	121°49.42'	121°48.54'	121°47.13'	121°46.54'	121°45.69'	121°47.54'	121°47.63'	121°48.53'	121°48.18'

Appendix 1. Chemical analyses . . . (continued).

Sample no.	Volcanic rocks of the High Cascades									
	BR-128	BR-131	BR-133	BR-134	MI-553	MI-136	MI-554	MI-692	MI-698	BR-139
Unnormalized results (wt. %):										
SiO ₂	54.97	53.22	63.72	63.60	64.47	70.75	71.75	66.53	66.46	60.15
Al ₂ O ₃	18.46	19.47	17.85	17.90	17.25	15.55	15.77	17.21	17.54	19.19
TiO ₂	1.153	1.158	0.808	0.798	0.614	0.438	0.441	0.677	0.627	0.806
FeO*	7.31	8.48	5.12	5.09	4.24	2.95	2.94	4.36	4.25	6.07
MnO	0.123	0.134	0.091	0.096	0.081	0.073	0.073	0.088	0.089	0.104
CaO	7.90	8.70	5.28	5.56	4.96	2.84	2.78	4.55	4.25	6.76
MgO	5.03	5.16	1.96	2.46	2.21	0.78	0.85	2.19	1.68	3.61
K ₂ O	0.86	0.58	1.52	1.49	1.58	1.99	2.05	1.58	1.52	0.96
Na ₂ O	4.13	3.56	5.02	4.87	4.88	5.19	5.35	4.93	4.98	4.20
P ₂ O ₅	<u>0.276</u>	<u>0.298</u>	<u>0.187</u>	<u>0.178</u>	<u>0.144</u>	<u>0.103</u>	<u>0.104</u>	<u>0.153</u>	<u>0.185</u>	<u>0.101</u>
Total	100.21	100.76	101.56	102.04	100.429	100.66	102.108	102.268	101.581	101.95
Normalized results (wt. %):										
SiO ₂	54.46	52.38	62.43	62.02	63.92	70.08	70.07	64.78	65.15	58.65
Al ₂ O ₃	18.29	19.16	17.49	17.45	17.10	15.40	15.40	16.76	17.20	18.71
TiO ₂	1.14	1.14	0.79	0.78	0.61	0.43	0.43	0.66	0.61	0.79
Fe ₂ O ₃ **	7.97	9.18	5.52	5.46	4.62	3.21	3.16	4.67	4.58	6.51
MnO	0.12	0.13	0.09	0.09	0.08	0.07	0.07	0.09	0.09	0.10
CaO	7.83	8.56	5.17	5.42	4.92	2.81	2.71	4.43	4.17	6.59
MgO	4.98	5.08	1.92	2.40	2.19	0.77	0.83	2.13	1.65	3.52
K ₂ O	0.85	0.57	1.49	1.45	1.57	1.97	2.00	1.54	1.49	0.94
Na ₂ O	4.09	3.50	4.92	4.75	4.84	5.14	5.22	4.80	4.88	4.10
P ₂ O ₅	0.27	0.29	0.18	0.17	0.14	0.10	0.10	0.15	0.18	0.10
Trace elements (ppm):										
Ni	76	58	10	15	23	12	9	20	11	30
Cr	70	71	6	13	16	0	0	8	0	25
Sc	24	24	17	16	12	8	6	13	11	20
V	162	152	125	125	89	40	34	46	45	147
Ba	299	244	447	420	430	527	531	431	467	195
Rb	7	6	20	20	24	29	28	21	22	12
Sr	913	676	685	670	569	331	322	519	560	592
Zr	125	143	145	142	131	155	154	158	143	101
Y	17	21	14	15	15	14	15	17	14	13
Nb	5.5	10.3	6.4	7.4	6.4	9.6	8.4	8.3	8.5	2.8
Ga	18	19	17	21	18	18	17	18	17	21
Cu	31	66	45	41	65	19	38	55	52	42
Zn	69	75	56	58	58	48	49	66	65	58
Elev. (ft)	5450	5610	5820	5780	6120	5900	6000	6050	5970	5280
Lat.	44°46.64'	44°46.86'	44°45.36'	44°45.36'	44°45.24'	44°45.36'	44°45.09'	44°45.74'	44°45.68'	44°45.86'
Long.	121°48.51'	121°48.69'	121°48.22'	121°48.45'	121°48.22'	121°48.76'	121°48.69'	121°46.49'	121°47.94'	121°48.58'

Appendix 1. Chemical analyses . . . (continued).

Sample no.	Volcanic rocks of the High Cascades									
	BR-137	BR-132	BR-143	BR-144	BR-146	BR-148	BR-155	BR-149	BR-151	BR-153
Unnormalized results (wt. %):										
SiO ₂	63.38	55.79	65.21	54.64	53.60	56.71	56.94	54.86	55.45	53.85
Al ₂ O ₃	18.06	17.98	17.36	18.56	19.42	18.02	18.48	17.44	18.11	18.03
TiO ₂	0.699	1.087	0.692	1.108	1.096	1.075	1.085	1.204	1.261	1.385
FeO*	4.71	7.29	4.51	8.13	8.18	7.09	7.11	7.75	8.68	9.07
MnO	0.099	0.123	0.090	0.128	0.131	0.121	0.120	0.132	0.151	0.141
CaO	5.85	7.89	5.19	8.23	8.83	7.77	7.96	8.17	7.84	8.22
MgO	2.80	5.41	2.16	5.32	5.68	5.20	5.38	6.28	4.77	5.45
K ₂ O	1.37	0.81	1.54	0.71	0.63	0.88	0.82	0.90	0.94	0.81
Na ₂ O	4.74	4.06	4.82	3.85	3.68	4.11	4.08	3.99	4.04	3.89
P ₂ O ₅	0.149	0.313	0.191	0.231	0.258	0.309	0.310	0.351	0.483	0.327
Total	101.86	100.75	101.76	100.91	101.50	101.28	102.28	101.08	101.73	101.17
Normalized results (wt. %):										
SiO ₂	61.94	54.98	63.80	53.72	52.38	55.60	55.28	53.86	54.05	52.75
Al ₂ O ₃	17.65	17.72	16.98	18.25	18.98	17.67	17.94	17.12	17.65	17.66
TiO ₂	0.68	1.07	0.68	1.09	1.07	1.05	1.05	1.18	1.23	1.36
Fe ₂ O ₃ **	5.06	7.90	4.85	8.79	8.79	7.65	7.59	8.37	9.31	9.77
MnO	0.10	0.12	0.09	0.13	0.13	0.12	0.12	0.13	0.15	0.14
CaO	5.72	7.77	5.08	8.09	8.63	7.62	7.73	8.02	7.64	8.05
MgO	2.74	5.33	2.11	5.23	5.55	5.10	5.22	6.17	4.65	5.34
K ₂ O	1.34	0.80	1.51	0.70	0.62	0.86	0.80	0.88	0.92	0.79
Na ₂ O	4.63	4.00	4.72	3.78	3.60	4.03	3.96	3.92	3.94	3.81
P ₂ O ₅	0.15	0.31	0.19	0.23	0.25	0.30	0.30	0.34	0.47	0.32
Trace elements (ppm):										
Ni	28	97	15	75	84	93	91	121	58	70
Cr	19	103	15	63	74	101	104	172	77	75
Sc	19	23	16	24	23	21	23	23	25	30
V	111	155	97	196	189	160	160	185	156	221
Ba	408	280	467	253	240	299	273	278	352	290
Rb	17	9	22	9	8	10	9	11	13	8
Sr	623	773	636	645	680	761	780	719	586	560
Zr	131	159	144	121	131	161	157	168	173	141
Y	15	20	14	18	18	20	20	21	26	23
Nb	6.0	10.7	7.5	6.5	8.3	11.8	10.8	12.2	14.9	8.7
Ga	17	18	19	17	20	17	18	19	19	21
Cu	47	186	44	79	74	42	71	74	61	62
Zn	58	71	56	72	68	68	69	74	87	86
Elev. (ft)	5800	5520	4280	4260	3900	3700	3880	3420	3300	3420
Lat.	44°45.4'	44°45.71'	44°46.74'	44°46.87'	44°46.86'	44°46.79'	44°46.39'	44°46.73'	44°46.71'	44°46.57'
Long.	121°48.68'	121°48.23'	121°49.72'	121°49.81'	121°49.96'	121°50'	121°50.08'	121°50.12'	121°50.24'	121°50.33'

Conrey

Appendix 1. Chemical analyses . . . (continued).

Sample no.	Volcanic rocks of the High Cascades									
	BR-154	BR-156	BR-158	BR-5	BR-6	BR-22	BR-4	BR-159	BR-20	BR-21
Unnormalized results (wt. %):										
SiO ₂	53.29	59.53	55.57	55.18	55.69	55.43	55.14	55.64	56.41	55.87
Al ₂ O ₃	18.39	18.22	19.70	19.46	20.11	19.15	19.24	19.04	20.16	19.03
TiO ₂	1.362	1.195	0.957	0.960	0.977	0.991	0.993	1.006	1.008	1.069
FeO*	9.08	6.85	6.95	7.20	7.01	7.34	7.41	7.42	6.61	7.50
MnO	0.155	0.122	0.120	0.124	0.119	0.126	0.124	0.122	0.117	0.124
CaO	8.38	6.58	8.42	8.52	8.57	8.45	8.40	8.33	8.44	8.16
MgO	5.43	2.76	4.47	5.31	4.26	5.04	5.06	4.86	3.53	4.92
K ₂ O	0.80	1.05	0.77	0.69	0.76	0.73	0.72	0.76	0.84	0.74
Na ₂ O	3.88	4.91	4.01	3.79	3.90	3.93	3.84	3.97	4.15	3.99
P ₂ O ₅	0.322	0.307	0.245	0.215	0.219	0.222	0.221	0.225	0.255	0.235
Total	101.09	101.52	101.21	101.45	101.62	101.41	101.15	101.37	101.52	101.64
Normalized results (wt. %):										
SiO ₂	52.25	58.24	54.53	54.01	54.43	54.27	54.12	54.49	55.21	54.57
Al ₂ O ₃	18.03	17.83	19.33	19.05	19.65	18.75	18.88	18.65	19.73	18.59
TiO ₂	1.34	1.17	0.94	0.94	0.95	0.97	0.97	0.99	0.99	1.04
Fe ₂ O ₃ **	9.79	7.37	7.50	7.75	7.54	7.90	8.00	7.99	7.12	8.06
MnO	0.15	0.12	0.12	0.12	0.12	0.12	0.12	0.12	0.11	0.12
CaO	8.22	6.44	8.26	8.34	8.38	8.27	8.24	8.16	8.26	7.97
MgO	5.32	2.70	4.39	5.20	4.16	4.93	4.97	4.76	3.45	4.81
K ₂ O	0.78	1.03	0.76	0.68	0.74	0.71	0.71	0.74	0.82	0.72
Na ₂ O	3.80	4.80	3.93	3.71	3.81	3.85	3.77	3.89	4.06	3.90
P ₂ O ₅	0.32	0.30	0.24	0.21	0.21	0.22	0.22	0.22	0.25	0.23
Trace elements (ppm):										
Ni	71	10	54	74	43	68	67	59	26	73
Cr	69	7	55	76	58	70	79	69	48	63
Sc	26	20	21	22	23	26	24	23	21	22
V	193	166	150	163	167	168	165	175	151	176
Ba	296	343	267	238	261	260	254	262	299	232
Rb	7	13	9	10	9	10	7	9	9	9
Sr	559	688	653	649	654	645	646	647	667	659
Zr	138	149	131	118	126	123	124	125	139	124
Y	22	20	17	16	18	18	19	18	20	18
Nb	7.7	8.6	7.6	6.3	7.3	7.5	7.7	7.7	8.5	8.4
Ga	20	19	19	20	20	18	18	17	19	19
Cu	70	47	70	75	55	79	43	62	53	75
Zn	82	70	67	68	62	66	67	65	68	70
Elev. (ft)	3540	4120	4720	5200	3480	4300	5100	4860	3980	3720
Lat.	44°46.54'	44°46.22'	44°46.39'	44°46.18'	44°48.52'	44°47.11'	44°46.35'	44°46.45'	44°47.52'	44°47.46'
Long.	121°50.23'	121°49.96'	121°49.57'	121°48.98'	121°52.66'	121°50.25'	121°49.02'	121°49.31'	121°50.96'	121°50.98'

Appendix 1. Chemical analyses . . . (continued).

Sample no.	Volcanic rocks of the High Cascades									
	MJ-BR1	MJ-BR3	MJ-CV1	BR-CV2	BR-135	RD-46-1	BR-19	WFINB	MJ-#011	MJ-#013
Unnormalized results (wt. %):										
SiO ₂	54.28	55.78	55.86	56.16	53.59	55.74	56.32	56.27	56.58	56.84
Al ₂ O ₃	18.49	18.62	18.58	18.45	19.87	17.79	18.24	19.00	18.02	18.22
TiO ₂	1.106	1.113	1.110	1.166	1.082	1.050	1.090	1.159	0.972	0.964
FeO*	7.76	7.33	7.31	7.68	7.87	7.05	7.13	7.41	6.82	6.63
MnO	0.124	0.130	0.125	0.128	0.130	0.119	0.123	0.128	0.112	0.110
CaO	8.15	7.60	7.64	7.62	9.00	7.77	7.75	6.86	7.58	7.43
MgO	4.77	4.77	4.75	4.68	5.05	5.47	5.12	4.23	4.77	4.77
K ₂ O	0.72	0.93	0.94	0.98	0.60	0.81	0.83	0.84	0.80	0.79
Na ₂ O	3.86	4.15	4.18	4.23	3.83	3.98	4.12	3.97	3.27	3.18
P ₂ O ₅	0.227	0.271	0.265	0.262	0.272	0.292	0.307	0.254	0.176	0.173
Total	99.49	100.69	100.76	101.36	101.29	100.07	101.03	100.12	99.10	99.11
Normalized results (wt. %):										
SiO ₂	54.14	55.00	55.04	54.99	52.50	55.31	55.36	55.79	56.40	56.67
Al ₂ O ₃	18.44	18.36	18.31	18.07	19.46	17.65	17.93	18.84	17.96	18.17
TiO ₂	1.10	1.10	1.09	1.14	1.06	1.04	1.07	1.15	0.97	0.96
Fe ₂ O ₃ **	8.51	7.95	7.92	8.27	8.48	7.70	7.71	8.08	7.56	7.35
MnO	0.12	0.13	0.12	0.13	0.13	0.12	0.12	0.13	0.11	0.11
CaO	8.13	7.49	7.53	7.46	8.82	7.71	7.62	6.80	7.56	7.41
MgO	4.76	4.70	4.68	4.58	4.95	5.43	5.03	4.19	4.75	4.76
K ₂ O	0.72	0.92	0.93	0.96	0.59	0.80	0.82	0.83	0.80	0.79
Na ₂ O	3.85	4.09	4.12	4.14	3.75	3.95	4.05	3.94	3.72	3.61
P ₂ O ₅	0.23	0.27	0.26	0.26	0.27	0.29	0.30	0.25	0.18	0.17
Trace elements (ppm):										
Ni	62	71	63	64	56	96	82	58	61	60
Cr	58	61	65	62	69	103	95	47	70	66
Sc	26	24	25	24	26	24	24	21	21	23
V	193	157	153	167	184	143	162	152	145	161
Ba	245	364	352	353	212	283	294	315	277	259
Rb	8	10	10	10	8	9	10	11	11	11
Sr	647	758	770	730	695	803	781	548	724	718
Zr	122	127	127	120	134	155	161	145	128	127
Y	17	17	18	18	18	19	19	20	15	15
Nb	8.6	7.1	8.0	7.3	9.8	10.0	11.1	8.2	6.0	5.0
Ga	19	21	17	19	20	17	22	18	18	16
Cu	78	65	121	51	61	83	64	58	60	39
Zn	75	79	87	71	71	78	69	76	72	75
Elev. (ft)	4950	4840	4580	4500	5840	2900	4100		3040	3140
Lat.	44°46.36'	44°46.51'	44°46.99'	44°46.98'	44°45.36'	44°48.08'	44°47.99'		44°46.55'	44°46.23'
Long.	121°48.91'	121°49.13'	121°49.72'	121°49.76'	121°48.7'	121°53.59'	121°50.98'		121°56.84'	121°55.69'

Conrey

Appendix 1. Chemical analyses . . . (continued).

Sample no.	Volcanic rocks of the High Cascades									
	MJ-#020	MJ-#025	MJ-#029	BHS-20†	MJ-#019	MJ-#028	BR-67	BR-74	BHS-21§	BR-72
Unnormalized results (wt. %):										
SiO ₂	56.79	56.79	56.62	57.77	57.25	58.24	58.62	56.69	61.13	60.97
Al ₂ O ₃	18.20	18.18	18.07	18.61	18.36	18.65	18.34	18.34	18.83	18.37
TiO ₂	0.963	0.962	0.985	0.978	0.984	0.870	0.938	0.953	0.943	0.956
FeO*	6.85	6.74	6.75	6.75	6.83	6.01	6.48	7.47	5.74	5.62
MnO	0.109	0.107	0.111	0.111	0.114	0.095	0.102	0.129	0.095	0.098
CaO	7.22	7.30	7.39	7.71	6.67	6.89	7.20	7.45	6.67	6.46
MgO	4.81	4.87	4.82	4.66	4.68	4.23	4.24	5.93	3.26	2.93
K ₂ O	0.77	0.77	0.80	0.86	0.82	0.83	0.90	0.79	0.97	1.01
Na ₂ O	3.19	3.20	3.37	4.22	3.15	3.22	4.24	3.74	4.58	4.69
P ₂ O ₅	0.169	0.169	0.175	0.191	0.185	0.145	0.194	0.129	0.165	0.174
Total	99.07	99.09	99.09	101.86	99.04	99.18	101.25	101.62	102.38	101.28
Normalized results (wt. %):										
SiO ₂	56.63	56.63	56.44	56.34	57.11	58.07	57.53	55.38	59.37	59.87
Al ₂ O ₃	18.15	18.13	18.01	18.15	18.32	18.59	18.00	17.92	18.29	18.04
TiO ₂	0.96	0.96	0.98	0.95	0.98	0.87	0.92	0.93	0.92	0.94
Fe ₂ O ₃ **	7.59	7.47	7.48	7.24	7.57	6.66	6.99	8.03	6.13	6.07
MnO	0.11	0.11	0.11	0.11	0.11	0.09	0.10	0.13	0.09	0.10
CaO	7.20	7.28	7.37	7.52	6.65	6.87	7.07	7.28	6.48	6.34
MgO	4.80	4.86	4.80	4.54	4.67	4.22	4.16	5.79	3.17	2.88
K ₂ O	0.77	0.77	0.80	0.84	0.82	0.83	0.88	0.77	0.94	0.99
Na ₂ O	3.63	3.64	3.83	4.12	3.58	3.66	4.16	3.65	4.45	4.61
P ₂ O ₅	0.17	0.17	0.17	0.19	0.18	0.14	0.19	0.13	0.16	0.17
Trace elements (ppm):										
Ni	71	67	57	61	81	55	60	88	32	31
Cr	84	82	67	74	119	34	52	158	22	23
Sc	20	19	22	22	19	14	22	22	19	22
V	163	157	166	159	155	144	164	183	134	132
Ba	235	240	273	241	286	201	214	266	260	262
Rb	9	11	10	9	12	13	11	13	11	10
Sr	694	709	715	715	676	784	703	555	751	739
Zr	128	128	128	127	140	135	139	93	125	127
Y	14	16	16	16	17	16	18	15	15	16
Nb	5.0	6.0	7.0	6.1	8.0	5.0	7.6	3.9	5.0	5.2
Ga	18	21	20	20	18	18	20	17	18	19
Cu	49	46	26	28	217	36	51	71	47	44
Zn	70	67	64	62	85	68	61	70	56	60
Elev. (ft)	3360	3620	3540	3580	3400	4450	5000	4840	4880	4840
Lat.	44°46.26'	44°45.55'	44°45.62'	44°45.65'	44°46.42'	44°45.81'	44°45.44'	44°45.28'	44°45.1'	44°45.12'
Long.	121°55.6'	121°53.84'	121°54.21'	121°54.23'	121°55.73'	121°53.79'	121°52.29'	121°52.54'	121°52.41'	121°52.44'

† K-Ar age 0.857±0.060 Ma;

§ K-Ar age 1.47±0.06 Ma (Sherrod and Conrey, this volume)

Appendix 1. Chemical analyses . . . (continued).

Sample no.	Volcanic rocks of the High Cascades									
	MJ-56	BR-70	MJ-72	BR-31	BR-29	BR-30	BR-33	BR-34	BR-44	BR-44R
Unnormalized results (wt. %):										
SiO ₂	58.55	59.51	57.79	57.39	59.34	58.50	56.78	56.78	56.78	56.84
Al ₂ O ₃	18.61	19.17	19.06	19.65	17.22	17.52	19.79	19.79	19.79	19.78
TiO ₂	0.912	0.875	0.765	1.073	1.392	1.364	0.920	0.920	0.920	0.922
FeO*	5.70	5.62	6.03	6.72	7.83	7.84	6.33	6.33	6.33	6.31
MnO	0.092	0.089	0.104	0.110	0.137	0.134	0.104	0.104	0.104	0.103
CaO	7.04	6.97	7.01	7.93	6.33	6.75	7.83	7.83	7.83	7.83
MgO	3.83	4.04	4.15	3.48	2.92	3.10	4.24	4.24	4.24	4.20
K ₂ O	0.80	0.88	0.85	0.85	1.14	1.06	0.70	0.70	0.70	0.70
Na ₂ O	3.57	4.40	3.32	4.37	4.84	4.77	3.88	3.88	3.88	3.87
P ₂ O ₅	0.125	0.139	0.106	0.276	0.362	0.339	0.161	0.161	0.161	0.160
Total	99.23	101.69	99.19	101.85	101.51	101.38	100.74	100.74	100.74	100.72
Normalized results (wt. %):										
SiO ₂	58.34	58.20	57.61	55.98	58.01	57.26	57.11	56.85	56.01	56.09
Al ₂ O ₃	18.54	18.75	19.00	19.17	16.83	17.15	18.36	17.93	19.52	19.52
TiO ₂	0.91	0.86	0.76	1.05	1.36	1.34	1.15	0.94	0.91	0.91
Fe ₂ O ₃ **	6.31	6.05	6.68	7.21	8.42	8.44	7.40	7.16	6.87	6.85
MnO	0.09	0.09	0.10	0.11	0.13	0.13	0.11	0.10	0.10	0.10
CaO	7.01	6.82	6.99	7.74	6.19	6.61	7.25	7.44	7.72	7.73
MgO	3.82	3.95	4.14	3.39	2.85	3.03	2.88	4.47	4.18	4.14
K ₂ O	0.80	0.86	0.85	0.83	1.11	1.04	0.93	0.86	0.69	0.69
Na ₂ O	4.06	4.30	3.77	4.26	4.73	4.67	4.53	4.06	3.83	3.82
P ₂ O ₅	0.12	0.14	0.11	0.27	0.35	0.33	0.28	0.19	0.16	0.16
Trace elements (ppm):										
Ni	42	57	45	36	3	12	15	63	48	47
Cr	23	22	33	27	3	18	19	73	49	47
Sc	16	19	19	20	21	23	23	24	23	24
V	146	161	151	156	202	210	159	165	144	159
Ba	239	201	229	290	399	356	288	219	211	223
Rb	9	9	8	9	15	13	11	10	9	9
Sr	721	842	661	819	557	567	724	729	751	754
Zr	114	116	99	148	162	156	144	132	136	136
Y	15	13	14	18	23	23	20	16	16	17
Nb	4.0	3.4	4.0	8.3	11.1	10.4	8.1	7.1	6.1	6.8
Ga	19	18	19	17	21	19	17	21	19	23
Cu	23	18	52	46	35	59	65	44	50	51
Zn	60	52	59	69	78	81	73	68	65	63
Elev. (ft)	5120	5260	6040	4800	5160	5000	4780	4760	5700	5700
Lat.	44°44.99'	44°44.99'	44°45.01'	44°45.47'	44°45.18'	44°45.39'	44°45.48'	44°45.64'	44°45.16'	44°45.16'
Long.	121°52.41'	121°52.2'	121°50.91'	121°49.58'	121°49.81'	121°49.6'	121°49.78'	121°50.03'	121°51.03'	121°51.03'

Appendix 1. Chemical analyses . . . (continued).

Sample no.	Volcanic rocks of the High Cascades									
	BR-47	BR-49	BR-50	BR-52	BR-60	BR-8	BR-10	BR-12	BR-39	BR-40
Unnormalized results (wt. %):										
SiO ₂	59.24	58.37	57.90	57.46	57.37	59.58	59.46	59.53	59.92	58.96
Al ₂ O ₃	18.78	18.53	18.42	18.59	18.63	19.02	18.66	18.55	18.71	18.98
TiO ₂	0.909	0.939	0.992	0.993	0.985	0.867	0.879	0.872	0.857	0.863
FeO*	6.23	6.50	6.61	6.97	6.74	5.90	5.98	5.88	5.85	5.92
MnO	0.103	0.111	0.111	0.116	0.114	0.097	0.097	0.100	0.098	0.094
CaO	7.43	7.41	7.49	7.51	7.67	6.98	7.38	7.35	7.41	7.24
MgO	4.33	4.37	4.55	4.91	4.73	3.89	4.11	3.93	4.07	3.95
K ₂ O	0.89	0.89	0.89	0.86	0.83	0.94	0.89	0.88	0.89	0.90
Na ₂ O	4.15	4.09	4.10	3.90	4.17	4.08	4.23	4.29	4.24	4.08
P ₂ O ₅	<u>0.184</u>	<u>0.184</u>	<u>0.199</u>	<u>0.184</u>	<u>0.210</u>	<u>0.157</u>	<u>0.175</u>	<u>0.174</u>	<u>0.168</u>	<u>0.154</u>
Total	102.25	101.39	101.26	101.49	101.45	101.51	101.86	101.56	102.21	101.14
Normalized results (wt. %):										
SiO ₂	57.59	57.20	56.81	56.23	56.18	58.35	58.03	58.28	58.29	57.96
Al ₂ O ₃	18.26	18.16	18.07	18.19	18.24	18.63	18.21	18.16	18.20	18.66
TiO ₂	0.88	0.92	0.97	0.97	0.96	0.85	0.86	0.85	0.83	0.85
Fe ₂ O ₃ **	6.66	7.01	7.13	7.50	7.26	6.36	6.42	6.33	6.26	6.40
MnO	0.10	0.11	0.11	0.11	0.11	0.10	0.09	0.10	0.10	0.09
CaO	7.22	7.26	7.35	7.35	7.51	6.84	7.20	7.20	7.21	7.12
MgO	4.21	4.28	4.46	4.80	4.63	3.81	4.01	3.85	3.96	3.88
K ₂ O	0.87	0.87	0.87	0.84	0.81	0.92	0.87	0.86	0.87	0.88
Na ₂ O	4.03	4.01	4.02	3.82	4.08	4.00	4.13	4.20	4.12	4.01
P ₂ O ₅	0.18	0.18	0.20	0.18	0.21	0.15	0.17	0.17	0.16	0.15
Trace elements (ppm):										
Ni	61	56	59	79	63	48	53	56	53	51
Cr	56	57	69	84	73	36	48	47	46	37
Sc	22	22	20	23	22	19	21	19	19	21
V	150	144	158	167	160	136	129	130	132	160
Ba	225	238	218	233	254	203	211	207	209	188
Rb	11	13	10	11	9	13	11	10	11	10
Sr	732	679	695	604	763	769	743	742	754	711
Zr	136	139	134	127	138	135	136	136	134	130
Y	16	16	15	17	16	16	15	15	14	14
Nb	8.3	7.3	7.5	8.0	8.4	7.0	6.8	7.6	6.1	5.5
Ga	21	17	21	19	19	19	20	22	21	18
Cu	29	48	46	51	34	31	55	41	33	18
Zn	64	66	67	70	70	57	62	62	61	58
Elev. (ft)	5360	5080	4740	4360	4440	4880	4920	5040	5220	5500
Lat.	44°45.28'	44°45.78'	44°46.14'	44°46.32'	44°46.75'	44°47.02'	44°46.81'	44°46.52'	44°46.22'	44°46.05'
Long.	121°50.72'	121°51.12'	121°50.78'	121°50.65'	121°51.27'	121°52.5'	121°52.01'	121°51.78'	121°51.6'	121°51.67'

Appendix 1. Chemical analyses . . . (continued).

Sample no.	Volcanic rocks of the High Cascades									
	BR-43	BR-26	BR-38	BR-28	MJ-697	MJ-696	MJ-695	BHS-23†	BR-138	MJ-693
Unnormalized results (wt. %):										
SiO ₂	58.47	58.17	58.66	69.46	59.83	59.90	59.23	59.52	57.87	57.39
Al ₂ O ₃	18.94	18.38	18.59	16.17	18.99	19.09	18.94	19.08	18.99	18.80
TiO ₂	0.877	0.959	0.949	0.502	0.819	0.889	0.921	0.930	1.044	1.008
FeO*	6.06	6.63	6.37	3.31	6.06	5.37	5.66	5.52	6.20	6.96
MnO	0.104	0.113	0.116	0.079	0.109	0.088	0.095	0.090	0.160	0.120
CaO	7.95	7.51	7.46	3.10	6.85	7.29	7.21	7.31	7.62	7.86
MgO	4.19	4.43	4.28	0.95	3.58	3.77	3.90	3.88	4.02	4.60
K ₂ O	0.84	0.89	0.90	2.05	0.95	0.73	0.81	0.81	1.03	0.85
Na ₂ O	4.02	4.15	4.20	5.41	4.10	4.47	4.48	4.39	4.37	4.17
P ₂ O ₅	0.143	0.200	0.190	0.135	0.103	0.190	0.215	0.216	0.293	0.298
Total	101.59	101.43	101.72	101.17	101.39	101.787	101.461	101.75	101.54	102.056
Normalized results (wt. %):										
SiO ₂	57.21	56.98	57.31	68.44	58.66	58.54	58.05	58.18	56.65	55.85
Al ₂ O ₃	18.53	18.00	18.16	15.93	18.62	18.66	18.56	18.65	18.59	18.30
TiO ₂	0.86	0.94	0.93	0.49	0.80	0.87	0.90	0.91	1.02	0.98
Fe ₂ O ₃ **	6.52	7.14	6.85	3.59	6.54	5.77	6.10	5.94	6.68	7.45
MnO	0.10	0.11	0.11	0.08	0.11	0.09	0.09	0.09	0.10	0.12
CaO	7.78	7.36	7.29	3.05	6.72	7.12	7.07	7.15	7.46	7.65
MgO	4.10	4.34	4.18	0.94	3.51	3.68	3.82	3.79	3.94	4.48
K ₂ O	0.82	0.87	0.88	2.02	0.93	0.71	0.79	0.79	1.01	0.83
Na ₂ O	3.93	4.06	4.10	5.33	4.02	4.37	4.39	4.29	4.28	4.06
P ₂ O ₅	0.14	0.20	0.19	0.13	0.10	0.19	0.21	0.21	0.29	0.29
Trace elements (ppm):										
Ni	50	57	55	11	31	37	35	35	37	67
Cr	39	69	57	0	29	34	32	30	35	67
Sc	22	22	24	8	20	19	18	19	19	21
V	158	159	153	32	144	120	116	142	158	153
Ba	173	232	229	627	225	193	228	221	383	335
Rb	11	11	10	29	12	4	6	7	8	10
Sr	697	671	675	486	592	1202	1213	1232	1350	789
Zr	122	137	138	207	102	123	132	133	149	155
Y	14	16	18	17	15	11	13	12	14	19
Nb	6.2	7.8	7.5	11.7	4.8	4.0	5.1	3.6	5.5	10.7
Ga	17	17	16	18	19	17	19	19	19	16
Cu	85	38	33	24	57	58	44	38	68	76
Zn	61	68	66	57	77	53	60	59	65	73
Elev. (ft)	5560	4880	4960	4960	5620	5550	5800	5860	5410	5720
Lat.	44°45.47'	44°46.06'	44°46.34'	44°45.54'	44°45.64'	44°45.77'	44°45.48'	44°45.47'	44°45.73'	44°45.18'
Long.	121°51.26'	121°50.95'	121°51.43'	121°50.12'	121°47.44'	121°47.14'	121°46.94'	121°47.58'	121°48.54'	121°46.35'

† K-Ar age 0.652±0.045 Ma (Sherrod and Conrey, this volume)

Appendix 1. Chemical analyses . . . (continued).

Sample no.	Volcanic rocks of the High Cascades		
	MI-699	BD-13	BD-17
Unnormalized results (wt. %):			
SiO ₂	60.31	51.99	57.91
Al ₂ O ₃	18.39	17.47	17.29
TiO ₂	1.032	1.333	0.993
FeO*	6.31	8.70	6.39
MnO	0.105	0.148	0.116
CaO	6.79	9.47	7.57
MgO	2.81	8.33	6.02
K ₂ O	1.17	0.63	1.07
Na ₂ O	4.50	3.33	4.04
P ₂ O ₅	0.273	0.266	0.272
Total	101.69	101.67	101.67
Normalized results (wt. %):			
SiO ₂	58.94	50.70	56.60
Al ₂ O ₃	17.97	17.04	16.90
TiO ₂	1.01	1.30	0.97
Fe ₂ O ₃ **	6.78	9.33	6.87
MnO	0.10	0.14	0.11
CaO	6.64	9.24	7.40
MgO	2.75	8.12	5.88
K ₂ O	1.14	0.61	1.05
Na ₂ O	4.40	3.25	3.95
P ₂ O ₅	0.27	0.26	0.27
Trace elements (ppm):			
Ni	15	151	141
Cr	16	262	191
Sc	20	28	20
V	149	200	145
Ba	340	248	361
Rb	15	8	12
Sr	537	675	1000
Zr	145	135	150
Y	20	22	16
Nb	9.7	8.6	7.2
Ga	21	18	20
Cu	77	57	89
Zn	81	70	63
Elev. (ft)	5240	3700	3080
Lat.	44°45'	44°58.85'	44°51.7'
Long.	121°45.9'	121°45.9'	121°53.2'

Appendix 2: Generalized lithologic log for CTGH-1




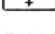

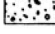


Compiled by David R. Sherrod, U.S. Geological Survey, Menlo Park, Calif. 94025
and Richard M. Conrey, Washington State University, Pullman, Wash. 99164

CTGH-1 hole was rotary drilled in the upper 161 m and cored in the lower 1,302 m (total depth 1,463 m). The cuttings and core were logged on site for Thermal Power Company by Angela McDannel and Doug Goodwin. We modify their lithologic descriptions by incorporating 40 chemical analyses (Conrey and Sherrod, this volume) and the study of 96 thin sections from drill core. The original onsite log is available in detailed and generalized form (publications CTGH-1-4 and CTGH-1-3) from the University of Utah Research Institute:

University of Utah Research Institute
391 Chipeta Way, Suite C
Salt Lake City, Utah, 84108-1295
(ph. 801-524-3422)

The Appendix 2 log also shows fracture density and magnetic polarity. Fracture density is generalized from the onsite drill log, in which the degree of fracturing in core was listed as absent, light, moderate, heavy, or intense. Magnetic polarity shows the upward component of the magnetic polarity (normal, N; reversed, R; or indeterminate, I) of 79 drill core samples as measured with a fluxgate magnetometer by Neil Woller in 1986. The three circled polarity measurements were determined by Shaul Levi of the College of Oceanography, Oregon State University, using alternating-field demagnetization methods (Table A2-1).

EXPLANATION OF CTGH-1 DRILL LOG

-  Till--Only in upper 12 m
-  Lava flows--Chiefly basaltic andesite, with lesser basalt and andesite. Locally includes abundant breccia
-  Lava flows and domes(?)--Chiefly andesite, with lesser dacite. Includes minor breccia
-  Lava flows--Chiefly basalt
-  Volcanic breccia--Includes lahars, flow breccia, and possible surge deposits
-  Tuff and lapilli tuff--Probably intermediate to silicic in composition; single chemical analysis is dacite
-  Olivine analcinite--Lava flow at 778-788 m
-  Basalt sill--At 621-683 m. Offshoots at lower depths recognized in thin section but too thin to show

Fluxgate magnetometer polarity determinations

- N Normal
- R Reversed
- I Indeterminate

Alternating field magnetic polarity determinations

- (N) Normal
- (R) Reversed

Table A2-1. Magnetization of samples from CTGH-1¹

Sample no. (=depth in ft)	Demagnetizing field (Oe)	Moment (M) (10 ⁻³ emu/gm)	Relative declination	Relative inclination	Wt. (gm)	χ^2 (10 ⁻³ G/Oe)	Q ³	Polarity
639	0	0.360	162°	-68°	32.61	1.55	0.5	
do.	50	0.302	141°	-68°				
do.	100	0.246	141°	-71°				
do.	200	0.192	140°	-73°				Reversed
3277	0	0.456	160°	36°	33.28	1.52	0.6	
do.	50	0.541	158°	55°				
do.	100	0.509	158°	62°				
do.	200	0.413	157°	64°				Normal
4779	0	0.387	169°	-43°	33.17	2.67	0.3	
do.	50	0.179	155°	18°				
do.	100	0.196	144°	52°				
do.	200	0.121	144°	59°				Normal

Notes:

- ¹ Determinations by Shaul Levi, College of Oceanography, Oregon State University
- ² χ (chi) = susceptibility.
- ³ Q = natural remanence divided by induced moment (Q>1 indicates most of moment is natural remanence; Q<1 indicates most is induced). Induced moment taken as (0.50) χ .

Appendix 2. Generalized lithologic log for CTGH-1.

Fracture density low – high	Depth (m)	Lithology	Interval		Description (Descriptions are from drill cuttings to depth of 161 m [527 ft])
			(m)	(ft)	
	0		0-12	0-40	Till. Comprises cobbles and boulders of basalt and basaltic andesite
	50				
	100		12-247	40-809	Basalt and basaltic andesite lava flows. Dark- to medium-gray, aphyric to slightly porphyritic
	150		(161)	(527)	(Descriptions are from drill core below this depth)
	200				
	250		247-258	809-857	Volcanic breccia. Lapilli and blocks ranging in composition from mafic to silicic. Matrix is yellowish-brown ash, crystals, and lithic fragments. We interpret these rocks as lahars on basis of heterolithic composition
	300		258-339	847-1,112	Andesite. Medium-light-gray and slightly porphyritic. Probably a lava flow or dome
	350		339-347	1,112-1,138	Laharic breccia. Lapilli and blocks of basalt and(or) basaltic andesite, with fewer silicic fragments in clayey matrix of crystals and lithic fragments. Probably a lahar, on basis of heterolithic composition
			347-375	1,138-1,230	Basaltic andesite. Medium-dark-gray, slightly porphyritic
			375-393	1,230-1,291	Volcanic breccia. Reddish-orange-brown, subangular to subrounded lapilli and blocks of basalt and basaltic andesite in matrix of crystals and lithic fragments

Appendix 2 (continued).

Fracture density low – high	Depth (m)	Lithology	Interval (m)	Interval (ft)	Description
	400	R			
	450	I	393-479	1,291-1,570	Andesite lava(?) and minor breccia. Medium-brown to dark-gray, slightly porphyritic
	500	N	479-502	1,570-1,647	Volcanic breccia. Medium-dark-gray and grayish-brown lapilli and blocks of mafic or intermediate lava in matrix of crystal-lithic tuff. Palagonitic in part. May be surge deposits
		N	502-508	1,647-1,666.5	Basaltic andesite lava. Olive-gray, very slightly porphyritic
		N	508-516	1,666.5-1,694	Volcanic breccia. Bedding ranges from laminated to cross-bedded. May be surge deposits
		N	516-543	1,694-1,781.5	Basaltic andesite lava. Slightly porphyritic
	550	N	543-548	1,781.5-1,798	Volcanic breccia (surge deposit?)
		N	548-555	1,798-1,820	Andesite lava, slightly porphyritic. Clay coats fractures and fills vesicles
		N	555-557	1,820-1,826	Lapilli tuff (air-fall?)
		N	557-600	1,826-1,969	Basaltic andesite, slightly porphyritic
	600	N	600-603	1,969-1,979	Lapilli tuff (air-fall?)
		N	603-621	1,979-2,036	Basalt and basaltic andesite, slightly porphyritic
	650	N	621-683	2,036-2,240	Basalt sill. Contains several subhorizontal horizons about 7 cm thick where vesicles and limonitic alteration are concentrated. These horizons were interpreted by McDannel and Goodwin as flow contacts. From thin sections, we interpret entire sequence as a sill, perhaps with numerous internal intrusive (emplacement) contacts. Interval from 639-642 m (2095-2107 ft) described by McDannel and Goodwin as basaltic andesite (matrix) that contains gabbroic xenoliths 7-25 cm in diameter with sharp to diffuse margins
	700	R	683-706	2,240-2,317	Basaltic andesite, slightly porphyritic. May include offshoot of sill
	750	I	706-785	2,317-2,576	Basalt, slightly porphyritic. Three flows recognized, 10-50 m thick
		I	778-788	2,553-2,586	Olivine analcimite
		N	788-793	2,586-2,602.5	Crystal-lithic lapilli tuff (air-fall?)
	800	R	793-810	2,602.5-2,657	Lapilli tuff (ash-flow). Light-gray, angular to subrounded lapilli of lithic fragments, black glass, and collapsed pumice(?) in dark-gray matrix of crystal-lithic dacitic tuff

CTGH-1-drill log

Appendix 2 (continued).

Fracture density low – high	Depth (m)	Lithology	Interval		Description
			(m)	(ft)	
	850	R	810-821	2,657-2,694	Basaltic andesite breccia. Medium- to dark-gray, subangular to subrounded lapilli and blocks of andesite in matrix of crystal tuff. Interpreted by McDannel and Goodwin as primary breccia interspersed with blocks or thin flows(?) of unvesiculated andesite
		N	821-831	2,694-2,726	
		R	831-866	2,726-2,842	Lapilli tuff (surge deposits?). Medium-gray blocks and lapilli of mafic or intermediate lava in matrix of crystal tuff. Matrix locally palagonitic
	900	N	866-895	2,842-2,935	Basaltic andesite, slightly porphyritic
		I	895-900	2,935-2,951.5	Volcanic breccia (flow breccia?). Angular to subrounded lapilli and blocks in matrix of crystal-lithic tuff. Unit varies from clast- to matrix-supported. Interpreted as flow breccia by McDannel and Goodwin on basis of strung-out, elongated clasts of basaltic andesite
		R	900-902	2,951.5-2,960.5	Basaltic andesite, slightly porphyritic
	950	I			Volcanic breccia (flow breccia?). Similar to previous interval of volcanic breccia but predominantly clast-supported
		R			
		R			
	1,000	N			Basaltic andesite, slightly porphyritic. Lava flows and thick deposits of pyroclastic (flow?) breccia
		R			
		R			
	1,050	R	902-1,463	2,960.5-4,800	Lava flows 1-3 m thick and pyroclastic (flow?) breccia 1-8 m thick in interval 1,024-1,195 m (3,360-3,920 ft)
		R			
		R			
	1,100	N			
		R			
		R			
	1,150	R			
		R			
		R			

Appendix 2 (continued).

Fracture density low – high	Depth (m)	Lithology	Interval (m)	Interval (ft)	Description
	1,200	R			
		R			
		N			
		N			
	1,250	R			
		R			
		R			
		N			
	1,300	N			
		N	902-1,463	2,960.5-4,800	(continued as above) Basaltic andesite, slightly porphyritic. Lava flows and thick deposits of pyroclastic (flow?) breccia
		N			Lava flows generally thicker (4-6 m thick) than breccia (2-3 m thick) in interval 1,195-1,341 m (3,920-4,400 ft)
	1,350	R			
		R			
		R			
		N			
		N			
	1,400	N			
		N			
		N			
		N			
		R			
	1,450	N			
		N			
		N			
		N			
		N	1,463		Total depth 1463 m (4800 ft)

CTGH-1 drill log